ISSN: 2588-5596

JGT

Journal of Gas Technology

Volume 6 . Issue 2 . Winter 2021 . www.jgt.irangi.org

Journal of Gas Technology, JGT

Volume 6, Issue 2, Winter 2021

Publisher
Iranian Gas Institute

Contact Information
http://jgt.irangi.org
Email: ijgt.igi@gmail.com

EISSN: 2588-5596

Open Access Journal
Journal of Gas Technology is a peer reviewed, open access journal.

Table of Contents

JOURNAL OF GAS TECHNOLOGY

Volume 6 / Issue 2 / Winter 2021 / Pages 04-19

Journal Homepage: http://jgt.irangi.org

Skid-Mounted SMR Packages for LNG Production: Configuration Selection and Sensitivity Analysis

Laleh Shirazi[1*], Mehran Sarmad[1], Peyman Moein[1], Reza Hayati[1], Sanaz Anahid[1], Marziyeh Zare[2]

1. Gas Research Division, Research Institute of Petroleum Industry (RIPI), Tehran, Iran
2. Research & Technology Directorate of National Iranian Gas Company, Tehran, Iran

ARTICLE INFO

ORIGINAL RESEARCH ARTICLE

Article History:
Received: 22 July 2021
Revised: 30 August 2021
Accepted: 14 October 2021

Keywords:
LNG
Single Mixed Refrigerant
Optimization
Sensitivity & Economic analysis
Skid Design

DOR: 20.1001.1.25885596.2021.7.2.1.3

ABSTRACT

On review of skid-mounted LNG technology providers, single mixed refrigerant (SMR), ni-trogen expander and self-refrigerated processes have been used for LNG production in skid scale. However, SMR processes are more efficient and have lower rotating equipment. By RIPI comparative study on commercialized SMR processes and more than 100 patents in this topic, the SMR process with one phase separator (by 43% sharing in SMR processes), has been selected for skid LNG plant. Regarding to process complexity of multi-phase separators in SMR loop, these types of cycles were not selected. Otherwise SMR process without phase separator was not selected for skid LNG plant because of the freezing possibility of heavy hydrocarbon refrigerants in this configuration.

Several single-phase separator SMR processes can be used based on arrangement of equipment in liquefaction and refrigeration sections. By extensive study and according to skid design limitations (e.g., the minimum number of fixed and rotating equipment, minimum process complexity and dimension and etc.), two process arrangements has been selected, simulated and optimized. Also, a sensitivity analysis on the feed pressure and temperature as well as the composition of MR and feed was done. Energy consumption of these two configurations was calculated and the complexity of them was compared. According to the results obtained in this study and considering lower total annualized cost of LNG unit and the necessity of pro-cess simplicity in the skid scales, the best case was recommended for LNG skid-mounted packages.

How to cite this article
L. Shirazi, M. Sarmad, P. Moein, R. Hayati, S. Anahid, M. Zare. Skid-mounted SMR Packages for LNG Production: Configuration Selection and Sensitivity Analysis. Journal of Gas Technology. 2021; 6(2): 04 -13. (http://jgt.irangi.org/article_251669.html)

* Corresponding author.
E-mail address: shirazil@ripi.ir (L. Shirazi).

Available online 26 December 2021

1. Introduction

The increasing of LNG production volume in the world supports the significant contribution of growing natural gas demand by developing conventional & unconventional gas sources (Barcly and Shukri, 2007). Gas pipeline and Liquefied natural gas (LNG) are two major options for transferring natural gas from sources to end users. Lower operating cost of gas pipe-line in comparison with LNG is the main reason which it is generally used for transporting natural gas; although it needs high capital investment cost for long distances gas transmission in addition to limitation of gas transfer capacity (Moein et al., 2015).

LNG is natural gas (predominantly methane) that has been cooled down to liquid, at tempera-ture below -161ºC and pressure 101.325 kPa with its volume reduced by a factor of 600. LNG production, storage and safe transfer need costly and high-tech equipment (Cranmore and Stanton, 2000). Liquefied natural gas is considered as efficient, clean and economical energy sources. It is a fuel for the future; because its low NO_x and SO_x emissions combined with reduced CO_2 permanently improve the ecological balance (He et al. 2018). Using LNG for gas transferring from the remote gas resources to consumers has been done (Pfoser et al., 2018). According to IGU World Gas LNG Report in 2018 Edition, the nominal LNG production capacity has been increased up to 359.5 MTPA at the end of 2017.

There are two different LNG production capacities: The first one is base-load liquefaction plants with capacity more than 3.4 MTPA, the second one is small scale liquefaction plants with capacity lower than 1 MTPA per train (Yin et al., 2008). In the last decade, skid mount-ed or containerized LNG plant is suggested to provide a cleaner, abundant fuel source that is ideal for use with stranded gas sources not connected to a network. Small scale LNG plants are developed in recent decades regarding to new applications such as using natural gas in heavy vehicles and utilization of small gas resources (Yin et al., 2008; Kohler et al., 2014). Be-side the environmental and economic benefits of small-scale LNG development in the global supply chain, the capital investment cost per ton of LNG production is more than base-load LNG plants (Nguyen et al., 2016).

Skid mounted LNG plant is the intellectual choice for virtual pipelines, producing a replacea-ble fuel for diesel, high horsepower fuel applications including marine, rail, mining, drilling and other oil industrial fuel applications. The facilities are modular, compact, quick installa-tion, commissioning and running. The other benefits include lower construction costs, im-proved quality and safety, faster project execution, and easily moved and re-deployed in the future if desire. Skid mounted solutions for LNG processing mainly used in pipeline gas, oil-associated gas, flare gas, bio gas and other small scale conventional and unconventional gas sources.

According to the review of more than 20 skid-mounted LNG technology providers, single mixed refrigerant (SMR), nitrogen expander and self-refrigerated processes have been used for liquefaction process of skid scale and Iso-Container type LNG.

These liquefaction processes are different due to their equipment and operation costs and min-imum approach temperature in composite curves (Hatcher et al., 2012). Generally, the opera-tion cost (due to high efficiency) and the number of rotary equipment of SMR processes are lower than N_2-expansion cycles (Moein et al., 2016) and self-refrigerated processes. Process simplicity, single phase and non-toxic refrigerant, against high energy consumption per unit of LNG production and the more number of rotating equipment are the pros and cons of N_2 ex-pander process (Moein et al., 2015). Self-refrigerated processes use a part of inlet feed to liq-uefaction unit (treated gas) as refrigerant for LNG production. Typically, these processes work at high operating pressures (e.g., 250 barg) and they need an auxiliary cooling cycle like

pro-pane or ammonia for LNG production. One advantage of this cycle is using (or even not being used) low volume of pure refrigerant (e.g., propane) in liquefaction cycle and there will be no a lot of supply, storage, leakage and make up problems of refrigerants as a main issue in this process.

Among the mixed refrigerant processes, the single mixed refrigerant process is the simplest one (Cao et al., 2006) with simple multi stage compressors and one main cold box. This pro-cess can be used for all ranges of liquefaction production rates from small scale to base-load (Swenson, 1977). SMR processes can be divided into two categories. The first group process-es contain phase separators to separate the vapor and liquid phases of mixed refrigerant and the second one does not use any separator at mixed refrigerant loop (Venkatarathnam, 2008). The SMR processes with phase separator can be organized into single phase separator to more than four phase separators. Although increasing the number of separators increases process efficiency, but process complexities and foot print also increase (Yin et al., 2008).

The enthalpy of natural gas changes nonlinearly during liquefaction process because of com-plex nature of mixed hydrocarbons. The efficiency and entropy of liquefaction processes can be increased and decreased respectively by decreasing the temperature difference between hot and cold composite curves, in cryogenic heat exchangers. MR cycle requires no additional equipment such as turbo expander for reducing refrigerant temperature (Venkatarathnam, 2008). Also, power consumption in MR processes is very significant, so the optimization method is needed to minimize energy consumption. Some references in the open literature review different methods of MR process optimization. Gong et al. (2000) applied the BOX optimization tool and Wahl et al. (2013) used sequential quadratic programming (SQP) to op-timize the PRICO process. Lee et al. (2002) optimized a multi-stage MR system and mini-mized shaft work requirement by a graphical targeting technique. Aspelund et al. (2010) opti-mized the PRICO process by using of Tabu Search algorithm (TS) and Nelder-Mead Downhill Simplex (NMDS) method. Genetic algorithm used for optimization of SMR process by Cam-marata et al. (2001), Mokarizadeh and Mowla (2010), Taleshbahrami, H. and Saffari, H. (2010), Alabdulkarem et al. (2011), Li et al. (2012), Xu et al. (2013), He and Ju (2014), Moein et al. (2015), Ding et al. (2017) and Abdelhamid et al. (2017). Combination of the genetic algorithm and sequential quadratic programming used by Hwang et al. (2013) for optimizing a DMR LNG process. Particle-swarm paradigm coded in MATLAB connected to UniSim simu-lation software used by Khan and Lee (2013) and Khan et al. (2013) and MATLAB's built-in fmincon solver used by Jacobsen and Skogestad (2013) to optimize a SMR process. Austbo et al. (2014) applied Sequential optimization for SMR LNG process. Ngoc Pham et al. (2016) optimized the modified SMR LNG process using by multivariate Coggin's algorithm com-bined with process knowledge. Ali et al. (2018) optimized energy for SMR LNG process us-ing the metaheuristic vortex search algorithm. Qyyum et al. (2018) applied a hybrid modified coordinate descent (HMCD) algorithm to optimize the SMR LNG process.

Because of the nature of nonlinearity and thermodynamic complexity of the LNG processes, optimization of these processes should be performed by global search methods such as GA, Tabu Search (TS), or Simulated Annealing (SA). Due to the fact that GA does not require derivatives and initial points, it was chosen as the optimization method for the current research.

In this study, SMR process was selected for liquefaction of natural gas due to its more effi-cient; lower operating pressure and lower number of rotary equipment rather than the other refrigeration cycles. By comprehensive study on various SMR configurations in the liquefac-tion and refrigeration section arrangements, concerning skid design limitations (e.g. the mini-mum fixed and rotating equipment, minimum process complexity, minimum dimension

and etc.), two process arrangements has been selected, simulated in Aspen HYSYS and optimized by Genetic Algorithm to minimize required work for LNG production. The sensitivity analysis by feed specification and MR composition changes on the total required work were investi-gated. Energy consumption of these two configurations was calculated and compared with each other to select the best configuration.

2. SINGLE MIXED REFRIGERANT PROCESS CONFIGURATION SELECTION

As mentioned before, single mixed refrigerant processes can be classified into those that use phase separator and those that do not (Venkatarathnam, 2008). The most famous SMR pro-cess without phase separator (in refrigeration loop) is PRICO process by Black & Veatch. As a definition, when we count a phase separator that after separation of liquid and gas phases, each one enters to heat exchanger separately. So, in PRICO process, we do not have any phase separator given the above definition.

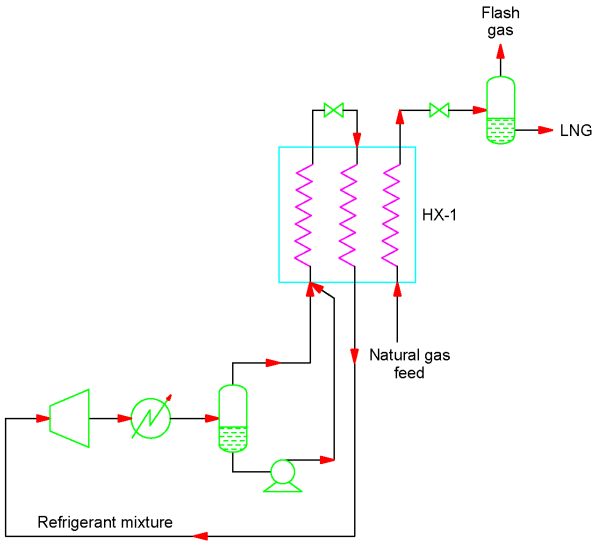

Figure 1. PRICO Liquefaction Process

In the PRICO process freezing possibility of high boilers in the refrigerant can be solved using phase separators that return heavy refrigerant components to the compressor at higher temper-atures, much above the freezing point of the heavy refrigerants (Venkatarathnam, 2008).

The SMR processes with phase separator can be organized into single to five phase separators. This categorization is based on patent analysis and not necessarily all of them in-dustrialized. Depending on different factors such as investment cost, operating costs and pro-cess complexity & flexibility; the optimal number of separators will be determined.

Although increasing the number of separators increases process efficiency, but process com-plexities also increase (Yin et al., 2008).

According to RIPI study on commercialized SMR processes and more than 100 patents in this topic, the order of SMR processes based on their contribution is as follows:

- Without phase separator: 21%
- 1-phase separator: 43%
- 2-phase separators: 23%
- 3-phase separators: 9%
- 4-phase separators: 3%
- 5-phase separators: 1%

Figure 2 shows a typical 1-phase separator SMR loop. In this configuration, the 2-phase mixed refrigerant stream, is separated to liquid and vapour streams PS-1 and enter to the cold box separately. There is no any separator in the flow path of the refrigerant and low-pressure re-frigerant enter to compressor package.

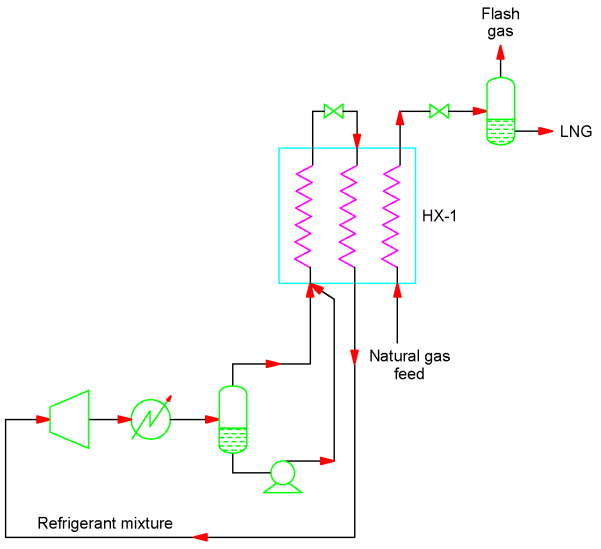

Figure 2. Typical 1-phase separator SMR loop

Figure 3 shows a typical 2-phase separators SMR loop. In this configuration, the 2-phase mixed refrigerant stream, is separated to liquid and vapour streams in PS-1 and enter to the cold box. After pre-cooling the vapour MR, this 2-phase stream is separated in the second phase separator (PS-2).

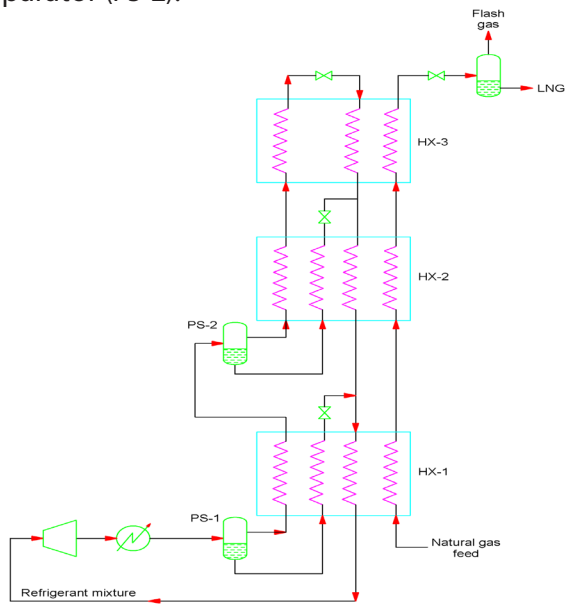

Figure 3. Typical 2-phase separators SMR loop

Figures 4, 5 and 6 show a typical three, four and five phase separators in the flow path of the mixed refrigerant. As seen, by increasing the number of phase separators, the complexity of the refrigerant cycle and cooling stages in cryogenic heat exchanger is greatly increased. Ap-proximately, the cooling stages are equal to the number of phase separator plus one.

Due to the freezing possibility of refrigerant high boilers in the PRICO process, a phase sepa-rator should be considered in the selected process. On the other hand, as shown above, the process complexity of more than 1 phase separator in SMR loop and also the considerations of small foot print in skid design, the SMR process with one phase separator (by 43% sharing in SMR processes) has been selected in this paper. The commercialized liquefaction units by companies such as Linde, Black & Veatch, Air Products and so on, also contains only the 0-phase, 1-phase and 2-phase separators in their refrigeration cycles.

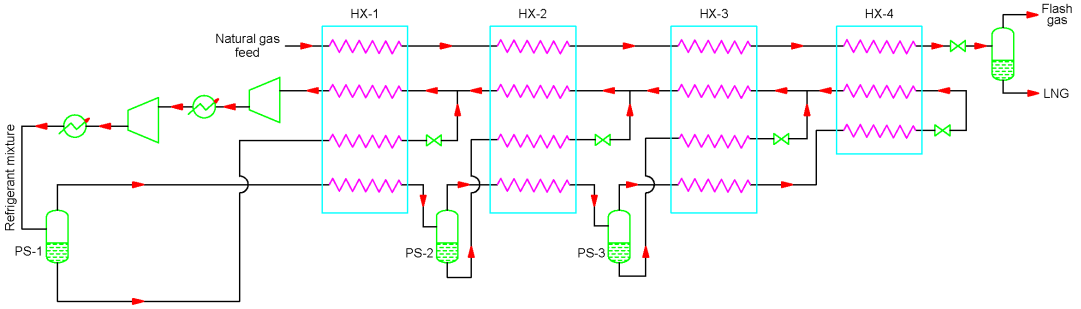

Figure 4. Typical 3-phase separators SMR loop

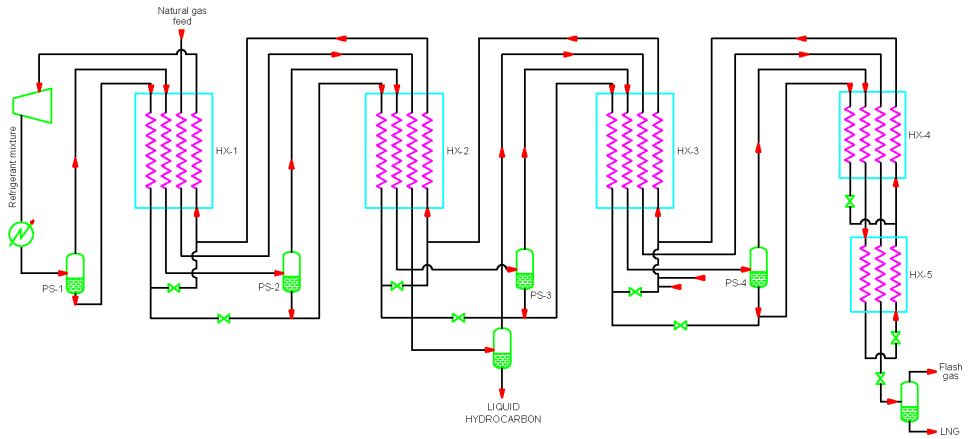

Figure 5. Typical 4-phase separators SMR loop

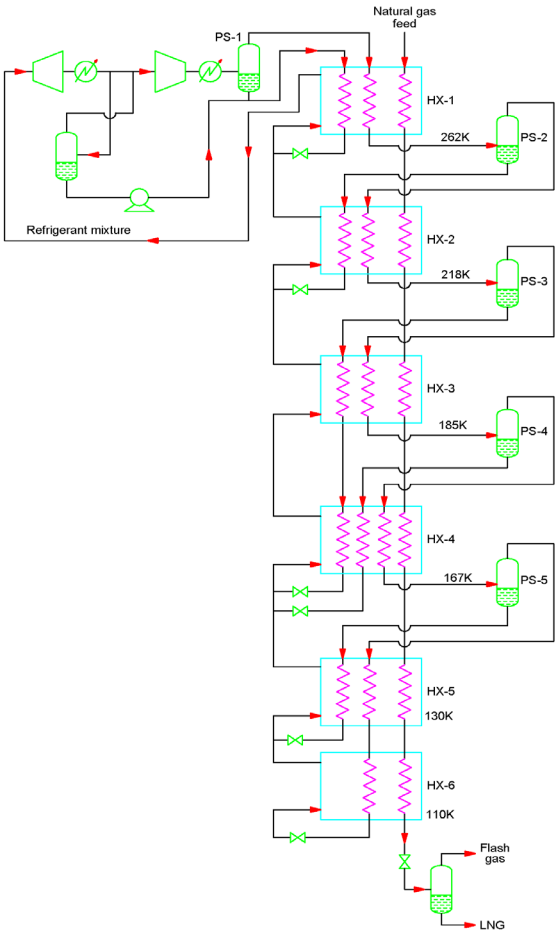

Figure 6. Typical 5-phase separators SMR loop

2.1. SMR PROCESS FOR SKID DESIGN

There are various types of SMR process with single phase separator in refrigeration cycle. These processes are different in the location of phase separator, the number of outlet low pres-sure refrigerant stream from cold box, the configuration of compression section, the presence of pump in compression cycle and etc. According to comprehensive study (simulation, optimi-zation, process analysis and etc.) of these configurations in RIPI and with respect to skid de-sign limitations (e.g., the minimum number of fixed and rotating equipment, minimum number of streams which has exchanged heat in cold box, minimum process complexity and etc.), two process arrangements has been selected (Schmidt, 2009; Heng and Wenhua, 2014).

2.1. SMR PROCESS SIMULATION (TWO CONFIGURATIONS)

According to section 2.1, two SMR process configurations have been selected for liquefaction unit. The flow sheets of these two processes modeled by Aspen HYSYS are shown in Figure 7.

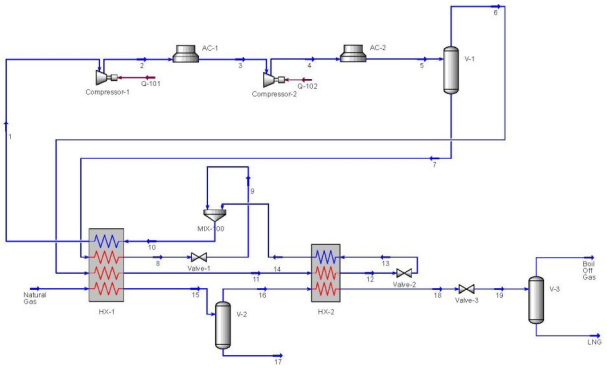

(a)

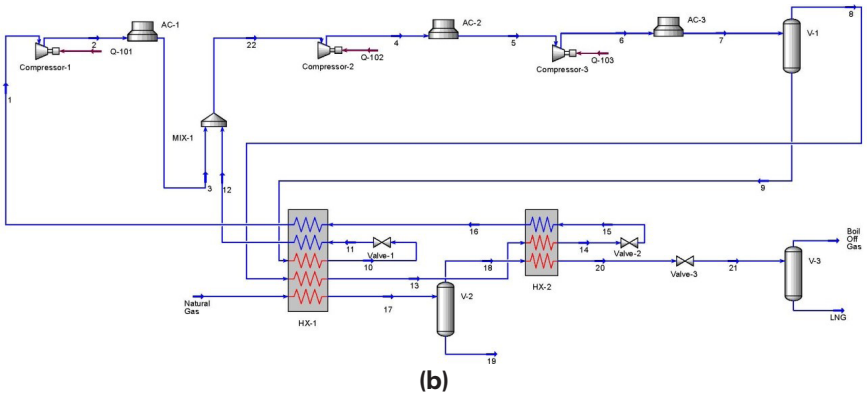

(b)

Figure 7. SMR process simulation of (a) Configuration Case I, (b) Configuration Case II.

As shown in Figure 7 (a), high pressure stream (stream No. 4) after leaving the last stage of the compressor and cooling in air cooler (AC-2), is divided into two phases (liquid and vapor) in a separator (V-1). These two streams enter the first heat exchanger (HX-1) individually and their temperature decreases. The cooled liquid stream passes through a throttling valve (stream No. 9). The cooled vapor phase goes to the second heat exchanger (HX-2) and after cooling, passes through a throttling valve and returns to the heat exchanger as a cold stream and after heat exchanging (stream No. 14), mixed with stream No. 9. The mixed stream enters to the first heat exchanger (HX-1) as a cold stream and after heat exchanging, enters the first stage of compression. In this process, the temperature of natural gas after two steps decreases to about -150 ºC and after throttling valve, LNG is produced at -161 ºC.

In Figure 7 (b), high pressure stream (stream No. 6) after leaving the third stage of the com-pressor and cooling in air cooler (AC-3), is separated into two phases (liquid and vapor) in a separator (V-1). Each of these streams enters to the first heat exchanger (HX-1) separately as hot streams. The cooled liquid stream after passing through a throttling valve returns to the heat exchanger as a cold stream and after heat exchanging (stream No. 12), mixes with steam No.3 and enters the second stage of compression. The cooled vapor phase goes to the second heat exchanger. The exit cold stream after passing through a throttling valve returns to the second heat exchanger (HX-2) as a cold stream and after heat exchanging goes to the first heat exchanger (HX-1). The outlet stream enters the first stage of compression. The tempera-ture of natural gas after two steps decreases to about -150 ºC and after throttling valve, LNG is produced at -161 ºC

Heavy hydrocarbons in natural gas can freeze at cryogenic temperatures in the liquefaction process. So, the amount of C_5^+ hydrocarbons should be decreased to less than 1000 ppmv be-fore LNG production. The separation of heavy hydrocarbons is done by condensation & grav-ity separation in the Heavies Separator (V-2) after pre-cooling of gas (typically @ -30 to -40 ºC) in the cold box. For this project, according to the feed gas composition the proper tem-perature for effective separation of C_5^+ hydrocarbons is -36 ºC based on simulation studies.

In this study, natural Gas (@ 25 ºC and 33 barg) including 86% methane, 5% nitrogen, 4% ethane and 5% C_3^+ has been used for 15 tons per day LNG production.

2.3. OPTIMIZATION PROBLEM

Power consumption in LNG processes is very significant, so the optimization methods are needed for minimizing operation costs. In order to optimize the energy consumption of these two liquefaction processes, GA method was used by connecting MATLAB to Aspen HYSYS process simulator. A MATLAB program code adapted from previous work (Moein et al., 2015; Moein et al., 2016) was developed to use GA optimization procedure on simulated pro-cesses in Aspen HYSYS Simulator. This MATLAB code calls the Aspen HYSYS simulation and transfers the data produced by GA to Aspen HYSYS. In this situation GA method acts as a controller and the Aspen HYSYS model is a server. The total required work of the pro-cess was considered as fitness function of GA method which should be minimized. Aspen HYSYS calculated the value of total required work in each generation and sent back to MATLAB to evaluate the fitness function value. So, there is a continuous linking between MATLAB optimization and HYSYS simulation.

As previously mentioned, the total required work of the process was defined as an objective function of the GA optimization method. The value of this objective function was calculated by Aspen HYSYS process simulator. Therefore, this objective function is a black box that contains an Aspen HYSYS model. The black box cannot provide gradient information or a reliable initial value. On the other hand, because of nonlinear property of mixed refrigerant processes, the objective function has multiple local minimum

points. So, a global search meth-od needless derivative and an initial value is required to prevail these challenges and thermo-dynamic complexity of the process. In this research genetic algorithm as a global search meth-od is used to optimize the SMR processes. GA is a search heuristic that mimics the process of natural evolution, which was invented by Holland (1975) and further developed by his students and colleagues.

2.4. OPTIMIZATION FORMULATION

In this research minimizing of total required work of the process was defined as an objective function of GA method which expressed as:

$$Minimize\ f(X) = \sum W_{Compressors} \quad (1)$$

In the above equation X is an adjusted variable vector including MR molar flow rates of components, the outlet pressure of MR compressor stages and the MR pressure after each throttling valve. Nitrogen, methane, ethane, propane and butane are used as the components of the mixed refrigerant. Other parameters such as natural gas composition and outlet LNG pressure and temperature is fixed during optimization. Thermodynamic properties of MR and NG were calculated by Peng-Robinson equation of state.

In this investigation three constraints were used for optimization of SMR processes. The first one is minimum approach temperature between hot and cold streams in plate-fin heat exchangers which should be greater than 2 ºC to satisfy reliability and feasibility of the process (ALPEMA, 2010). The second one is the temperature of MR in the inlet of each stages of compressor which should be greater than the dew temperature of the fluid in that pressure to prevent formation of liquid in the suction part of the compressors. The third one is pressure of those streams which will be mixed in the mixer that should be in the same pressure. These constraints are formulated as follow:

$$\Delta T_{min.HX-i} \geq 2\ ^{\circ}C$$

$$T_i \geq T_{dew,i}$$

$$P_{i,in} = P_{j,in} \qquad (for\ Mixers)$$

Where $\Delta T_{min.HX-i}$ represents the minimum approach temperature in heat exchanger i, T_i and $T_{dew,i}$ refer to operating temperature and dew point temperature of stream i and $P_{i,in}$ and $P_{j,in}$ illustrate the mixer pressure of inlet streams (i and j).

The last limitation was adjusted in Aspen HYSYS simulator while the first and second constraints are defined as the penalties for the objective function as shown below:

$$Minimize\ P(X.r) = f(x) + r\left(\sum_i [max\{0.g_i(x)\}]^2\right)$$

$$g_1(x) = 2 - \Delta T_{min,HX-i} \quad (2)$$

$$g_2(x) = T_{dew,i} - T_i$$

where r is the penalty factor, assumed here as 10+14. If all the constraints are satisfied, the second term in the right-hand side of Eq. (2) would be zero ($P(X,r) = f(x)$). Otherwise, the second term will be a large value that GA modifies the penalty function in the next generation. The tuning parameters of GA are listed in Table 1.

Table 1. Tuning parameters of GA

Tuning parameter	Value
Population size	300
Selection method	Tournament
Tournament size	4
Mutation method	Adaptive feasible
Crossover fraction	0.8
Crossover function	Two-point
Stopping criteria:	
Maximum number of generations	200
Objective function tolerance	10^{-6}

3. RESULTS AND DISCUSSIONS

The result of optimized cases is shown in Table 2.

Table 2. Result of process optimization

Description	Case I	Case II
MR Pressure (kPa)	3870	3810
MR Flow Rate (kg/h)	5787	5223
MR composition (mole %)	Methane: 32	Methane: 34
	Ethane: 29	Ethane: 27
	Propane: 3	Propane: 2
	Butane: 26	Butane: 28
	Nitrogen: 10	Nitrogen: 9
Net Compression Power (kW)	319	309
Specific Power Consumption (SPC) (kWh/kg LNG)	0.51	0.49

The composite curve of optimized cases is shown in Figure 8 (a) & (b).

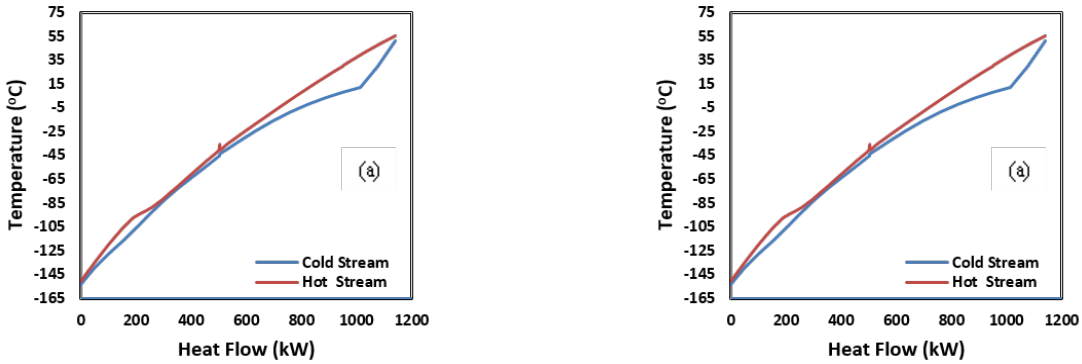

Figure 8. Composite curves of two heat exchangers in the cold box (a) Optimized Case I, (b) Opti-mized Case II

The results show that the "net compression power" of the Case I is only about 3.2% more than the Case II. However, given that the amount of LNG production in skid-mounted projects is low, the energy consumption is not important and the process simplicity has a higher priority. Furthermore, the fixed equipment cost of Case II is more than Case I due to the addition of a compression stage and air cooler in refrigeration cycle. Also, in commercial small scale liquefaction processes such as CB&I (Don Henry Coers & Jackie Wayne Sudduth, 1975) and Linde LIMUM-3 (Dr.-Carl-von, 2018) SMR processes, the mixing of low pressure MR streams has been done similar to process pattern of Case I.

3.1. SENSITIVITY ANALYSIS

Changing some operating parameters can affect the liquefaction process especially minimum approach temperature in PFHE. Some of these parameters are as follows:

1) Feed temperature
2) Feed pressure
3) Feed composition
4) MR composition

Changes in the feed temperature can be eliminated in treatment section or adjusted by chang-ing the amount of refrigerant flow rate. The feed pressure also can be set at inlet facility. However, the effect of unwanted feed gas temperature and pressure changes on minimum approach temperature of LNG heat exchanger is shown for Cases I and II in Figure 9 and Figure 10 in the range of 10 to 35 °C and 30 to 40 barg, respectively.

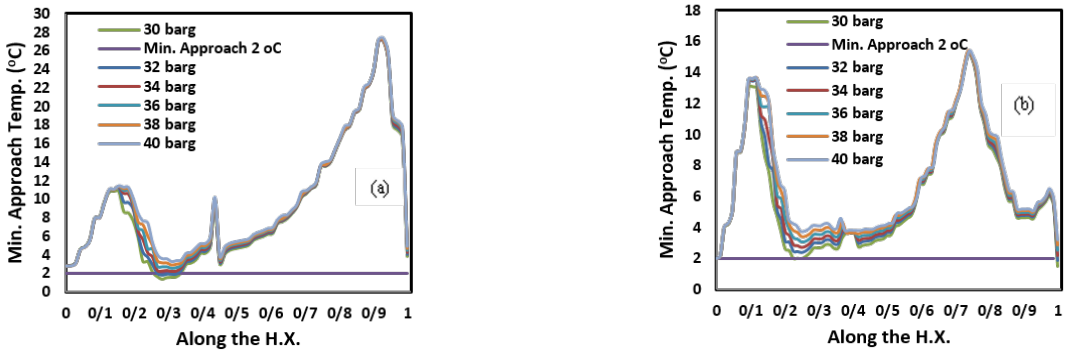

Figure 9. Effect of Feed Pressure on Min. Approach Temp. of (a) Case I, (b) Case II.

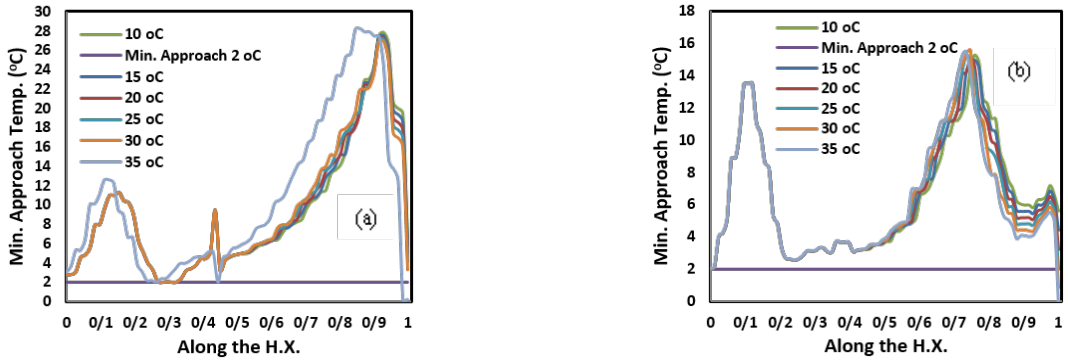

Figure 10. Effect of Feed Temp. on Min. Approach Temp. of (a) Case I, (b) Case II

As shown in Figure 9 (a), in Case I, by changing the pressure in the range of 30 to 40 barg, minimum approach temperature is less than 2 °C at feed pressure between 30 to 33 barg. So Case I is sensitive to changes in feed pressure. But in Case II, by changing the pressure in the range of 30 to 40 barg, minimum approach temperature in all pressures, is equal or higher than 2. Therefore, Case II is not sensitive to changes in feed pressure.

Also, as shown in Figure 10 (b), Case II is more sensible to feed temperature changes, due to decrease the minimum approach temperature less than 2 °C in the hot section of heat exchang-er.

Due to the different sources of gas supply in Iran, one of the most likely changes in specification of feed is the change in composition over the year. The effect of feed composition changes (methane content from 90% to 93%) on. minimum approach temperature of LNG heat ex-changer is shown in Figure 11 for Cases I and II.

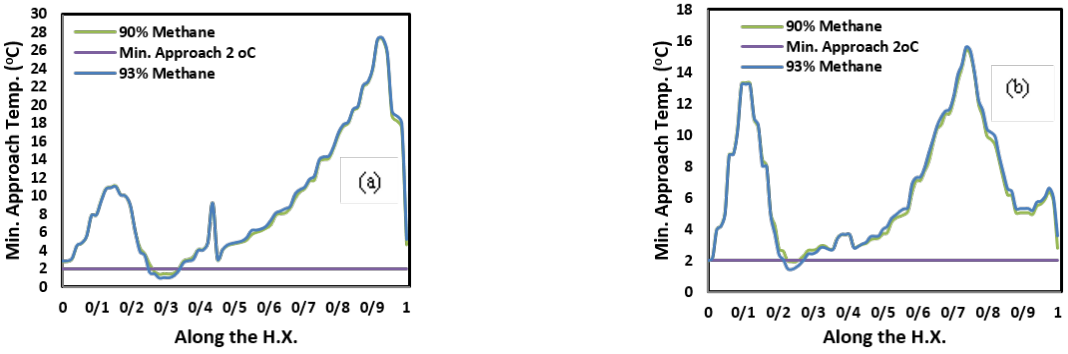

Figure 11. Effect of Feed Composition on Min. Approach Temp. of (a) Case I, (b) Case II

The initial mole fraction of methane in the feed gas is considered 86%. The variation range of methane content is considered from 86 to 93% mole according to maximum methane content in Iran gas pipelines. In Case I, by changing the concentration of methane in the mentioned range, minimum approach temperature is less than 2 ºC which indicates the sensitivity of this case to changes of methane content. In Case II by, changing the concentration of methane up to 90%, minimum approach temperature is equal or higher than 2 ºC and above 90%, minimum approach temperature is less than 2 ºC. So, Case I is more sensible to feed composition chang-es.

Due to leakage probability in the MR compressor, there is the possibility of changing the com-position of refrigerant during operation. This variation can be eliminated by make-up system to control MR composition. However, the effect of unwanted MR composition changes on min-imum approach temperature of LNG heat exchanger is shown in Figure 12, 13, 14, 15 and 16 for Cases I and II.

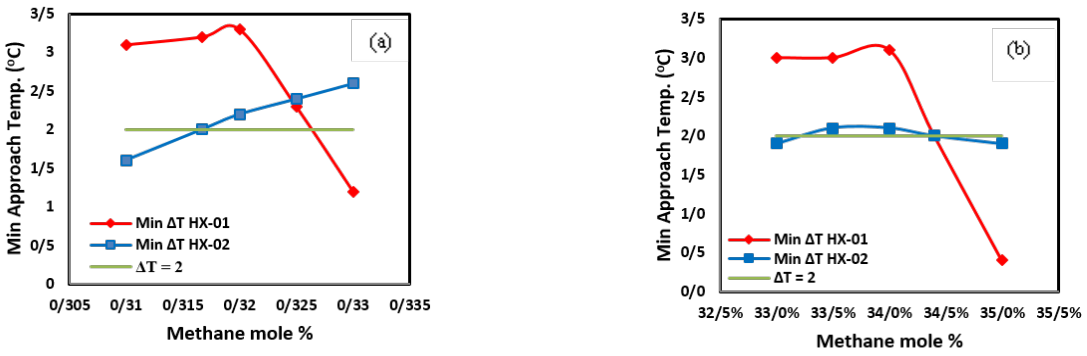

Figure 12. Min. Approach Temp. Sensitivity vs. Methane mole% of (a) Case I, (b) Case II.

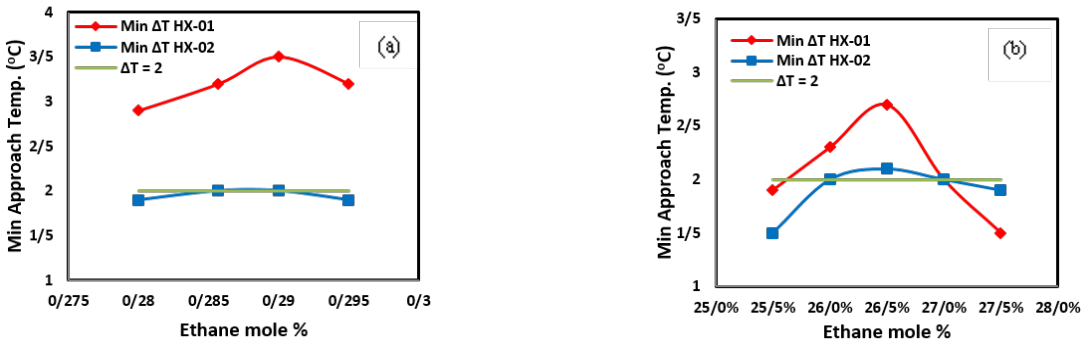

Figure 13. Min. Approach Temp. Sensitivity vs. Ethane mole% of (a) Case I, (b) Case II.

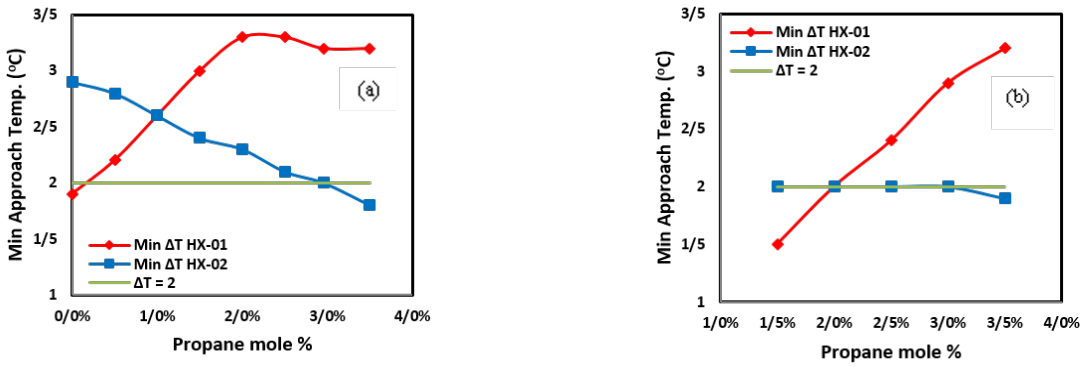

Figure 14. Min. Approach Temp. Sensitivity vs. Propane mole% of (a) Case I, (b) Case II.

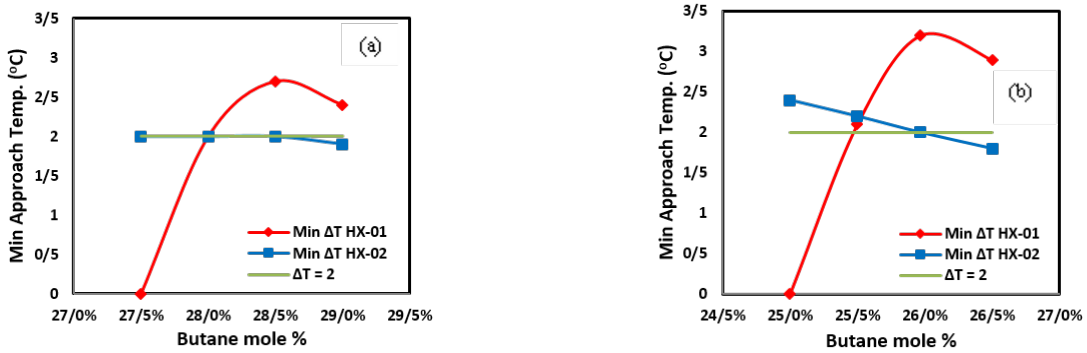

Figure 15. Min. Approach Temp. Sensitivity vs. Butane mole% of (a) Case I, (b) Case II.

Changes in the feed temperature can be eliminated in treatment section or adjusted by chang-ing the amount of refrigerant flow rate. The feed pressure also can be set at inlet facility. However, the effect of unwanted feed gas temperature and pressure changes on minimum approach temperature of LNG heat exchanger is shown for Cases I and II in Figure 9 and Figure 10 in the range of 10 to 35 oC and 30 to 40 barg, respectively.

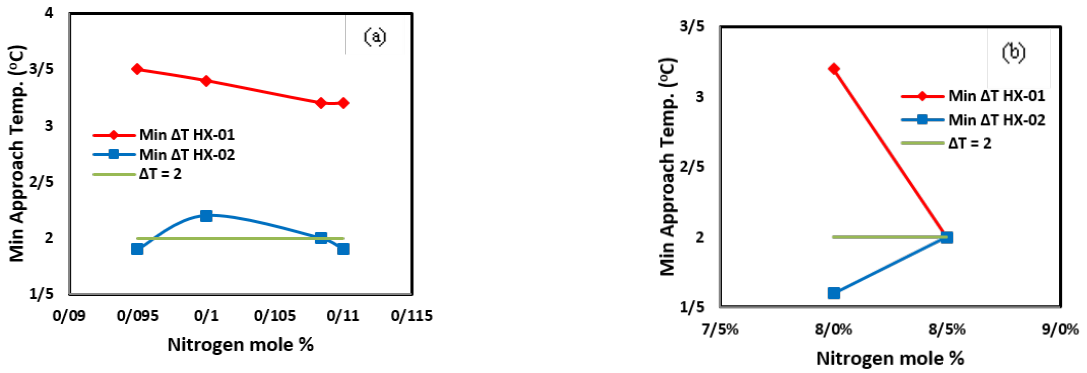

Figure 16. Min. Approach Temp. Sensitivity vs. Nitrogen mole% of (a) Case I, (b) Case II.

The results of MR sensitivity analysis is shown in Table 3. According to this table and Figures 12-16, Case II is more sensible to MR composition due to limited range of allowable changes in propane and nitrogen mole percent.

Table 3: MR composition Sensitivity

MR Component	Case I (mole %)	Case II (mole %)
Methane	31.0-33.0 (31.7)	33.0-35.0 (34.4)
Ethane	28.0-29.5 (28.6)	25.5-27.5 (27.0)
Propane	0.0-3.5 (3.0)	1.5-3.5 (2.0)
Butane	25.0-26.5 (26.0)	27.5-29.0 (28.0)
Nitrogen	9.5-11.0 (10.8)	8.0-8.5 (8.5)

The results of above sensitivity analysis are as follows:

- Case I is more sensible to feed pressure and composition changes
- Case II is more sensible to feed temperature and MR composition changes
- Propane content of MR fluid can be decreased to zero and 1% in Case I and II, re-spectively.

The comparison of two scenarios (Case I and II) shows that:

1) Energy consumption of Case I is slightly more than the Case II
2) Case II is more complicated than the Case I

According to above results, sensitivity analysis, and the small production rate of LNG in this project, the process simplicity is preferred to energy efficiency and the recommended process configuration is Case I.

4. ECONOMIC ANALYSIS

The preliminary cost estimation has been done for Case I and Case II. The equations which have been used for costs of purchased equipment are shown in table 4. The operating cost is calculated and compared by multiplying the power consumption (kW) of the compressors by working hours of a year by 3 cents per kWh as the electricity expense in Iran.

The cost data available from different sources are related to the past years and thus modification factors from Chemical Engineering Cost Index are used to update the costs of the reference year according to the following equation (Peters et al. 2003):

$$Cost_{reference\ year} = Cost_{original} \times \frac{Cost\ index_{reference\ year}}{Cost\ index_{original\ year}}$$

The comparison of economic results show that the purchased cost estimated for Case I is about 1,428,000 U$ whilst the purchased cost of Case II is estimated 1,716,000 U$. Also, the annual electricity cost for Case I & Case II is 66,000 U$ and 64,000 U$, respectively. i.e., the purchased cost for the Case II is 16.8% higher than the Case I. However, the electricity cost of for Case I is 3.1 % higher than the Case II.

Also, the total annualized cost of Case I & Case II is estimated by using of following equation (Towler et al., 2013):

$$Total\ Annualized\ Cost\ (TAC) = Capital\ cost \times \frac{i\ (i+1)^n}{(i+1)^{n-1}} + Operation\ cost$$

$$i = Discount\ Rate\ (8\%)$$

$$n = Plant\ Lifetime\ (20\ year)$$

The comparison of results show that the total annualized cost estimated for Case I is about 212,000 U$ whilst the total annualized cost of Case II is estimated 239,000 U$. So, the total annualized cost for Case II is 11.4% higher than the Case I.

Table 4. Purchased Cost of Equipment

Component	Purchased equipment cost expression
Plate fin heat exchanger	$C_{HX}=A_f \times \{C_a+C_b A_t^c\}$ (Sanaye et al., 2019, Mishra et al., 2004) C_{HX} : Heat exchanger cost ($) A_t : Heat transfer surface C_a = 30000 C_b = 750 A_f = 0.322 c = 0.8
Two-phase separator	$log_{10} C^{spe} = k_1 + k_2 \log_{10} V + k_3 [\log_{10} V]^2$ (Turton et al., 2008) C_{spe}: Separator cost ($) V : Separator volume ($m^3$) k_1 = 3.4974 k_2 = 0.4485 k_3 = 0.074
Compressor	$C = a + bs^n$ (Towler et al., 2013) C : Cost of compressor ($) a = 580,000 b = 20,000 n = 0.6 s = Power of compressor (kW)
Cooler	$C_C=1.218k(1 + f_d + f_p)Q^{0.86}$ (Couper et al., 2005, Ghorbani et al., 2017) C_C : Cost of cooler (k$) Q : Duty (MBTU/h) k : Tube material f_d : Design type f_p : Design pressure

Abbreviations

GA	Genetic Algorithm
LNG	Liquefied Natural Gas
MR	Mixed Refrigerant
NG	Natural Gas
MRC	Mixed-Refrigerant Cycles
SMR	Single Mixed Refrigerant
TS	Tabu Search
NMDS	Nelder-Mead Downhill Simplex
SA	Simulated Annealing

5. CONCLUSION

Single mixed refrigerant process was studied in skid LNG technology. Because of process complexity of more than 1 phase separator in SMR loop, these types of processes are not suitable for skid-mounted packages. On the other hand, freezing possibility of heavy hydrocarbons content of refrigerant in the SMR process without phase separator and also the consideration of small foot print of these processes in skid-mounted packages, one phase separator SMR process has been selected for this design. With respect to skid design limitations (e.g. the minimum fixed and rotating equipment, minimum process complexity, minimum dimension and etc.), two process arrangements has been selected, simulated and optimized by coupling of Aspen HYSYS as the process simulator and MATLAB as the optimizing software. GA optimization method was chosen in order to make sure a global optimum condition would be reached. Key parameters were optimized and the unit energy consumption was minimized as an objective function. Also, the effect of pressure, temperature and composition of feed and MR composition changes on the process performance (minimum approach temperature of LNG heat exchangers) was investigated. The results showed that case I is more sensible to feed pressure and feed gas composition changes. Case II is more sensible to feed temperature and MR composition changes. Energy consumption of case I is slightly more than Case II. According to optimization results, sensitivity analysis, total annualized cost estimation & small production rate of LNG, the recommended process configuration is Case I.

Acknowledgements

We gratefully acknowledge the support of Research & Technology Directorate of National Iranian Gas Company.

References

Abdelhamid, M.I., Ghallab, A.O., Ettouney, R.S., El-Rifai, M.A., 2017. Genetic Algorithm Optimization of a Small-Scale Natural Gas Liquefaction Process, International Journal of Chemical and Molecular Engineering, 11 (8), 574-578.

Alabdulkarem, A., Mortazavi, A., Hwang, Y., Radermacher, R., Rogers, P., 2011. Optimization of propane pre-cooled mixed refrigerant LNG plant, Applied Thermal Engineering, 31(6-7), 1091-1098.

Ali, W., Qyyum, M.A., Qadeer, K., Lee, M., 2018. Energy optimization for single mixed refrigerant natural gas liquefaction process using the metaheuristic vortex search algorithm, Applied Thermal Engineering, 129, 782-791.

The Brazed Aluminium Plate-Fin Heat Exchanger Manufacturers' Association (ALPEMA), Third Edition, 2010.

Aspelund, A., Gundersen, T., Myklebust, J., Nowak, M.P., Tomasgard, A., 2010. An optimization-simulation model for a simple LNG process, Comput Chem Eng, 34(10), 1606-1617.

Austbo, B., Lovseth, S.W., Gundersen, T., 2014. Annotated bibliography-Use of optimization in LNG process design and operation, Comput Chem Eng, 71, 391-414.

Barcly, M., Shukri, T., 2007. Enhanced Single Mixed Refrigerant Process For Stranded Gas Liquefaction, 15th International Conference & Exhibition on Liquefied Natural Gas (LNG 15). Barcelona, Spain, April 24-27.

Cammarata, G., Fichera, A., Guglielmino, D., 2001.

Optimization of a liquefaction plant using genetic algorithms, Appl Energy, 68(1), 19-29.

Cao, W., Lu, X., Lin, W., Gu, A., 2006. Parameter comparison of two small-scale natural gas liquefaction processes in skid-mounted packages, Applied Thermal Engineering, 26(8), 898-904.

Chemical Engineering Plant Cost Index (CEPCI), Chem. Eng., 2017.

Couper JR, Penney WR, Fair JR, Walas SM. Costs of individual equipment. Chem Process Equip 2005:663-9.

Cranmore, R.G., Stanton, E., 2000. Natural gas In: Dawe RA. (Editor), Modern petroleum technology, Volume 1, Upstream. Chichester: Institute of Petroleum (IP), John Wiley and Sons Ltd, 337-380.

Ding, H., Sun, H., Sun, Sh., Chen, Ch., 2017. Analysis and optimisation of a mixed fluid cas-cade (MFC) process. Cryogenics, 83:35-49.

Dr.-Carl-von, 2018. LNG Technology, Optimised solutions for small to world scale plants.

Ghorbani B, Hamedi MH, Amidpour M, Shirmohammadi R., 2017. Implementing absorption refrigeration cycle in lieu of DMR and C3MR cycles in the integrated NGL, LNG and NRU unit. Int J Refrig, 77:20-38.

Gong, M.Q., Wu, J.F., Luo, E.C., Zhou, Y., Liang, J.T., Zhang, L., 2000. Optimum composi-tion calculation for multicomponent cryogenic mixture used in J-T refrigerators. Adv Cryo Eng, 45, 283-290.

Hatcher, P., Khalilpour, R., Abbas, A., 2012. Optimization of LNG mixed-refrigerant processes considering operation and design objectives. Comput. Chem. Eng, 41, 123-133.

He, T., Ju, Y., 2014. Design and Optimization of a Novel Mixed Refrigerant Cycle Integrated with NGL Recovery Process for Small-Scale LNG Plant. Ind Eng Chem Res, 53 (13), 5545-5553.

He, T., Karimi, I.A., Ju, Y., 2018. Review on the design and optimization of natural gas liquefaction processes for onshore and offshore applications. Chemical Engineering Research and Design, 132, 89-114.

Heng, S., Wenhua, M., 2014. Two-section type single loop mixed refrigerant natural gas liquefaction process and device. CN102492505A.

Henry Coers, D., Wayne Sudduth, J., 1975. Refrigerant apparatus and process using multi-component refrigerant. US3932154A.

Holland, J.H., 1975. Adaption in Natural and Artificial Systems. first edition. MIT Press, Boston, 1975.

Hwang, J.H., Ku, N.K., Roh, M.I., Lee, K.Y., 2013. Optimal design of liquefaction cycles of liquefied natural gas floating, production, storage, and offloading unit considering optimal synthesis. Ind Eng Chem Res, 52(15), 5341-5356.

Jacobsen, M.G., Skogestad, S., 2013. Active constraint regions for a natural gas liquefaction process. J Nat Gas Sci Eng, 10, 8-13.

Khan, M.S., Lee, M., 2013. Design optimization of single mixed refrigerant natural gas liquefaction process using the particle swarm paradigm with nonlinear constraints. Energy, 49, 146-155.

Khan, M.S., Lee, S., Rangaiah, G.P., Lee, M., 2013. Knowledge based decision making method for the selection of mixed refrigerant systems for energy efficient LNG processes. Appl Energy, 111, 1018-1031.

Kohler, T., Bruentrup, M., Key, R.D., Edvardsson, T., 2014. Choose the best refrigeration technology for small-scale LNG Production. Hydrocarbon Processing, 45-52.

Lee, G.C., Smith, R., Zhu, X.X., 2002. Optimal synthesis of mixed-refrigerant systems for low temperature process. Ind Eng Chem Res, 41(20), 5016-5028.

Li, Y., Wang, X., Ding, Y., 2012. An optimal design methodology for large-scale gas lique-faction. Appl Energy, 99, 484-490.

Mishra M, Das PK, Sarangi SK., 2004, Optimum design of crossflow plate-fin heat exchang-

ers through genetic algorithm. International Journal of Heat Exchangers. 5, Iss 2, 379-401.

Moein, P., Sarmad, M., Khakpour, M., Delaram, H., 2016. Methane addition effect on a dual nitrogen expander refrigeration cycle for LNG production. J Natural Gas Sci and Eng, 33, 1-7.

Moein, P., Sarmad, M., Ebrahimi, H., Zare, M., Pakseresht, S., Zandieh Vakili, Sh., 2015. APCI-LNG single mixed refrigerant process for natural gas liquefaction cycle: Analysis and optimization. J Natural Gas Sci and Eng, 26, 470-479.

Mokarizadeh Haghighi Shirazi, M., Mowla, D., 2010. Energy optimization for liquefaction process of natural gas in peak shaving plant. Energy, 35, 2878-2885.

Ngoc Phama, T., Shariq Khan, M., Quang Minh, L., Amalia Husmil, Y., Bahadori, A., Lee, S., Lee, M., 2016. Optimization of modified single mixed refrigerant process of natural gas liquefaction using multivariate Coggin's algorithm combined with process knowledge. J Natural Gas Sci and Eng, 33, 731-741.

Nguyen, T.V., Damgaard Rothuizen, E., Brian E, Bruun A.H., 2016. Techno-economic optimization of three gas liquefaction processes for small-scale applications Proceedings of Ecos- The 29th International Conference on Efficiency, Cost, Optimization, Simulation and Envi-ronmental Impact of Energy Systems. June 19-23, Portorož, Slovenia.

Peters MS, Timmerhaus KD, West RE., 2003, Plant design and economics for chemical engi-neers. vol. 4. McGraw-Hill New York.

Pfoser, S., Schauer, O., Cost, Y., 2018. Acceptance of LNG as an alternative fuel: Determi-nants and policy implications. Energy Policy, 120, 259-267.

Qyyum, M.A., Long, N.V.D., Minh, L.Q., Lee, M., 2018. Design optimization of single mixed refrigerant LNG process using a hybrid modified coordinate descent algorithm. Cryogenics, 89, 131-140.

Sanaye S, Shams Ghoreishi SM., 2019, Energy, exergy and economic analyses of two modified and optimized small-scale natural gas liquefaction (LNG) cycles using N2 and N_2/CH_4 refrigerants with CO_2 precooling. Cryogenics (Guildf), 102:66-76.

Schmidt, H., 2009. Method for liquefaction of a stream rich in hydrocarbons. US20090205366A1.

Swenson, L.K., 1977. Single Mixed Refrigerant, Closed Loop Process for Liquefying Natural Gas. US Patent 4,033,735.

Taleshbahrami, H., Saffari, H., 2010. Optimization of the C3MR cycle with genetic algorithm. Transactions of the Canadian Society for Mechanical Engineering, 34 (3-4), 433-448.

Towler G. & Sinnott R., 2013, Chemical Engineering Design Principles, Practice and Econom-ics of Plant and Process Design. 320-325 & 412.

Turton R, Bailie RC, Whiting WB, Shaeiwitz JA., 2008, Analysis, synthesis and design of chemical processes. Pearson Education.

Venkatarathnam, G., 2008. Cryogenic Mixed Refrigerant Processes. New York, Springer, 151.

Wahl, P.E., Løvseth, S.W., Mølnvik, M.J., 2013. Optimization of a simple LNG process using sequential quadratic programming. Computers & Chem Eng, 56, 27- 36.

Xu, X., Liu, J., Jiang, C., Cao, L., 2013. The correlation between mixed refrigerant composi-tion and ambient conditions in the PRICO LNG process. Appl Energy, 102, 1127-1136.

Yin, Q.S., Li, H.Y., Fan, Q.H., Jia, L.X., 2008. Economic Analysis of Mixed-Refrigerant Cy-cle and Nitrogen Expander Cycle in Small Scale Natural Gas Liquefier. AIP Conference Pro-ceedings 985, 1159-1165.

JOURNAL OF GAS TECHNOLOGY

Volume 6 / Issue 2 / Winter 2021 / Pages 20-27

Journal Homepage: http://jgt.irangi.org

Heat Transfer Rate Enhancement in CGS Heaters Using a Tube Insert

Behnam Ranjbar[1], Faezeh mohammadi[1], Masoud Rahimi[2*],behzad khosravi[3], Nader Abbasi[3]

1. Department of Chemical Engineering, Kermanshah Branch, Islamic Azad University, Kermanshah, Iran
2. Department of Chemical Engineering, Razi University, Kermanshah, Iran
3. Iranian national gas company, Kurdistan province, Sanandaj, Iran

ARTICLE INFO

ORIGINAL RESEARCH ARTICLE

Article History:
Received: 21 Juen 2021
Revised: 08 August 2021
Accepted: 05 October 2021

Keywords:
Tube Insert
Pressure Reducing Station
Heater
Regulator
CGS

ABSTRACT

In this study, in order to increase the heat transfer rate in the heaters of the City Gas Station(CGS), a classic type of a tube insert was placed into its heating coils. The use of the inserts will lead to increase in the pressure drop that maybe treated as disadvantage of using inserts in some heat exchangers. However, in this case pressure drop is quite favor phenomenon as pressure should be reduced in city gas transfer line. The type of the given insert is spiral, and is made of seamless steel in accordance with the gas pipe production standard. The inserts are embedded in eight coil paths in the heater of Mavian pressure reducing station of in Kamyaran city of Kurdistan Province with capacity of 2500 m^3/h. Heat transfer enhancement up to 47% obtained, which is quite important from energy saving and environmental pollution control point of view.

DOR: 20.1001.1.25885596.2021.7.2.2.4

How to cite this article
B. Ranjbar, F. mohammadi, M. Rahimi, B. khosravi, N. Abbasi. Heat Transfer Rate Enhancement in CGS Heaters Using a Tube Insert. Journal of Gas Technology. 2021; 6(2): 20 -27. (http://jgt.irangi.org/article_251675.html)

* Corresponding author.
E-mail address: masoudrahimi@yahoo.com (M. Rahimi)

Available online 26 December 2021

1. Introduction

Pressure reducing stations are located at the entrance to cities to reduce the high pressure of gas that flows from refineries to consumption points. This decrease in pressure is associated with a decrease in the gas temperature due to the Joule-Thomson coefficient, which, in turn, involves numerous problems such as freezing of the water and the blockage of the transmission line. In order to prevent such problems, the temperature of the gas should be increased before the pressure decreases in the station. Nowadays this temperature rise is achieved by thermal heaters using natural gas. A heaters used in the gas stations is a type of heaters in which the gas is placed inside a tube series and hot water around the pipes in a uniformly homogeneous surface with a balanced temperature. In fact, firstly, the water is heated indirectly and the water transmits this heat to the flowing gas. Hence, these heaters are also called as indirect heaters. One of the main problems with the use of this kind of heaters is the high fuel consumption, which in most cases is natural gas, so due to the low efficiency of this type of heaters, finding solutions to increase their efficiency has always been considered.

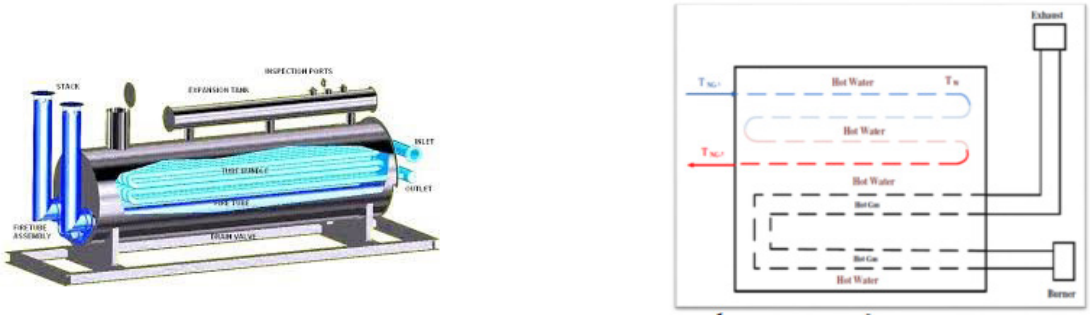

a) A general view (Farzaneh-Gord et al., 2006) **b) heating mechanism**

Figure 1. A conventional CGS gas heater layout

In a CGS gas heater, the burning of natural gas in the torch generates hot gases, and these gases cause to product the warm water due to passage from the heater. Natural gas flows from one side of the pipe and is surrounded by warm water inside the heater. This tube circulates inside the heater in several steps, and finally the temperature of the gas within it will be extremely desirable. A scheme of a classical heater which is called "linear heater" is shown in the Fig 1.

In the process of reducing pressure in constant volume, any reduction in pressure will lead to the decrease in temperature. Therefore, in gas pressure reduction systems, we will always be faced with a decrease in gas temperature. Therefore, in the gas pressure reduction systems, we will always be faced with a decrease in gas temperature. As a result, when the temperature of the gas approaches the dew point of the gas, the steam of the liquids associated with the gas, such as water and heavier hydrocarbons, is converted to liquid and at low ambient temperature at the facility causing frostbite. Since the gas temperature entering to station is 15 degrees, this pressure drop causes condensation and crystallization. This reduction in pressure causes the condensation and formation of crystals in the path and equipment of the station and ultimately reduces the life of the equipment and damage to the station. As a result, adding a heater unit in the station is essential and inevitable (Cullender, 1955).

One of the main problems with using this kind of heaters is the high fuel consumption, which is usually natural gas. Since the efficiency of this kind of heaters is low, finding solutions to increase their efficiency has always been considered. In this regard, many studies have

been done to optimize energy consumption and, consequently, reduce fuels consumption of the heaters.

Heat transfer and friction coefficient of circular spiral- shaped tube with different torsion ratios were investigated by Pathipakka and Sivashanmugam (Pathipakka and Sivashanmugam, 2010) in two complete conditions of these components and short length with regular intervals. They found that these components could be used in a short length, like full length, to increase the heat rate, and only a small amount of pressure drop would increase.

Bhuiya et al. (2013) carried out a lot of laboratory studies on the use of pipes equipped with double spiral with different angles and concluded that the Nussselt number and the friction coefficient increase by decreasing the helical angle in the same conditions. Sarma et al. (2005) have also presented a series of equations for predicting friction coefficients and heat transfer coefficients in tubes equipped with twisted tapes for a wide range of Reynolds and Prandtl Numbers. There is a good agreement between laboratory data and the presented equations.

In a study, the effects of twisted tape insert with square-shaped wings containing several holes in the fluid flow and heat transfer in heat exchangers were investigated by Suri et al. (2017). Hence, under the same operating conditions in exchangers having tube insert with square-shaped wings and numerous holes, the thermal performance coefficient was higher than that of a tube insert without wing.

Rahimi et al. (2009) showed that among the various types of twist strips, including the classic twisted tape, perforated twisted tape, notched twisted tape, Jagged twisted tape; Nusselt number, and thermal performance coefficient for this serrated insert is more than other cases. Thianpong et al. (2012) studied the effects of a simple spiral tape in the tube with a fixed heat flux in a laboratory and indicated that by decreasing the twist ratio of the tape, heat transfer and pressure drop are increased. The effect of twisted tapes in the form of the regular and quadruple arrangement in thermal exchangers was examined by Samruaisin et al. (2018.) In the mode in which tapes were placed in the form of the regular and quadruple strips, the heat transfer rate and the coefficient of friction were less than that mode in which the tapes had occupied the entire space of the tube in the form of the quadruple.

2. The studied heater characteristics

The capacity of the aforementioned heater is 3000 standard cubic meter per hour (SCMH) which was built by Aria Petro Jam Company in 2008. The inside of the heater chamber is consists of the mixture of the distilled water and antifreeze, in which 8 coil paths with a diameter of 2 inches pass through the mixture. The thickness of each coil is 5 mm and the weight of each coil is considered to be 200 kg. Due to the fact that the work pressure of the heater is PSI 1050, high pressure equipment should be used. In order to prevent heat loss in the outlet of the heater, the outlet should be insulated. If the shell is full of distilled water, it's weight is 5000 kg and if shell is empty, it's weight is 1000 kg. It is obvious that the temperature increases due to increasing the capacity of the heater. To increase the temperature of the mixture inside heater chamber, the warming pan is used, which it's feed is supplied from the outlet gas of the station with a diameter of 1 inches. The amount of this feed is very significant therefore, before entering the feed into the heater, a turbine meter is installed on the heater for measuring the consumption of this energy.

Figure 2. A real photograph of heating coil

Figure3. A real photograph of station's warming pan

3. Tube insert implementation

In the construction of the station's heater mentioned above, the coil pipes with a diameter of 2 inches have been used. Due to the fact that the length of the coil is 170 cm, it should use an insert that covers enough the pipe surface. Considering the above, the dimensions of these inserts were selected according to the figure below, as the length of these tube inserts is 160 cm and their steps and the diameters for given tubes are 4 cm.

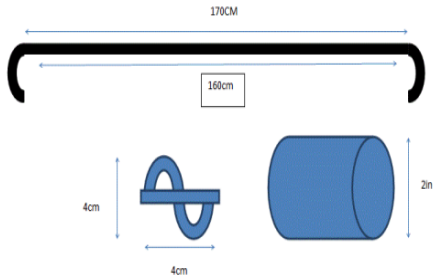

Figure 4. the geometry of the employed insert

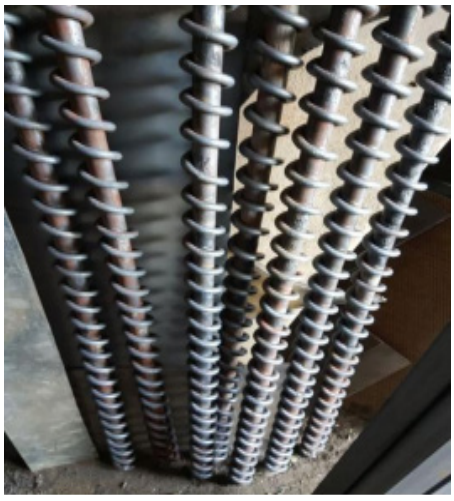

Figure 5. A real photograph of the inserts

3.1. Destruction test

The corrosion parameter is a necessary factor that should be measured during the process. As far as using an insert in tube cause a rotational fluid motion on the lateral tube wall, it can cause erosion corrosion For this purpose, before the test, the thickness is measured by the thickness gauge device. and then after the installation of the insert, the intended number is re-measured, which is considered as the difference of the corrosion criterion. The device is based on the Multigauge 5700 Datalogger model of the Trichtex company in the United Kingdom. This works on ultrasonic wave transmission. A transmitted ultrasound pulse travels though both the coating and the metal and reflects from the back wall. The returned echo then reverberates within the metal, with only a small portion of the echo travelling back through the coating each time. The timing between the small echoes gives us the timing of the echoes within the metal, which relate to the metal thickness.

3.2. Test procedure

At the first stage, necessary tests are carried out for heaters in which the insert has not been used, and the results related to the parameters of temperature, pressure and consumable flow rate are be measured and then the structure of the desired inserts are used. Finally, the results are compared. The measuring points are illustrated in Fig.6.

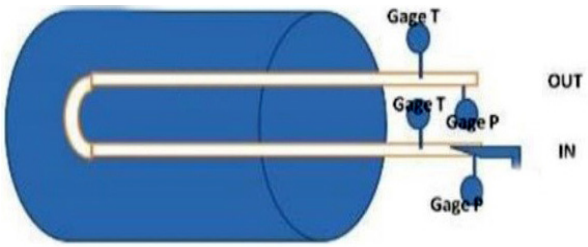

Figure 6. the schematic of how to measure the parameters

In the measurement, before installation of the insert, the input and output data related to temperature and pressure were recorded. The average time interval for each test is

approximately one hour in order to reach to steady state condition. The pressure and temperature values measured at different water temperatures of 35, 40, 45, 50, 55 and 60 ºC. Also, in order to obtain more accurate results, and calculating fluid properties including viscosity, density, and thermal conductivity of fluid, as well as specific heat, the average fluid temperature was used.

3.3 Measurement results

According to the heater temperature setting, the results of inlet and outlet temperatures as well as measured pressure drop are listed in Table 1.

Table 1. Range of parameters

Heater temp (ºC)		Ti (ºC)	To (ºC)	ΔP(bar)
35	Without insert	19	36	0.15
	With insert	13	38	0.47
40	Without insert	20	41	0.13
	With insert	17	44	0.51
45	Without insert	21	45	0.1
	With insert	19	49	0.40
50	Without insert	20	47	0.1
	With insert	21	53	0.38
55	Without insert	22	49	0.09
	With insert	23	54	0.37
60	Without insert	25	50	0.88
	With insert	26	53	0.34

3.4. Data Reduction

to use laboratory results optimally, the measured data is reducible as follows: in the first step, the heat transforming rate is calculated as below (Shabanian et al., 2011):

$$Q = mC_p\,(T_0 - T_i) \quad (1)$$

On the other hand, the amount of heat transfer which conveys from the fluids to the ambient condition is calculated as below

$$Q = hA\,(\widetilde{T_W} - T_b) \quad (2)$$

$\widetilde{T_W}$ indicates the pipes' surface temperature and in under study industrial sample, is a water temperature of the heater and T_b indicates the fluids mass temperature, which is obtained from the following relationship:

$$T_0 = (T_i + T_0)/2 \quad (3)$$

The equation to calculate the average heat transfer rate and NASLET is as follows

$$h = mc_p(T_0 - T_i) / A(\widetilde{T_W} - T_i) \quad (4)$$

$$Nu_m = (hD_h)/k \quad (5)$$

Furthermore, the Reynolds's number and average friction rate is specified through the following equations:

$$Re = (puD_h)/\mu \quad (6)$$

$$f = (2D\Delta P)/(pLu^2) \quad (7)$$

One of the most important factors in the comparison of heat transfer using the structure of inserts is the parameter of the percentage of improvement in heat transfer, which is visible in the form of increase at the heat transfer in the embedded insert mode relative to the non-embedded -insert mode.

$$\%\Delta T_e = \frac{\Delta T_{with\ insert} - \Delta T_{without\ insert}}{\Delta T_{without\ insert}} \times 100 \quad (8)$$

4. Discussuion

4.1 Heat Transfer enhancement evaluation

According to measured results and by using data reduction procedure, the following results are listed for heat transfer parameters in Table2.

Table .2 Comprehensive results at various temperatures

Heater temp (°C)		Measured value			Calculated value					
		Ti (°C)	To (°C)	ΔP(bar)	u(m/s)	Re	f	h (w/m².k)	Nu	% increase in h
35	Without insert	19	36	0.15	22.16	50651.4	0.28	5.85	61.54	47
	With insert	13	38	0.47	24.5	57431	0.72	61.12	71.91	
40	Without insert	20	41	0.13	22.16	50809	0.25	52.01	59	28.51
	With insert	17	44	0.51	24.51	56205	0.78	66.88	76.85	
45	Without insert	21	45	0.1	22.16	50651	0.18	47.24	53	25
	With insert	19	49	0.4	24.51	56030	0.61	64.13	72.87	
50	Without insert	20	47	0.1	22.16	50651	0.18	38.65	43.9	18.51
	With insert	21	53	0.38	24.3	50630	0.58	57.88	65.77	
55	Without insert	22	49	0.09	22.16	50651	0.17	32.59	36.99	14.81
	With insert	23	54	0.37	24.51	50631	0.57	44.17	50.2	
60	Without insert	25	50	0.88	22.16	50651	0.16	26.58	30.2	8
	With insert	26	53	0.34	24.51	56031	0.52	29.11	33.08	

From Table 2, it can be concluded that the use of insert inside the heater improves heat transfer. Hence, increasing the Nusselt parameters and the heat transfer coefficient.

The main mechanism of increasing the temperature in a canal which has a screwed tape is creating a secondary flow due to the presence of a tangential component of velocity and increasing velocity near the wall of the tube. The fluid passing around it cause to move a part of the fluid flow perpendicular to the direction of the primary flow. This flow is known as the rotational flow. This increases the temperature gradient across the cross-section and leads to an increase in the heat transfer rate. In other words, the rotational flow generated by the strip, which leads to an increase in the heat transfer of the centrifugal displacement, plays an important role in the heat transfer of the rotational flow (Jacobi and Shah, 1995).

As expected from the studies in literature, the use of these inserts has led to an increase in pressure drop and, consequently, a friction coefficient. Considering that the increase in pressure occur before the regulator, hence it improves the demanding pressure drop reduction.

From the results of Table 2, it is found that at low water temperatures due to the difference in the driving force of the temperature, the use of inserts is very effective. Hence, the highest efficiency of use of the inserts is at temperatures of 35 and 40°C. At 35°C, improved heat-transfer of 47%was obtained. Also, at high water temperatures, Nusselt number has less variation than low temperatures, so that use of the inserts could not be effective at a water temperature of 60°C in heater. A slight increase in speed and, consequently, the Reynolds-number are of cases considered in the gas supply facilities. This can be an effective point in the issues of corrosion.

4.2. Economical and energy saving evaluation

Considering the importance of the role of energy and the conservation of non-renewable energy sources, and considering the high energy consumption of pre-heating gas in gas pressure reduction stations, it is important to check and calculate the amount of energy. To achieve this goal, the amount of fuel intended for heating which is natural gas is measured by turbine meters at different temperatures of the reservoir. By considering the recent parameter, you can calculate the efficiency of the heater and the amount of savings resulting from the use of this insert.

$$V^{\bullet} = Q^{\bullet}_{Heater} / \mu \times LHV \quad (9)$$

LHV is a low heat value of the fuel, which is 34129 kj/m^3 by using the region's gas analysis, and also, μ is the efficiency of the heater, which can be changed using the insert.

$$Q^{\bullet}_{Heater}\left(\frac{Kj}{h}\right)= m^{\bullet}\left(\frac{Kg}{h}\right)\times \mathrm{CP}\left(\frac{\mathrm{KJ}}{\mathrm{Kg^{\circ}k}}\right)\times \Delta \mathrm{T} \quad (10)$$

The following results are adapted by using the above equations.

Table 3. Checking the consumption of heaters by using insert

	Different heater temperatures	Consumption rate without insert (cubic meter per hour)	Efficiency without insert	Consumption rate with insert (cubic meter per hour)	Efficiency with insert
1	35	0.3	0.23	0.15	0.7
2	40	0.35	0.25	0.16	0.71
3	45	0.43	0.23	0.18	0.68
4	50	0.49	0.23	0.2	0.65
5	55	0.51	0.22	0.2	0.63

From Table 3, it can be concluded that the use of insert in addition to saving energy, also increases the efficiency of the heater. After ensuring that the energy consumption is reduced according to the above table, in this section the amount of savings resulted from the insert will be estimated by Rial. Given that the cost per cubic meter of gas is about fifty cents equal to half a dollar, and the dollar is set at 100000 Rials, it should be noted that the use of heaters in most areas is considered to be about 8 months, Therefore, the basis of calculation is considered to be 8 months during the year.

Table 4. Estimated costs by using insert

	Heater temperatures (degrees Celsius)	amount of energy savings (cubic meter per hour)	Energy saving cost per hour (Rials)	Energy price per day (Rials)	Energy price per month (Rials)	Energy price per year (Rials)
1	35	0.15	7500	180000	5400000	4320000
2	40	0.19	9500	228000	6840000	5472000
3	45	0.25	12500	300000	9000000	7200000
4	50	0.29	14500	348000	1044000	8352000
5	55	0.31	15500	372000	11160000	8920000
6	60	0.29	14500	348000	10440000	8352000

The average savings resulting from the use of inserts in a heater with a capacity of 2500 Cubic meters per hour, according to the current table, are about seventy million Rials. It is worth noting that this amount will be significant in high capacity heaters. On the other hand, the cost of making this inserts in eight coil direction is 20,000,000 Rials. On the of construction of this unit in eight coils is 20,000,000 Rials, which is estimated at 30,000,000 Rials by calculation of installation costs, including welding and controlling at the station.

According to the National Gas Company's program, heater repairs are planned for a period of 8 years. At best, the inserts may be used for at least 5 years, in other words, the depreciation of use of inserts is about 5 years, which is equivalent to ten million Rials each year. Considering all of

the above, as well as taking into account the costs of building and installing these inserts at the Mavian Station, it will be possible to save 60 million Rials each year.

5.Conclusion

The present study focuses on the heat transfer and pressure drop on the heater in pressure reducing station through the helicoid spiral insert. The increase in the Nusselt number indicates that the heat transfer rate has been increased, and as it was shown, the highest Nusselt number was reported to be 76.85. The percentage of heat transfer improvement of 47% indicates that the increase at heat transfer rate is optimal. Due to the amount of energy savings and ease the manufacturing process of the inserts, the use of the inserts intended have increased the efficiency of the heater. As already mentioned, the use of Insert in the structure of the heaters due to the desirability of pressure drop can be a good alternative to other methods for increasing the heat transfer.

Acknowledgement

The authors wish to express their thanks to Iranian national gas company, Kurdistan province, for support of this research.

References

Bhuiya, M.M.K., Chowdhury, M.S.U., Saha, M., Islam M.T., 2013.Heat transfer and friction factor characteristics in turbulent flow through a tube fitted with perforated twisted tape inserts. Int J Heat Mass Transf. 46, 49-57. https://doi.org/10.1016/j.icheatmasstransfer.2013.05.012

Cullender, M.H., 1955. The Isochronal Performance Method of Determining the Flow Characteristics of Gas Wells. SPE. 6.

Farzaneh-Gord, M., Hashemi, S., Sadi, M., 2007. Energy Destruction in Iran's Natural Gas Pipe Line Network. Energy Exploration & Exploitation. 25, 393-406. https://doi.org/10.1260/014459807783791809

Jacobi, A.M., Shah, R.K., 1995. Heat transfer surface enhancement through the use of longitudinal vortices: A review of recent progress. Exp Therm Fluid Sci. 11, 295-309. https://doi.org/10.1016/0894-1777(95)00066-U.

Pathipakka, G., Sivashanmugam, P., 2010. Heat transfer behaviour of nanofluids in a uniformly heated circular tube fitted with helical inserts in laminar flow. Superlattices Microstruct. 47, 349-360. https://doi.org/10.1016/j.spmi.2009.12.008.

Rahimi, M., Shabanian, S.R., Alsairafi, A.A., 2009. Experimental and CFD studies on heat transfer and friction factor characteristics of a tube equipped with modified twisted tape inserts. Chem Eng Process. 48, 762-770. https://doi.org/10.1016/j.cep.2008.09.007.

Sarma, P.K., Kishore, P.S., Rao, V.D., Subrahmanyam, T., 2005. A combined approach to predict friction coefficients and convective heat transfer characteristics in A tube with twisted tape inserts for a wide range of Re and Pr. Int J Therm Sci. 44, 393-398. https://doi.org/10.1016/j.ijthermalsci.2004.12.001.

Suri, A.R.S., Kumar, A., Maithani, R., 2017. Heat transfer enhancement of heat exchanger tube with multiple square perforated twisted tape inserts: Experimental investigation and correlation development. Chem Eng Process. 116, 76-96. https://doi.org/10.1016/j.cep.2017.02.014.

Samruaisin, P., Changcharoen, W., Thianpong, C., Chuwattanakul, V., Pimsarn, M., Eiamsa-ard, S., 2018. Influence of regularly spaced quadruple twisted tape elements on thermal enhancement characteristics. Chem Eng Process.128, 114-123. https://doi.org/l10.1016/j.cep.2018.04.014

Shabanian, S., Rahimi, M., Shahhosseini, M., Alsairafi, A., 2011. CFD and experimental studies on heat transfer enhancement in an air cooler equipped with different tube inserts. Int J Heat Mass Transf. 38, 383-390. https://doi.org/10.1016/j.icheatmasstransfer.2010.12.015.

Thianpong, C., Eiamsa-ard, P., Promvonge, P., Eiamsa-ard, S., 2012. Effect of perforated twisted-tapes with parallel wings on heat tansfer enhancement in a heat exchanger tube. Energy Procedia. 14, 1117-1123.

JOURNAL OF GAS TECHNOLOGY

Volume 6 / Issue 2 / Winter 2021 / Pages 28-44

Journal Homepage: http://jgt.irangi.org

Techno-Economic Analysis of Flare Gas to Gasoline (FGTG) Process through Dimethyl Ether Production

Mostafa Jafari[1], Ali Vatani[1*],Mohammad Shahab Deljoo[1], Amirhossein Khalili-Garakani[2]

1. Institute of Liquefied Natural Gas (I-LNG), School of Chemical Engineering, College of Engineering, University of Tehran, Tehran, Iran
2. Chemistry and Process Engineering Department, Niroo Research Institute, Tehran, Iran

ARTICLE INFO

ORIGINAL RESEARCH ARTICLE

Article History:
Received: 04 Juen 2021
Revised: 30 July 2021
Accepted: 11 September 2021

Keywords:
Flare Gas
DME
Gasoline
Hydrogen
Operating Profit
Asaluyeh

DOR: 20.1001.1.25885596.2021.7.2.3.5

ABSTRACT

It is well known that burning flare gases and releasing them into the atmosphere has become one of the problems of the oil, gas, and petrochemical industries. If these industries can produce energy or valuable materials from flare gases, it will be very profitable and less harmful to the environment. The purpose of this investigation is to design, simulation and economic evaluation the process of converting flare gas to dimethyl ether (DME) for the production of gasoline, Liquefied petroleum gas (LPG), and hydrogen by Aspen HYSYS v.11 software. The flare gas to gasoline (FGTG) process can be indirect or direct DME production (two scenarios). In the economic comparison of these scenarios, the total product sales, operating profit, total capital cost, desired rate of return (ROR), and payoff period (POP) will be calculated. The economic evaluation results show that using the FGTG process with direct DME production (second scenario) instead of the FGTG process with indirect DME production (first scenario), increases the product sales and operating profit by about 55% and 65%, and also the total capital cost and utility cost is decreased by about 30% and 50%, respectively. Finally, the desired ROR in the FGTG process with direct DME production and indirect DME production is 52 percent/year and 33 percent/year, and the POP for the second scenario is approximately 1.1 years earlier than the first scenario.

How to cite this article
M. Jafari, A. Vatani, M.S. Deljoo, A.H. Khalili-Garakani. Techno-Economic Analysis of Flare Gas to Gasoline (FGTG) Process through Dimethyl Ether Production. Journal of Gas Technology. 2021; 6(2): 28 -44. (http://jgt.irangi.org/article_251676.html)

* Corresponding author.
E-mail address: avatani@ut.ac.ir (A. Vatani)

Available online 26 December 2021

1. Introduction

Iran is blessed with substantial energy resources, including natural gas and crude oil. In energy terms, Iran's proven natural gas reserves, approximated at about 34 billion cubic meters, are known to be considerably more than its oil resources. Crude oil consumption was more than 100 million barrels per day, according to figures released by British Petroleum Company (BP's) in 2019. However, in 2021, global crude oil consumption has reached 92 million barrels per day (Jaccard, et al. 2018). The main reason is the transition from fuels and fossil energy to reversible and clean energies such as hydropower, solar energy, wind energy, Etc. (Icaza, et al. 2021). Organization of the Petroleum Exporting Countries (OPEC) statistics show that Iran has the third-longest lifespan of oil reserves among the 140 OPEC member countries. According to these statistics, Iran's oil reserves will exist for another 138 years (Karamelikli, et al. 2017). Due to shortages of oil reserves in the future, efforts to replace synthetic fuels instead of crude oil have taken place (Puricelli, et al. 2021). Synthetic fuels can be produced from natural gas, coal, flare gases, biogas, Etc. Flaring is one of the most controversial issues dealing with today's problems of the energy industry and its environmental effects. Gas flaring poses a series of adverse health, ecological and economic outcomes. Although the purpose of the flaring system is to maintain the safety of engineers, workers, and equipment, burning in the flare tower produces some intermediate products, which are finally transformed to CO2 and H2O (Davoudi, et al. 2014). Flare gases can be used in many methods, for example, enhanced oil recovery (EOR), DME Production, gasoline production, hydrogen production, compressed natural gas (CNG) production, LPG production, ethylene recovery, combined heat and power (CHP) generation, desalinated water generation, Etc. (Iora et al. 2014; Saidi et al. 2018; Jafari et al. 2020a). Three conventional synthetic methods for gasoline production from flare gas are the Fischer-Tropsch (FT) process, the conversion of DME to gasoline (DTG), and the conversion of Methanol to gasoline (MTG) (Wan et al. 2018). The synthetic methods of gasoline production are illustrated in Figure 1. In the MTG and DTG process, the selectivity for gasoline production is approximately 80%. In contrast, in the FT process, it is approximately 30% and the remainder of the production of heavy liquid hydrocarbons (Materazzi and Holt, 2019).

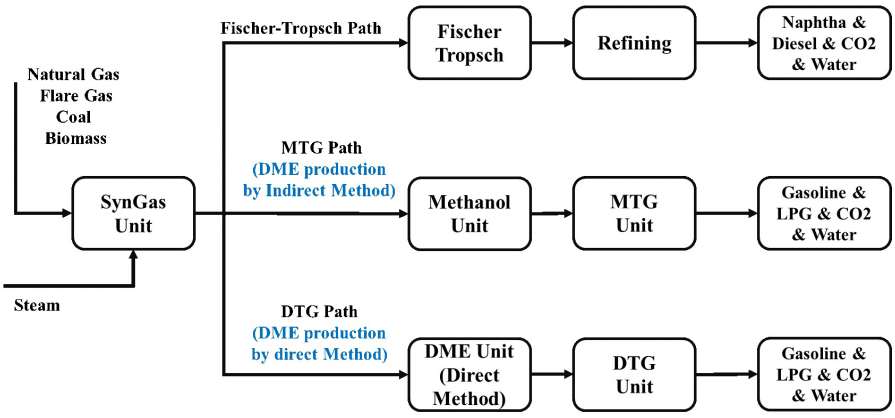

Figure 1. Gasoline Synthesis method: Fischer-Tropsch (FT), Methanol to Gasoline (MTG), and DME to Gasoline (DTG) (Wang et al. 2016)..

Few studies have been performed on the conversion of the FGTG Process. In a study by Lee et al. (1995), the technical comparison between the MTG and DTG processes has been investigated. The results showed The DTG process offers advantages over the Mobil MTG process in several areas. These include heat duty and heat of reaction, hydrocarbon product yield, synthesis gas conversion, and process efficiency. In a study by Stanley et al. (2009), the

feasibility of converting flare gas to gasoline using the GTL process as a profitable method to reduce the amount of flaring in Nigeria has been investigated. Rahimpour et al. (2012) simulated and economically evaluated three different methods of flare gas recovery (FGR) (gasoline production, power generation, and gas compression). Simulation of these processes was performed in Aspen HYSYS software. The results showed that power generation has a higher ROR and faster payoff period (POP), and, finally, gasoline production has a higher annual profit. In a study by Zolghafari et al. (2017), Technical characterization and economic evaluation of FGR in various gas-processing plants have been investigated. Three methods, including GTL, gas turbines generation (GTG), and gas to ethylene (GTE), have been simulated using Aspen HYSYS. the results showed that the GTG method is one of the most economical methods and the GTE method has the higher annual profit. In a study by Hajizadeh et al. (2018), technical and economic evaluation of flare gas recovery in a Fajr-e Jam gas refinery have been investigated. Three methods for FGR were investigated, including two novel methods. The first two methods considered liquefaction and LPG production by implementing flare gases as feed for the existing LPG unit. Different parameters were studied in feed liquefaction and LPG production. The third studied option is using a three-stage compression unit to compress the flare gases. The results showed that the ROR for liquefaction and LPG methods is above 200%. In a study by Jafari et al. (2018), simulation and technical analysis of the Integrated FGTG process have been investigated. In this paper, an integrated FGTG process for converting flare gas to gasoline is simulated using the Aspen HYSYS software. The simulation results demonstrate that by recycling all gas emissions, such as off-gas from the methanol and MTG units back into the process, gasoline productivity and LPG productivity can be increased on average 55% and 10%. In a study by Jafari et al. (2020b), simulation and economic evaluation of a poly-generation system for co-production of power, steam, CH_3OH, H_2 and, CO_2 from flare gas have been investigated (figure 2). In this paper, the poly-generation system has been used for converting flare gas to energy and various products such as power, steam, methanol, H_2, and CO_2. A poly-generation system has a lower raw material cost, utility cost, and operating cost than the corresponding single-product processes. The simulation results showed that using 9690 kg/h of flare gas, 8133 kg/h methanol, 653.7 kg/h H_2, 46950 kg/h N_2, 9103 kg/h CO_2, 109850 kg/h MP steam, and 3.7 MW power have been produced. Also, the total capital cost and the operating profit of the poly-generation system are 71 million USD and 115 million USD/year, respectively, and the payoff period is 1.5 years.

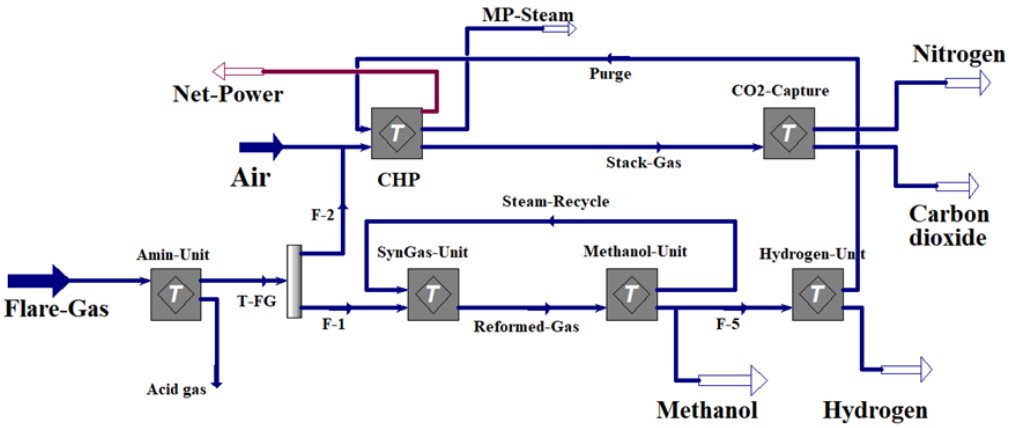

Figure 2. Block Flow Diagram (BFD) of conversion of flare gas into products in a poly-generation system (Jafari et al. 2020b).

The difference between the MTG and DTG processes is that the DME is produced indirectly in the MTG path, but in the DTG path, the DME is produced directly. In the Chemical Industry, the indirect method of DME producing is more than the direct method. The indirect method involves two synthesis steps: Methanol production from synthesis gas and dehydration of the methanol. Whereas the direct synthesis converts synthesis gas to DME using a hybrid of bi-functional. Considering the potential of producing various products from flare gases and preventing environmental pollution, in this project, an attempt is made to techno-economic analysis for the FGTG process using conventional processes. In articles published in previous years, no detailed studies have been conducted on the economic evaluation of the FGTG method. The innovations of this paper are the simulation of the conversion of flare gas to dimethyl ether (direct and indirect DME production method) with the aim of co-production of LPG, gasoline, and hydrogen and economic comparison of these processes. In the economic comparison of these processes, the total capital cost, operating profit, total utility cost, desired ROR, and the POP will be calculated.

2. Materials and Methods

South Pars and the Asaluyeh region are some of the country's largest sources of flare gas producers. Flaring is one of the most controversial issues dealing with today's problems of the energy industry and its environmental effects. Although the purpose of the flaring system is to maintain the safety of engineers, workers, and equipment, burning in the flare tower produces some intermediate products, which are finally transformed to CO_2 and H_2O (Jafari et al. 2020b). Currently, in the South Pars area, 45 burners are burning a huge volume of flare gases. 25% of all flared gas in Iran burns in the Asaluyeh region. The properties of Asaluyeh flare gases are given in Table 1.

Table 1. Characteristics of gases sent to Asalouyeh flare (Ziyarati at al. 2019).

Mole fraction	Component
Methane	0.851
Ethane	0.050
Propane	0.019
Ethane and C_4^+	0.018
CO_2	0.022
N_2	0.035
H_2S	0.005

On average, 8100 tons of flare gas is produced per day. This massive volume of burnt flare gases and their pollutants can certainly cause environmental problems in the Assaluyeh region and seriously impact human health. Therefore, planning for the collection and use of flare gases will have an excellent economic justification. Flare gas in the Asaluyeh region mainly contains methane, which is an excellent opportunity to produce valuable products such as gasoline and LPG. Simulation of conversion of flare gases into desired products was performed in Aspen HYSYS v. 11 software. The thermodynamic equation used in this simulation is PRSV, but some units require a different fluid package to be performed with very high accuracy. The fluid packages used in the various units are given in Table 2 (Lopez et al. 2017). The economic evaluation of this process was carried out using specialized economic evaluation software called Aspen Process Economic analyzer v. 11 or APEA. Features of this software include the possibility of connecting to simulation software such as Aspen HYSYS, Aspen Plus, PRO/II, mapping of various process equipment in simulation models, dimensioning of equipment, and cost estimation.

Table 2. Describe the specific fluid packages for each unit (Attary et al. 2018; Hajilary et al. 2020; Moradi et al. 2021 and Nejat et al. 2018).

Fluid Package	Description
Acid-Gas:	This fluid package is used for the Amine Treatment Unit. This new ability to purify acidic gases in Aspen HYSYS allows this to remove the acidic contaminant in the simulation with very high precision by choosing this thermodynamic equation; there is no need to define the reactions of amine and acid gases per unit of amine.
PRSV:	This fluid package is used for the Synthesis Gas Production Unit. The PRSV model is a two-fold modification of the Peng-Robinson equation of state that extends the application of the original Peng-Robinson method for moderately non-ideal systems. It is successfully expanded to handle non-ideal systems giving results as good as those obtained using excess Gibbs energy functions like the Wilson, NRTL, or UNIQUAC equations.
UNIQUAC:	This fluid package is used for the Methanol and DME Synthesis Unit. This equation presented by Abrams in 1975 uses Guggenheim's statistical mechanics and quasi-chemical theory to illustrate the fluid-structure. This equation, like the equation, NRTL can predict the behavior of LLE and VLE systems.
Peng Robinson:	This fluid package is used for the Hydrogen purification and Gasoline production unit. The Peng-Robinson (PR) model is ideal for VLE calculations for hydrocarbon systems. Several enhancements to the original PR model were made to extend its range of applicability and to improve its predictions for some non-ideal systems. For oil, gas, and petrochemical applications, the Peng-Robinson equation is usually recommended.

3. Process description of FGTG unit

This section describes the simulation of the process of converting flare gas to gasoline (FGTG). DME is the intermediate product of this process and will convert to gasoline. There are two scenarios (figure 3 & figure 4) for the production of DME:

1. FGTG Process with Indirect DME Production (first scenario).
2. FGTG Process with Direct DME Production (second scenario).

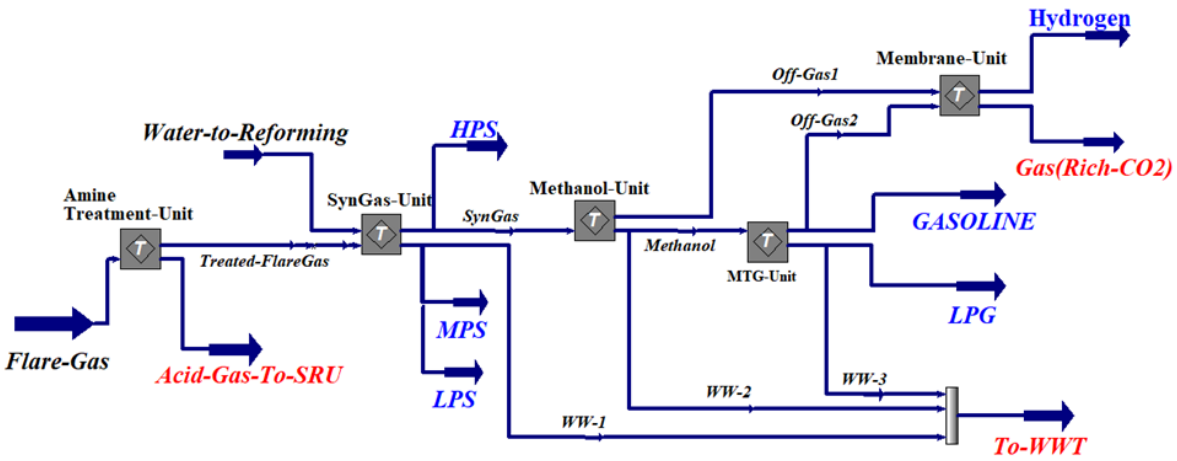

Figure 3. BFD of FGTG Process with Indirect DME Production

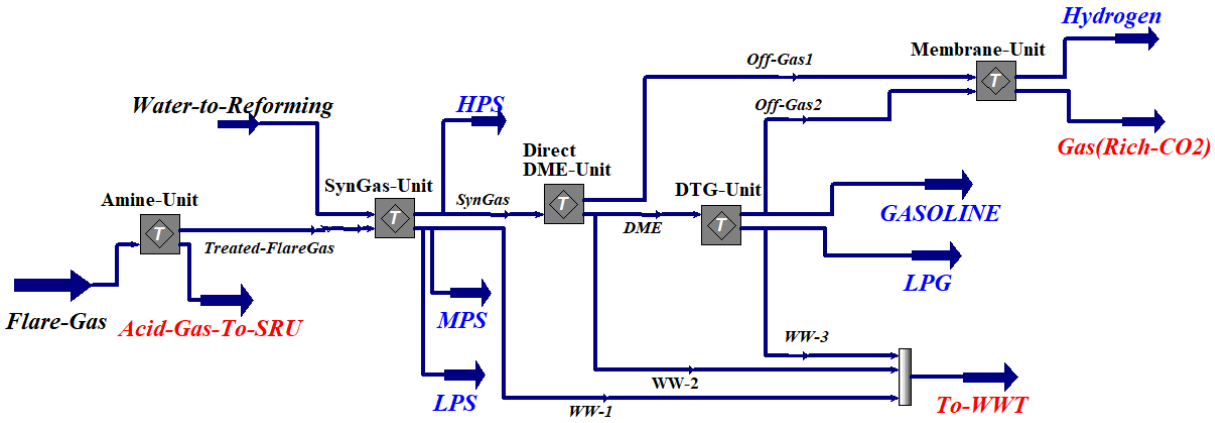

Figure 4. BFD of FGTG Process with Direct DME Production

The initial stage in the FGTG process is Amine Treatment Unit (figure 5). The flare gas enters the amine treatment unit with the specifications given in table 1, at a volume flow rate of 188500 m^3/h (Mass flow rate: 148.1 Ton/h) at 30 ºC and a pressure of 100 kPa. The H2S in the flare gas is first separated in the Amine Treatment Unit and then sent to the synthesis gas production unit in these two scenarios. Many factors are involved in choosing the proper process for sweetening the gas; the most important are feed inlet temperature and pressure, selectivity, the mass fraction of acidic gases, final characteristics of treated gas, process economics, and environmental issues that influence. H2S is highly toxic and also acidic, which can cause corrosion. The solvent used in this process is MDEA, and the process pressure is 30000 kPa (Luo et al. 2014).

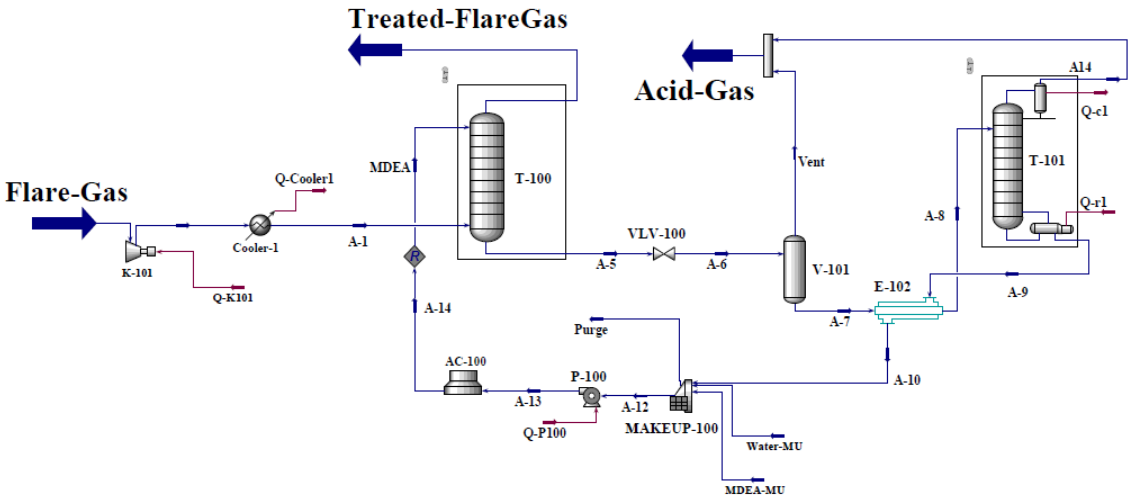

Figure 5. Schematic of Amine Treatment unit as configured in the Aspen HYSYS software environment (Luo et al. 2014).

The second stage in the FGTG process is the synthesis gas production unit (figure 6). The treated flare gas enters the synthesis gas production unit at a temperature of 50 ºC and pressures 3000 kPa with water at a temperature of 25 ºC and pressure 100 kPa. In the synthesis gas production unit, the ratio of H_2/CO is 4(Ghasemzadeh et al. 2016 and Jones et al. 2009). The amine treatment unit and synthesis gas production unit are the same in both scenarios. The first reactor is operated as a pre-reformer for reforming the heavier hydrocarbon components. Reactions 1 to 6 occur in the pre-reforming reactor. The conversion value in all reactions is 100%~~.~~ the second reactor reforms methane. Reactions 7 and 8 occur in

the reforming reactor. Low-pressure steam (LPS), medium-pressure steam (MPS), and high-pressure steam (HPS), produces from the hot synthesis gas leaving the pre-reforming reactor.

In the first scenario, the synthesis gas is sent to the methanol unit, and methanol is produced. The produced methanol is then sent to the MTG unit. In this unit, methanol will first be converted to DME and then convert to liquid hydrocarbons. The process of methanol synthesis (figure 7) involves several steps, including compression of the synthesis gas, synthesis cycle, synthesis reactions and catalysts, and the purification of methanol. The synthesis gas can be converted to methanol by an exothermic reaction at an average temperature of 210-270 °C and a 50 - 100 bar pressure in the presence of a copper alumina catalyst. The main reactions involved in methanol reactors are exothermic for an equilibrium model involving two reactions (Eq. 8 & 9).

$C_2H_6 + 2H_2O \rightarrow 2CO + 5H_2$	Reforming ethane	(1)
$C_3H_8 + 3H_2O \rightarrow 3CO + 7H_2$	Reforming propane	(2)
$i\text{-}C_4H_{10} + 4H_2O \rightarrow 4CO + 9H_2$	Reforming i-butane	(3)
$n\text{-}C_4H_{10} + 4H_2O \rightarrow 4CO + 9H_2$	Reforming n-butane	(4)
$i\text{-}C_5H_{12} + 5H_2O \rightarrow 5CO + 11H_2$	Reforming i-pantane	(5)
$n\text{-}C_5H_{12} + 5H_2O \rightarrow 5CO + 11H_2$	Reforming n-pantane	(6)
$CH_4 + H_2O \leftrightarrow CO + 2H_2$	Steam Methane Reforming	(7)
$CO + H_2O \leftrightarrow CO_2 + H_2$	Water Gas Shift	(8)
$CO_2 + 3H_2 \leftrightarrow CH_3OH + H_2O$	Methanol Synthesis Reaction	(9)

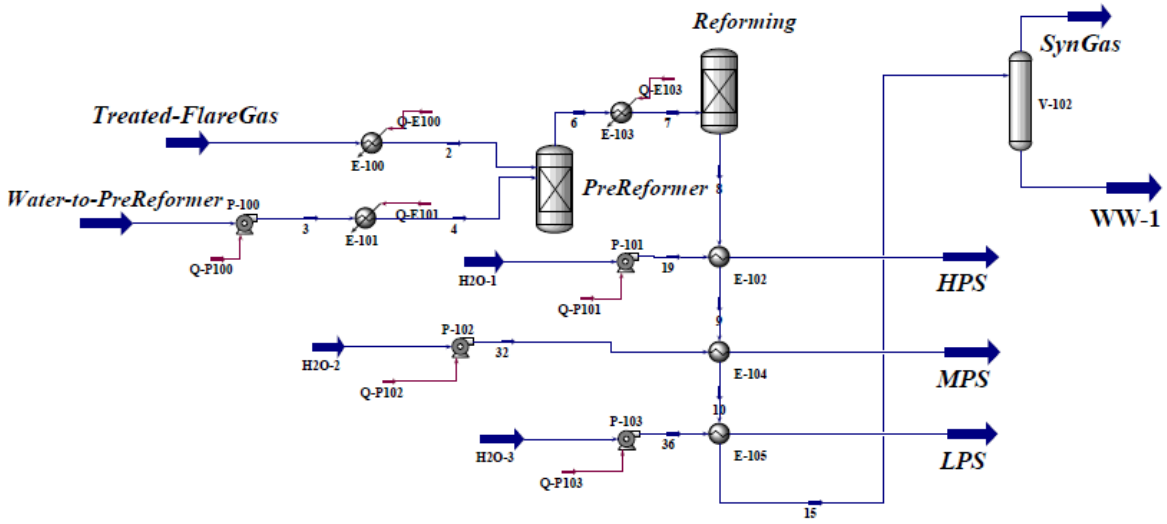

Figure 6. Schematic of synthesis gas production as configured in the Aspen HYSYS software environment (Ghasemzadeh et al. 2016).

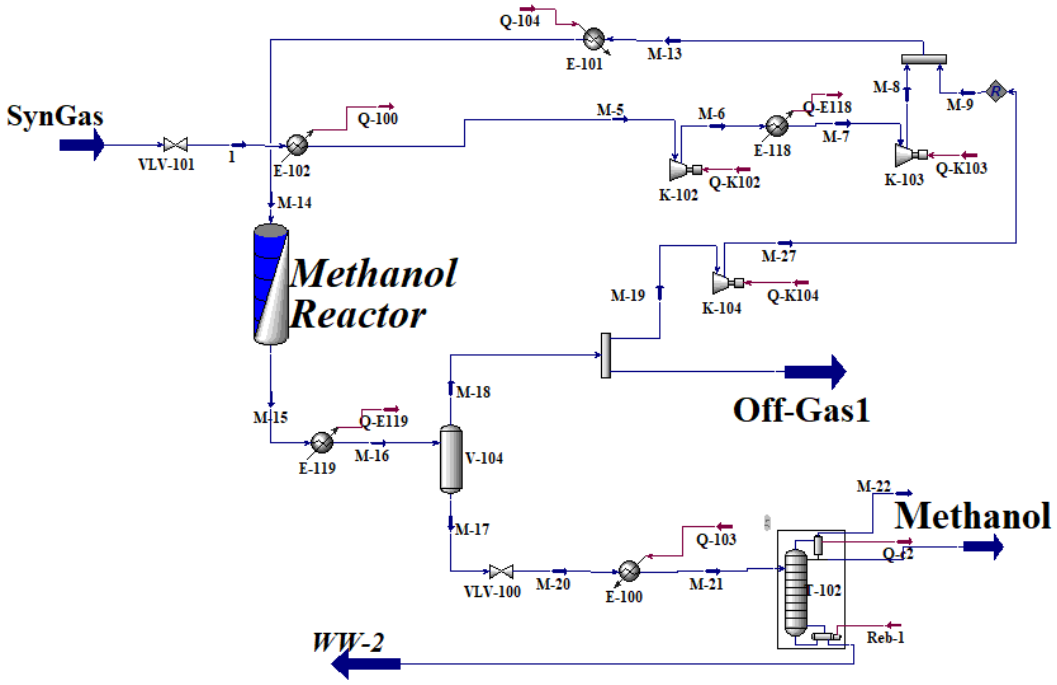

Figure 7. Schematic of methanol production unit as configured in the Aspen HYSYS software environment (Sunny et al. 2016).

Mobil operated the first MTG plant in New Zealand, producing gasoline of approximately 92-RON (Research Octane Number) quality, based on a process developed in the 1970s (Nian et al. 2013). The basis of the process of MTG is to convert methanol to DME and then to other hydrocarbons. The reaction is the strongly exothermic conversion of methanol to hydrocarbon products, and adiabatic temperature increase to about 600 °C is associated. MTG reaction paths are summarized by Eq. 10 to 14:

$$2CH_3OH \leftrightarrow DME + H_2O \quad (10)$$

$$DME \rightarrow Light\ Olefins + H_2O \quad (11)$$

$$Light\ Olefins + DME \rightarrow Heavy\ Olefins + H_2O \quad (12)$$

$$Heavy\ Olefins \rightarrow Aromatics + Paraffin \quad (13)$$

$$Aromatics + DME \rightarrow Higher\ Aromatics + H_2O \quad (14)$$

The first step is the dehydration reaction of methanol, resulting in the equilibrium mixture of DME, methanol, and water. DME is then converted to light olefins. DME then converts light olefins (mostly propylene and butene) into heavier olefins, which can then react with each other to form aromatics and paraffin. A schematic of the MTG process configured in the Aspen HYSYS software environment is illustrated in Figure 8. This is applied to an integrated plant-wide FGTG process for converting flare gas to hydrocarbon fuel products, including gasoline and LPG.

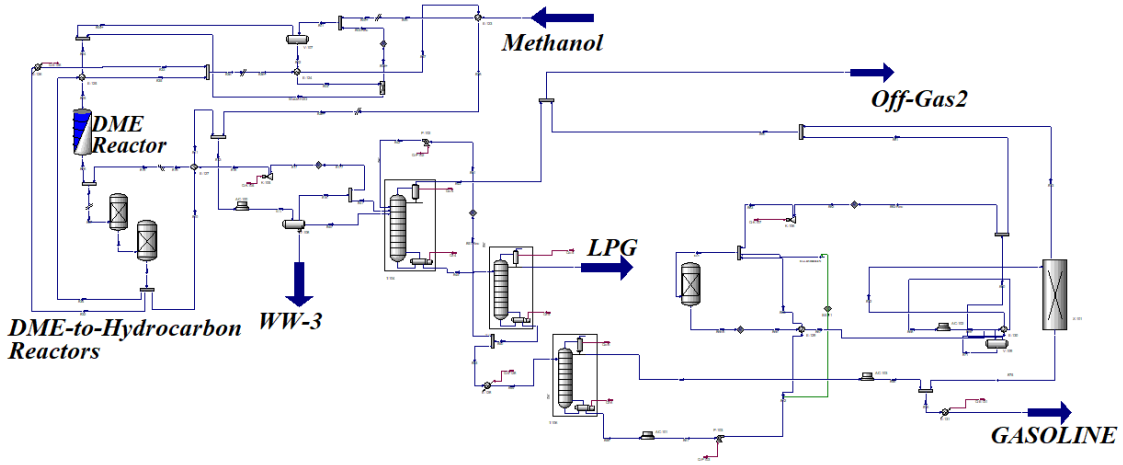

Figure 8. Schematic of MTG unit as configured in the Aspen HYSYS software environment (Hindman et al. 2013).

In the Second scenario, the synthesis gas is directly converted to DME. The produced DME is then sent to the DTG unit. In this unit, DME is converted to liquid hydrocarbons. Recently, a combination of the methanol co-production and dehydration of the methanol process for the direct synthesis of DME from the syngas at one reactor has been developed. The direct synthesis of DME from the syngas follows the three significant reactions 15, 16, and 17 and generally reaction 18. The reactions take place in the DME production, namely:

$$CO_2 + 3H_2 \leftrightarrow CH_3OH + H_2O$$ Methanol synthesis (15)

$$2CH_3OH \leftrightarrow CH_3OCH_3 + H_2O$$ Methanol dehydration (16)

$$CO + H_2 \leftrightarrow H2 + CO_2$$ Water gas shift: (17)

$$3CO + 3H_2 \leftrightarrow CH_3OCH_3 + CO_2$$ Overall reaction: (18)

The schematic of the DME production (direct Method) process and DTG process configured in the Aspen HYSYS software environment is illustrated in Figures 9 & 10.

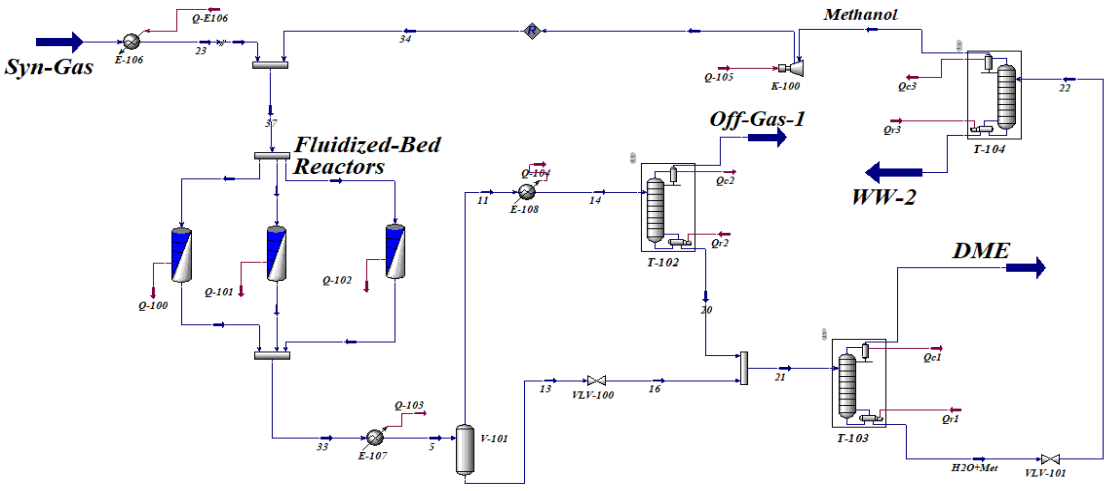

Figure 9.Schematic of DME production (direct method) as configured in the Aspen HYSYS software environment (Jones et al. 2009).

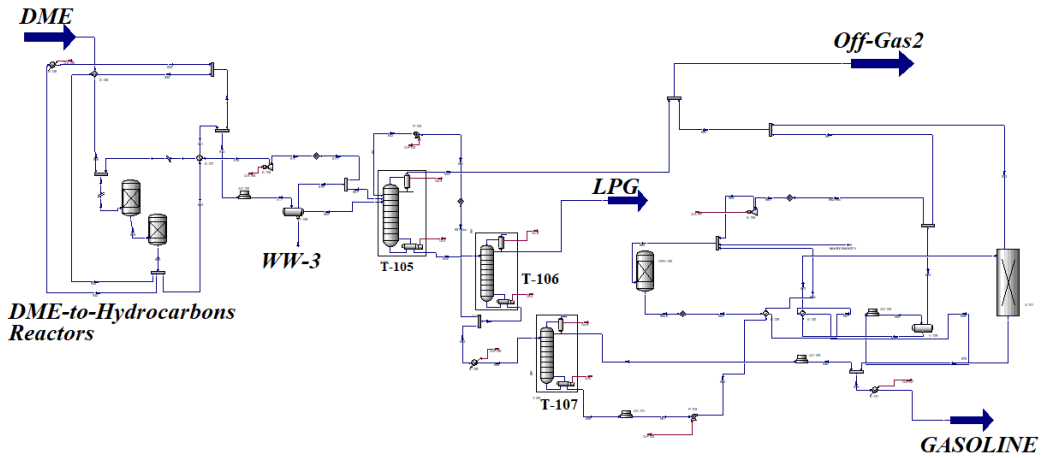

Figure 10. Schematic of DTG unit as configured in the Aspen HYSYS software environment (Hindman et al. 2013).

The off-gases produced from the methanol production unit, DME production unit, MTG unit, and DTG unit are rich in H_2. Pure H_2 can be one of the essential products along with gasoline and LG. Selling pure hydrogen and gasoline, and LPG can significantly impact the overall profit of the process and ROR. Membrane processes have been used to purify hydrogen. A schematic of the Membrane process configured in the Aspen HYSYS software environment is illustrated in Figure 11. In this process, two-stage silica membranes are used in series. The permeance and pressure gradient of silica membranes are given in Table 3.

Table 3. Properties of hydrogen permeance and selectivity of silica membrane (Saebea et al. 2019).

Specifications	Values
Stream pressure (kPa)	1300
Pressure gradient (kPa)	1200
Permeance of H_2 $\frac{m^3}{m^2.hr.pa}$	0.0003225
Permeance of CH_4 $\frac{m^3}{m^2.hr.pa}$	6.45×10^{-8}
Permeance of C_2H_6 $\frac{m^3}{m^2.hr.pa}$	8×10^{-8}
Permeance of C^+_2 $\frac{m^3}{m^2.hr.pa}$	5×10^{-9}

Since there is no membrane simulation in Aspen HYSYS software, another simulator software is needed. Since the PRO/II software can simulate a membrane system, this membrane is first simulated in this software and, then using the PRO/II software output, the same performance of the membrane in Aspen HYSYS software component splitter equipment has been implemented (Ghasemzadeh et al. 2017).

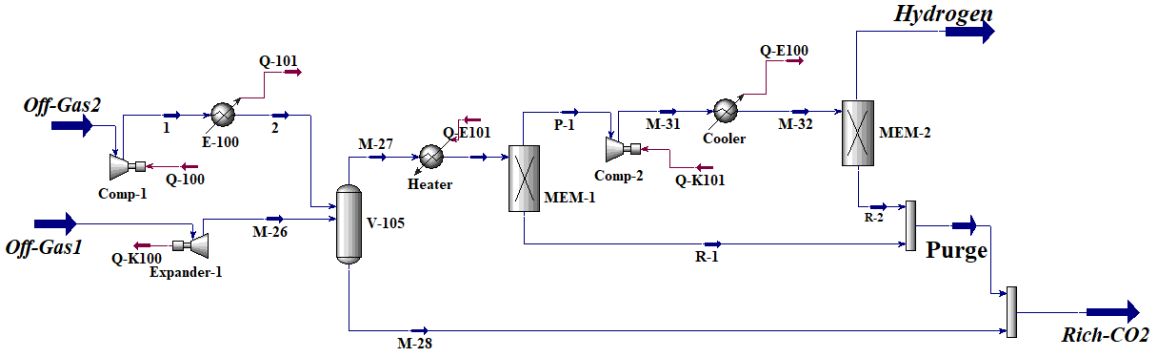

Figure 11. Schematic of Membrane Process for Hydrogen purification unit as configured in the Aspen HYSYS software environment (Jafari et al. 2020b).

4. Economic evaluation of FGTG Unit

In the following, it should be considered whether the production of gasoline from flare gases will be economically profitable or not. The most important issue in the economic evaluation of the chemical processes is obtaining the equipment cost, total installed cost, total capital cost, total operating cost, total utilities cost, operating profit, desired rate of return, and payoff period (POP) (Jafari and Khalili-Garakani., 2021a).

The operating profit of this process is defined as (Jafari et al. 2019):

Operating Profit = (Products Sales Price) - (Raw materials Price + Utility Cost)

Since the design of the FGTG is innovative, the design should be carefully evaluated in terms of economic. On the other hand, for the FGTG process, an accurate economic comparison shall be made between the direct or indirect production method of DME from flare gases to determine which has a higher desired ROR and an earlier payoff period. The following is a list of some commonly used terminology in economic evaluation with its description (Jafari et al. 2019):

- Equipment cost in APEA represents the cost of purchasing equipment, and total installed cost represents the total direct material and labor costs associated with the project component. Due to the items that are included in the installed cost, in APEA software, the installed cost is more than the equipment cost.
- Total utilities cost refers to the cost of cooling water, refrigerant, hot oil, steam, power, etc., annually.
- The total capital cost of this process is defined as: Total Capital Cost = Fixed Capital Cost + Working Capital Cost

  capital cost includes the following:

  ✓ Direct costs: Equipment and setting, piping, civil, structural steel, instrumentation and controls, electrical equipment and materials, insulation, paint, etc.

  ✓ Indirect field costs: Engineering and supervision, start-up and commissioning, construction expenses - fringe benefits, burdens, insurance, equipment rental, field services, temporary constructions, etc.

  ✓ Indirect non-field costs: freight, taxes and permits, engineering, and material procurement, contingency, allowances for unpredictable events, other project costs, etc.
- The POP refers to the amount of time it takes to recover the total capital cost. The POP of this process is defined as: POP = Fixed Capital Cost / Net Profit
- The desired ROR of this process is defined as: ROR = (Net Profit / Fixed Capital Cost)

The right decisions made during economic evaluation operations, such as choosing the right type of equipment and utility, will significantly impact the correct economic evaluation. At the beginning of the work, the stream price of feed and product are entered to determine if the unit design capable of profitability or not (Jafari et al. 2019). Table 4 shows the stream prices of flare gas, products, and utilities. Hydrogen fuel prices range from 12 USD to more than 14 USD per kilogram, but the most common price is 12 USD per kg.

Table 4. Stream price for flare gas, products and utility

Stream Name	Cost	Unit	Ref.
Flare Gas (Raw material)	0.02	USD/m^3	[35, 19]
Water & cooling water (Raw material & Utility)	0.00418	USD/Ton	[19]
Gasoline (Product)	880	USD/Ton	[36]
LPG (product)	1000	USD/Ton	[37]
Hydrogen (product)	12000	USD/Ton	[38]
HP steam (product & Utility)	4.52	USD/Ton	[19]
MP steam (product & Utility)	4.36	USD/Ton	[19]
LP steam (product & Utility)	4.17	USD/Ton	[19]
Refrigerant (Utility)	2.71	USD/GJ	[19]

After determining the raw material cost, total products sales, the type of consumption utility of equipment is selected. A key step in APEA software is the mapping of equipment. For example, a distillation column in Aspen HYSYS might be mapped into several items such as a trayed or packed tower, a kettle-type reboiler, an overhead condenser, a reflux pump, etc. The default material of construction for all equipment is carbon steel. However, the materials used in the construction of the equipment can be changed according to conditions such as high temperature, high pressure, or corrosion. After mapping and sizing operations, the economic evaluation in the APEA software will be completed and the results will be reported (Meng et al. 2018).

5. Results and discussion

In these two simulated configurations (direct and indirect production of DME gases sent to flare for simultaneous production of gasoline, LPG, hydrogen, and steam at different levels), the connection between the flows in the main flowsheet and sub-flows sheet is established. In table 5 and Table 6 are compared the products produced and the rate of utility consumption in the two processes for co-generation of gasoline, LPG, and hydrogen.

The simulation results showed that using the FGTG process with direct DME production (second scenario) instead of the FGTG process with indirect DME production (first scenario) decreases the mass flow rate of gasoline and LPG produced by about 55% and 35%. The reason for the low production of gasoline and LPG in the second scenario is that the ratio of H_2/CO is high. If the H_2/CO is higher than 3, more methanol will be produced in the first scenario, resulting in more gasoline and LPG. If the H_2/CO is less than 3, the methanol will be produced less in the first scenario, and DME will be produced more in the second scenario. Also, the results show that using the second scenario instead of the first scenario increases the mass flow rate of hydrogen produced by about 100%. Since steam production is done at the same synthesis gas unit, LPS, MPS, and HPS production are the same in two processes. This table shows that the purification and separation of hydrogen from off-gas flows next to gasoline can be very profitable.

Generally, using the second scenario instead of the first scenario increases the sum of gasoline, LPG, hydrogen, and steam production at different levels by about 55%. Since hydrogen production is more expensive than gasoline and LPG, producing more hydrogen will be more profitable. Also, the total utilities cost in the second scenario in terms of power, heating, and cooling is less than in the first scenario. However, the water production of the first scenario is much more compared to the second scenario. Finally, the simulation results show that using the first scenario instead of the second scenario increases the total utilities consumption by about 50%.

Table 5. Flow rates and price of purchases of flare gas and utilities

	FGTG with Indirect DME Production (first scenario)				FGTG with Direct DME Production (second scenario)			
Feeds & Utilities	Mass flow	Unit	Cost flow	Unit	Mass flow	Unit	Cost flow	Unit
Flare Gas	148.1	Ton/h	3770	USD/h	148.1	Ton/h	3770	USD/h
Water	1361	Ton/h	5.69	USD/h	1361	Ton/h	5.69	USD/h
Power	579.1	GJ/h	9149.78	USD/h	384.4	GJ/h	6073.52	USD/h
Cooling-water	2848	GJ/h	605.2	USD/h	2544	GJ/h	540.6	USD/h
HP Steam	4119.2	GJ/h	10298	USD/h	3391	GJ/h	8477.5	USD/h
MP Steam	2204.3	GJ/h	4849.46	USD/h	658.7	GJ/h	1449.14	USD/h
LP steam	754	GJ/h	754	USD/h	131.9	GJ/h	250.61	USD/h
Refrigerant	0	GJ/h	0	USD/h	176	GJ/h	477.136	USD/h

Table 6. Flow rates and Price of Product Sales

	FGTG with Indirect DME Production (first scenario)				FGTG with Direct DME Production (second scenario)			
Products	Mass flow	Unit	Cost flow	Unit	Mass flow	Unit	Cost flow	Unit
HP steam	869.1	Ton/h	3700.19	USD/h	869.1	Ton/h	3700.1933	USD/h
MP steam	124.5	Ton/h	542.82	USD/h	124.5	Ton/h	542.82	USD/h
LP steam	227.2	Ton/h	948.37	USD/h	227.2	Ton/h	948.36915	USD/h
Hydrogen	12.51	Ton/h	150120	USD/h	25.69	Ton/h	308280	USD/h
Gasoline	76.09	Ton/h	66959.2	USD/h	49.48	Ton/h	43542.4	USD/h
LPG	15.54	Ton/h	15540	USD/h	11.46	Ton/h	11460	USD/h
Gas (Rich CO_2)	19.27	Ton/h	0	USD/h	125.5	Ton/h	0	USD/h
Acid Gas	3.95	Ton/h	0	USD/h	3.95	Ton/h	0	USD/h
to-WWT	130.4	Ton/h	0	USD/h	55.11	Ton/h	0	USD/h

Table 7, is showed a summary of the economic comparison of the FGTG process in two scenarios. The results show that both methods of FGTG can be very profitable. On the other hand, the FGTG process with direct DME production (second scenario) is better than the FGTG process with indirect DME production (first scenario). The results show that using the first scenario instead of the second scenario increases the equipment cost, total installed cost, and total capital cost by about 30%, 35% and 23%, respectively. Also, using the second scenario instead of the first scenario increases the net profit and total operating profit by about 20% and 65%. ROR of the second scenario is 52% and for the first scenario is 33%. Finally, the POP for the second scenario is approximately 1.1 years earlier than the first scenario.

Table 7. Summary of the Economic comparison of the FGTG Process with Indirect DME Production and FGTG Process with Direct DME Production

	FGTG with Indirect DME Production (first scenario)	FGTG with Indirect DME Production (first scenario)	Unit
Total Raw Materials Cost	32.57	32.57	MUSD/year
Total Product Sales	2054.68	3183.61	MUSD/year
Total Utilities Cost	199.14	130.50	MUSD/year
Operating Profit	1822.97	3020.54	MUSD/year
Total Equipment Cost	265.00	204.00	MUSD
Total Installed Cost	301.00	223.00	MUSD
Fixed Capital Cost	1075.17	828	MUSD
Working Capital Cost	190	146	MUSD
Total Capital Cost	1265.17	974.00	MUSD
Net Profit	354.80	430.56	MUSD/Year
Desired Rate of Return	33	52	Percent/Year
Payoff Period	3.00	1.90	Year

6. Conclusions

This work has addressed simulation and economic comparison of the process of converting 148 Ton/h (188500 m^3/h) of flare gas to gasoline, LPG, and hydrogen with two scenarios (indirect or direct production of DME).

Aspen HYSYS v.11 was used to carry out the process simulation studies. Also, Comparison and economic analysis of these two scenarios for the simultaneous production of gasoline and other products were presented in APEA v.11. The H_2S in the flare gas is first separated in the Amine Treatment Unit and then sent to the synthesis gas production unit in these two scenarios. In the synthesis gas production unit, the ratio of H_2/CO is 4. The amine treatment unit and synthesis gas production unit are the same in both scenarios. In the direct process of producing DME, the treated flare gas is converted directly to DME, but in the indirect method, the treated flare gas is first converted to methanol and then to DME. The following are the main results obtained from the simulation and economic evaluation:

- ✓ The first scenario (FGTG process with indirect DME Production) produces 76.09 ton/h of gasoline, 15.54 ton/h of LPG, and 12.51 ton/h of hydrogen. But in the second scenario (FGTG process with direct DME production), 49.98 ton/h of gasoline, 11.46 ton/h of LPG, and 25.69 ton/h of hydrogen will be produced.
- ✓ Gasoline and LPG production are higher in the first scenario, but hydrogen production is higher in the second scenario.
- ✓ Total utilities cost in the first scenario increased by about 50% than in the second scenario.
- ✓ Operating profit in the second scenario increased by about 65% than in the first scenario.
- ✓ Raw material cost in the two scenarios was equal, and total product sales in the second scenario increased by about 55% than in the first scenario.
- ✓ Capital cost in the first scenario increased by about 30% than in the second scenario.
- ✓ The desired ROR in the first scenario is 33% and in the second scenario is 52%.
- ✓ POP for the first scenario is 3 years and in the second scenario is 1.9 years.

Further research is needed to increase the production of products such as gasoline and LPG, sensitivity analysis of CO_2-rich gas return to the syngas unit to increase production. Also, the wastewater stream will be returned to the process after treatment to avoid excessive water consumption in the process. Multi-objective and single-objective optimizations are also needed to reduce energy consumption, reduce capital costs, and increase valuable products such as gasoline, LPG, and hydrogen.

Nomenclature

FGR	Flare gases recovery
ROR	Rate of Return
POP	Payoff Period
DME	Dimethyl Ether
LPG	Liquefied petroleum gas
FGTG	Flare Gas to Gasoline
OPEC	Organization of the Petroleum Exporting Countries
BP	British Petroleum
FT	Fischer-Tropsch
DTG	Dimethyl Ether to Gasoline
MTG	Methanol to Gasoline
GTL	Gas to Liquids
EOR	Enhanced Oil Recovery
CNG	Compressed Natural Gas
CHP	Combined Heat and Power
APEA	Aspen Process Economic Analyzer
BFD	Block Flow Diagram
PFD	Process Flow Diagram
MDEA	Methyl Diethanolamine
LPS	Low-Pressure Steam
MPS	Medium-Pressure Steam
HPS	High-Pressure Steam
GTG	Gas Turbines Generation
GTE	Gas to Ethylene
MUSD	Million United Stated Dollars
P.O. Period	Payoff period
RON	Research Octane Number

References

Attary, M., 2018. On the numerical solution of nonlinear integral equation arising in conductor like screening model for realistic solvents. Mathematical Sciences, 12(3), pp.177-183. https://doi.org/10.1007/s40096-018-0257-1

Davoudi, M., Aleghafouri, A. and Safadoost, A., 2014. Flaring networks assessment in South Pars Gas processing plant. Journal of Natural Gas Science and Engineering, 21, pp.221-229. https://doi.org/10.1016/j.jngse.2014.08.008

Ghasemzadeh, K., Jafari, M. and Babalou, A.A., 2016. Performance investigation of membrane process in natural gas sweeting by membrane process: Modeling study. Chemical Product and Process Modeling, 11(1), pp.23-27. https://doi.org/10.1515/cppm-2015-0054

Ghasemzadeh, K., Jafari, M. and Basile, A., 2017. Theoretical Study of Various Configurations of Membrane Processes for Olefins Separation. International Journal of Membrane Science and Technology, 4, pp.1-7. http://dx.doi.org/10.15379/2410-1869.2017.04.01.01

Hajilary, N., Rezakazemi, M. and Shahi, A., 2020. CO_2 emission reduction by zero flaring startup in gas refinery. Materials Science for Energy Technologies, 3, pp.218-224. https://doi.org/10.1016/j.mset.2019.10.013

Hajizadeh, A., Mohamadi-Baghmolaei, M., Azin, R., Osfouri, S. and Heydari, I., 2018. Technical and economic evaluation of flare gas recovery in a giant gas refinery. Chemical Engineering Research and Design, 131, pp.506-519. https://doi.org/10.1016/j.cherd.2017.11.026

Hindman, H., 2013, June. Methanol to gasoline technology. In The Twenty-third International Offshore and Polar Engineering Conference. OnePetro.

Icaza, D., Borge-Diez, D. and Galindo, S.P., 2021. Proposal of 100% renewable energy production for the City of Cuenca-Ecuador by 2050. Renewable Energy, 170, pp.1324-1341. https://doi.org/10.1016/j.renene.2021.02.067

Iora, P., Bombarda, P., Gómez Aláez, S.L., Invernizzi, C., Rajabloo, T. and Silva, P., 2016. Flare gas reduction through electricity production. Energy Sources, Part A: Recovery, Utilization, and Environmental Effects, 38(21), pp.3116-3124. https://doi.org/10.1080/15567036.2015.1129471

Jaccard, M., Hoffele, J. and Jaccard, T., 2018. Global carbon budgets and the viability of new fossil fuel projects. Climatic Change, 150(1), pp.15-28. https://doi.org/10.1007/s10584-018-2206-2

Jafari, M., Ashtab, S., Behroozsarand, A., Ghasemzadeh, K. and Wood, D.A., 2018. Plant-wide Simulation of an Integrated Zero-Emission Process to Convert Flare Gas to Gasoline. Gas Processing Journal, 6(1), pp.1-20. 10.22108/GPJ.2018.111048.1028

Jafari, M., Ghasemzadeh, K., Yusefi Amiri, T. and Basile, A., 2019. Comparative Study of Membrane and Absorption Processes Performance and their Economic Evaluation for CO_2 Capturing from Flue Gas. Gas Processing Journal, 7(2), pp.37-52. 10.22108/GPJ.2019.116263.1053

Jafari, M., Sarrafzadeh, M.H. and Ghasemzadeh, K., 2020a. Simulation and economic evaluation of heat and power generation from flare gases in a combined cycle power plant. Energy Equipment and Systems, 8(4), pp.307-322. 10.22059/EES.2020.241289

Jafari, M., Vatani, A. and Deljoo, M.S., 2020b. Simulation and Economic Evaluation of Polygeneration System for Coproduction of Power, Steam, CH_3OH, H_2, and CO_2 from Flare Gas. Iranian Journal of Oil and Gas Science and Technology, 9(4), pp.93-114. 10.22050/IJOGST.2020.227023.1547

Jafari, M. and Garakani, A.K., 2021a. Techno-Economic Analysis of Heavy Fuel Oil Hydrodesulfurization Process for Application

in Power Plants. Iranian Journal of Oil & Gas Science and Technology, 10(1), pp.40-65. http://dx.doi.org/10.22050/ijogst.2020.254534.1569

Jafari, M., Nezhadfard, M. and Khalili-Garakani, A. 2021b. Simulation and Economic Analysis of Combined Desalinated Water and Power Generation from Associated Gases of Cheshmeh Khosh. Iranian Journal of Oil and Gas Science and Technology, 10(1), pp. 01-014. 10.22050/IJOGST.2020.219350.1536

Jones, S.B. and Zhu, Y., 2009. Techno-economic analysis for the conversion of lignocellulosic biomass to gasoline via the methanol-to-gasoline (MTG) process.

Karamelikli, H., Akalin, G. and Arslan, U., 2017. Oil exports and non-oil exports: Dutch disease effects in the Organization of Petroleum Exporting Countries (OPEC). Journal of Economic Studies. https://doi.org/10.1108/JES-01-2016-0015

Lee, S., Gogate, M. and Kulik, C.J., 1995. Methanol-to-gasoline vs. dme-to-gasolne II. process comparison and analysis. Fuel science & technology international, 13(8), pp.1039-1057. https://doi.org/10.1080/08843759508947721

Lopez-Echeverry, J.S., Reif-Acherman, S. and Araujo-Lopez, E., 2017. Peng-Robinson equation of state: 40 years through cubics. Fluid Phase Equilibria, 447, pp.39-71. https://doi.org/10.1016/j.fluid.2017.05.007

Luo, X., Wang, M., Oko, E. and Okezue, C., 2014. Simulation-based techno-economic evaluation for optimal design of CO_2 transport pipeline network. Applied Energy, 132, pp.610-620. https://doi.org/10.1016/j.apenergy.2014.07.063

Materazzi, M. and Holt, A., 2019. Experimental analysis and preliminary assessment of an integrated thermochemical process for production of low-molecular weight biofuels from municipal solid waste (MSW). Renewable Energy, 143, pp.663-678. https://doi.org/10.1016/j.renene.2019.05.027

Meng, H., Wang, M., Aneke, M., Luo, X., Olumayegun, O. and Liu, X., 2018. Technical performance analysis and economic evaluation of a compressed air energy storage system integrated with an organic Rankine cycle. Fuel, 211, pp.318-330. https://doi.org/10.1016/j.fuel.2017.09.042

Moradi, M., Ghorbani, B., Ebrahimi, A. and Ziabasharhagh, M., 2021. Process integration, energy and exergy analyses of a novel integrated system for cogeneration of liquid ammonia and power using liquefied natural gas regasification, CO_2 capture unit and solar dish collectors. Journal of Environmental Chemical Engineering, 9(6), p.106374. https://doi.org/10.1016/j.jece.2021.106374

Nejat, T., Movasati, A., Wood, D.A. and Ghanbarabadi, H., 2018. Simulated exergy and energy performance comparison of physical-chemical and chemical solvents in a sour gas treatment plant. Chemical Engineering Research and Design, 133, pp.40-54. https://doi.org/10.1016/j.cherd.2018.02.040

Nian, C.W. and You, F., 2013. Design of methanol plant. In EURECHA Student Contest Problem Competition ESCAPE-23 Symp. (p. 25).

Pauletto, G., Galli, F., Gaillardet, A., Mocellin, P. and Patience, G.S., 2021. Techno economic analysis of a micro-Gas-to-Liquid unit for associated natural gas conversion. Renewable and Sustainable Energy Reviews, 150, p.111457. https://doi.org/10.1016/j.rser.2021.111457

Puricelli, S., Cardellini, G., Casadei, S., Faedo, D., Van den Oever, A.E.M. and Grosso, M., 2021. A review on biofuels for light-duty vehicles in Europe. Renewable and Sustainable Energy Reviews, 137, pp.110398. https://doi.org/10.1016/j.rser.2020.110398

Rahimpour, M.R., Jamshidnejad, Z., Jokar, S.M., Karimi, G., Ghorbani, A. and Mohammadi, A.H., 2012. A comparative study of three different methods for flare gas recovery of Asalooye

Gas Refinery. Journal of Natural Gas Science and Engineering, 4, pp.17-28. https://doi.org/10.1016/j.jngse.2011.10.001

Saidi, M., 2018. Application of catalytic membrane reactor for pure hydrogen production by flare gas recovery as a novel approach. International Journal of Hydrogen Energy, 43(31), pp.14834-14847. https://doi.org/10.1016/j.ijhydene.2018.05.156

Saebea, D., Authayanun, S. and Arpornwichanop, A., 2019. Process simulation of bio-dimethyl ether synthesis from tri-reforming of biogas: CO_2 utilization. Energy, 175, pp.36-45. https://doi.org/10.1016/j.energy.2019.03.062

Stanley, I.O., 2009. Gas-to-Liquid technology: Prospect for natural gas utilization in Nigeria. Journal of natural gas science and engineering, 1(6), pp.190-194. https://doi.org/10.1016/j.jngse.2009.12.001

Sunny, A., Solomon, P.A. and Aparna, K., 2016. Syngas production from regasified liquefied natural gas and its simulation using Aspen HYSYS. Journal of Natural Gas Science and Engineering, 30, pp.176-181. https://doi.org/10.1016/j.jngse.2016.02.013

Wan, Z., Li, G.K., Wang, C., Yang, H. and Zhang, D., 2018. Effect of reaction conditions on methanol to gasoline conversion over nanocrystal ZSM-5 zeolite. Catalysis Today, 314, pp.107-113. https://doi.org/10.1016/j.cattod.2018.01.017

Wang, Z., He, T., Li, J., Wu, J., Qin, J., Liu, G., Han, D., Zi, Z., Li, Z. and Wu, J., 2016. Design and operation of a pilot plant for biomass to liquid fuels by integrating gasification, DME synthesis and DME to gasoline. Fuel, 186, pp.587-596. https://doi.org/10.1016/j.fuel.2016.08.108

Ziyarati, M.T., Bahramifar, N., Baghmisheh, G. and Younesi, H., 2019. Greenhouse gas emission estimation of flaring in a gas processing plant: Technique development. Process Safety and Environmental Protection, 123, pp.289-298. https://doi.org/10.1016/j.psep.2019.01.008

Zolfaghari, M., Pirouzfar, V. and Sakhaeinia, H., 2017. Technical characterization and economic evaluation of recovery of flare gas in various gas-processing plants. Energy, 124, pp.481-491. https://doi.org/10.1016/j.energy.2017.02.084

JOURNAL OF GAS TECHNOLOGY

Volume 6 / Issue 2 / Winter 2021 / Pages 45-52

Journal Homepage: http://jgt.irangi.org

Natural Gas Transmission in Dense Phase Mode

Mortaza Zivdar[1*], Moslem Abofarakh[2]

1. Professor, Chemical Engineering Department University of Sistan and Baluchestan, Zahedan, Iran
2. Msc. Student, Chemical Engineering Department University of Sistan and Baluchestan, Zahedan, Iran

ARTICLE INFO

ORIGINAL RESEARCH ARTICLE

Article History:
Received: 26 March 2021
Revised: 13 May 2021
Accepted: 29 June 2021

Keywords:
Dense Phase
Natural Gas Transmission
Pipelines
Simulation

ABSTRACT

Natural gas transmission processes in the pipeline encounter many problems, such as the high cost of purchasing and maintaining compressors in pressure boosting stations, the formation of gas hydrates, the formation of two-phase fluid, noise pollution, and service and maintenance costs of the pipeline. To solve these problems, natural gas transmission in the supercritical state (dense phase state) is recommended. Unfortunately, there is limited information on the transmission of natural gas in the dense phase. In this research, the natural gas transmission of Iran's fourth national pipeline in the supercritical state has been studied, and the results have been compared with the normal state. By performing this process in the dense phase mode, the number of pressure stations was reduced from 10 stations in the normal mode to 4 stations in the dense phase mode. The results of this study also showed that the pressure drop and energy of compressors in the dense phase state were reduced by 59% and 60%, respectively.

DOR: 20.1001.1.25885596.2021.7.2.4.6

How to cite this article
M. Zivdar, M. Abofarakh. Natural Gas Transmission in Dense Phase Mode. Journal of Gas Technology. 2021; 6(2): 45 -52.
(http://jgt.irangi.org/article_251677.html)

* Corresponding author.
E-mail address: mzivdar@eng.usb.ac.ir (M. Zivdar)

Available online 26 December 2021

1. Introduction

Despite the advances in renewable energy, natural gas is still one of the primary needs for society and industry. The important issue, after dehydration and sweetening of natural gas, is the transmission of natural gas to industries, cities, and countries. There are methods such as pipeline, gas compression, conversion of natural gas to liquid, conversion of natural gas to valuable liquids, and etc.) Thomas, 2003(. The pipeline method is the most common method of transporting natural gas in most countries. However, the transmission of natural gas through the pipeline has problems such as the high cost of purchasing and maintaining compressors at pressure stations, the formation of gas hydrates, the presence of the two-phase fluid within the pipeline, noise pollution, and the cost of servicing and maintaining the pipeline (Dai et al, 2017; Wenyue, 2013; Wang and Xuan, 2013). Various works have been done to reduce the problems related to gas transmission in the pipeline. Shiekh (2013) examined the gas transmission process in the pipeline to minimize transmission costs. The results of this study showed that by optimizing design variables, such as diameter, the distances between the pressure stations, and condenser outlet pressure, the cost of gas transmission through the pipe reduced (Shiekh, 2013). Liu et al (2014) studied the gas transfer process to reduce energy consumption. The results of this study showed that by optimizing the pressure station and temperature parameters, energy consumption was reduced by 11 to 16% (Liu et al, 2014). Wu et al (2018) reviewed studies on pipeline optimization. Finally, they reported optimization algorithms that required less computation (Wu et al, 2018). According to the reviewed studies, all works were focused on optimizing design variables to reduce the problems and costs of the gas transmission pipelines. The results of these researches show that although using these methods was useful in reducing gas transmission problems in the pipeline, the use of new methods for further improvement of the performance of gas transmission in pipelines is needed. Gas transmission in the pipeline in the dense phase mode is a suggestion to reduce the problems related to gas transmission in the normal state. In fact, in the dense phase state, the density of the fluid is similar to that of liquids, and its viscosity is similar to the gases. Due to the dual nature of the fluid, some problems created during the transfer of gas in the normal state are eliminated. To transfer natural gas to the dense phase state, the gas pressure should be higher than the maximum pressure in the phase diagram (Cricondenbar) and also the gas temperature should be higher than the critical temperature and lower than the maximum temperature in the two-phase region (Cricondentherm) (Moshfeghian, 2012; Zivdar and Abrofarakh, 2021). Despite the advantages of gas transmission in the dense phase state, there are not enough studies pertinent to gas transmission in the dense phase mode. This study considered the natural gas transmission of Iran's fourth pipeline in the dense phase state. The results of this case were compared with the results of gas transmission in normal conditions to show how dense phase has a better performance.

2. Mathematical

The one-dimensional equations of continuity, energy and momentum for the gas inside the pipeline are shown as follows, respectively (Helgaker and Ytrehus, 2012).

Continuity:

$$\frac{\partial \rho}{\partial t} + \frac{\partial (\rho u)}{\partial x} = 0 \quad (1)$$

Energy:

$$\rho C_v \left(\frac{\partial T}{\partial t} + u \frac{\partial T}{\partial x} \right) + T \left(\frac{\partial p}{\partial T} \right)_\rho \frac{\partial u}{\partial x} = \frac{f \rho u^3}{2D} - \frac{4U}{D} (T - T_a) \quad (2)$$

Momentum:

$$\frac{\partial (\rho u)}{\partial t} + \frac{\partial (\rho u^2 + p)}{\partial x} = -\frac{f \rho u |u|}{2D} - \rho g \sin\theta \quad (2)$$

In these equations ρ is density, u is velocity, C_v is Heat capacity at constant volume, T is temperature, p is pressure, f is the friction factor, and D is the diameter of the pipeline.

3. Case study

In this research, the aim is to transfer the natural gas of the fourth national pipeline to the dense phase state and compare it with the normal mode. Tables 1 and 2 show the natural gas components and the fourth national pipeline information, respectively.

Table 1. Gas components of the fourth national pipeline

Components	Percentage of molar fraction (%)
C_1	90
C_2	5
C_3	0.6
NC_4	0.1
NC_5	0.06
C_6	0.02
C_7	0.02
N_2	3.2
CO_2	1

Table 2. Fourth pipeline information

Parameter	value
D (in)	56
Pin (Psia)	1250
Tin (°F)	120
L (km)	1140
n (lbmol/hr)	250000

Figure 1 shows the different areas of natural gas of the fourth national pipe line in the phase diagram

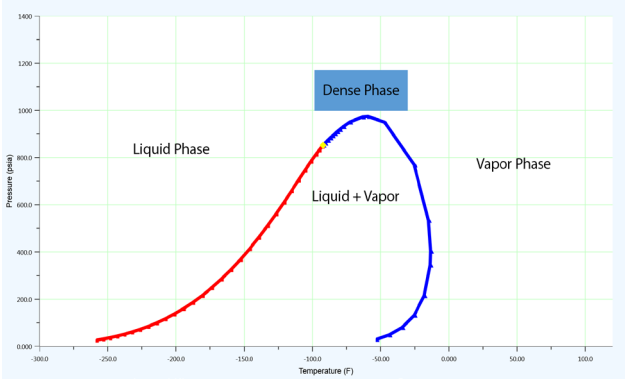

Figure 1. Different areas of natural gas of the fourth national pipeline in the phase diagram

According to Figure 1, to transfer the natural gas to the dense phase, the gas pressure and temperature along the entire length of the pipeline should be greater than 974 Pisa and -92 °F, respectively.

4. Simulation

In this section, pipeline simulations are performed in both normal and dense phase state with Aspen Plus software. One of the important parameters in the simulation is the selection of the appropriate thermodynamic package to calculate the physical and thermodynamic properties of the system. In this research, the Peng Robinson thermodynamic model is used (Kamal, 2002).

4.1. Simulation of the fourth pipeline in normal mode

The fluid enters the pipeline with the pressure of 1250 Pisa and enters the pressure station with a pressure of 1133 Pisa. Each pressure boosting station includes a compressor and a heat exchanger whose job is to bring the gas condition to the inlet state of the pipeline. In fact, Outlet gas from each section of the pipeline enters the pressure boosting station, and its pressure is increased. The temperature is also increased using a heat exchanger to reach the inlet temperature. There are 10 pressure boosting stations along the entire length of the pipeline, and each station is 114.5 km away from the next station. The simulation of the fourth pipeline with Aspen Plus software is shown in Figure 2.

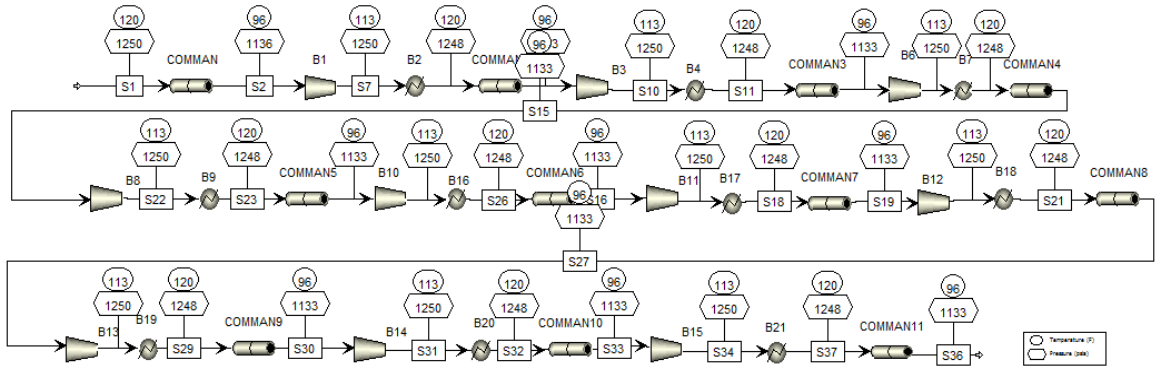

Figure 2. Fourth pipeline simulation in normal mode

4.1. Natural gas simulation of the fourth pipeline in dense phase mode

To transfer the gas to the dense phase area, it should be cooled from 120°F to -60°F at a constant pressure since the gas inlet pressure is more than 974 Pisa. Figure 3 shows the cooling of the inlet gas in a phase diagram.

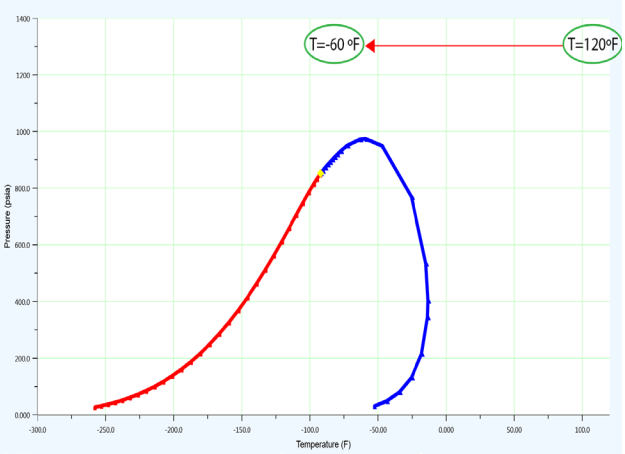

Figure 3. Cooling of natural gas at constant pressure

In the dense phase state, gas enters the pipeline with a temperature of -60°F and a pressure of 1250 Pisa. Since the pressure drop in the supercritical state is less than the normal state, less pressure boosting stations are needed in the supercritical state. The simulation of the fourth pipeline in supercritical mode with Aspen Plus software is shown in Figure 4. According to the less reduction of the pressure drop, it was found that the pressure boosting stations has been decreased from 10 to 4, while the distance between each pressure station and the next station is 228 km. The outlet pressure in each section before entering the pressure boosting station was equal to 1130 Pisa. In this case, 4 stations are responsible for bringing the gas to the temperature and natural gas pressure in the initial state. In fact, the outlet gas from each section of the pipeline enters the pressure boosting station, and its pressure increases to 1250 Pisa, then enters the heat exchanger to reach a temperature of -60°F.

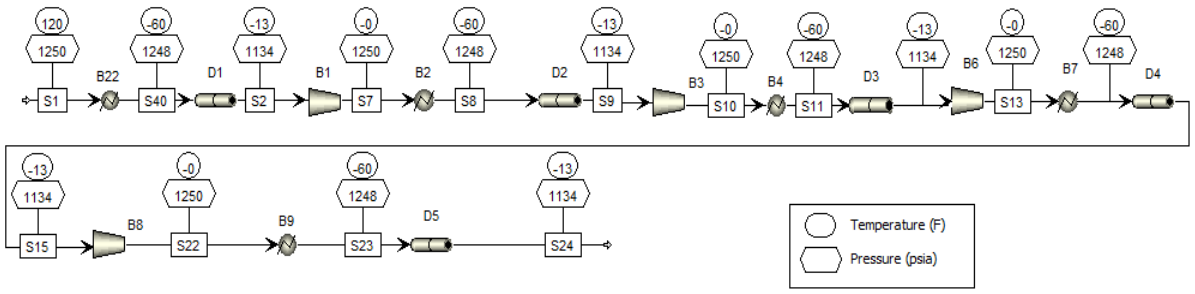

Figure 4. Fourth national pipeline simulation in dense phase mode

5. Results and discussion

In this research, the fourth pipeline is simulated in both normal and supercritical conditions. The results obtained from these two cases are compared as:

5.1. Temperature and pressure changes in supercritical state

Figure 5 shows the phase diagram of temperature and pressure changes in the supercritical state along 228 km of the pipeline. In this figure, state 1 shows the temperature and pressure conditions of the inlet, and state 2 shows the outlet conditions.

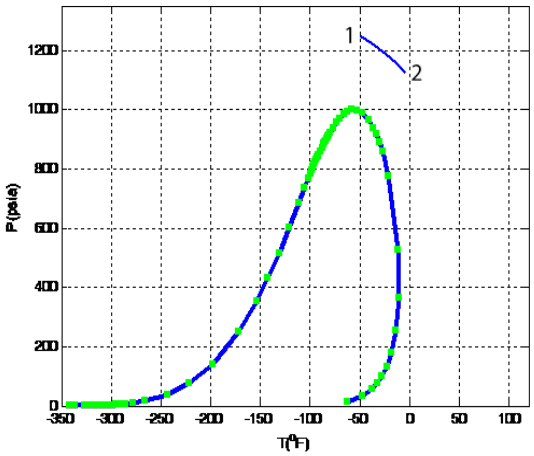

Figure 5. Temperature and pressure changes in the pipeline in supercritical state: 1: Input conditions 2: outlet conditions from the pipeline

5.2. Checking of hydrate formation in the supercritical state

Figure 6 is considered to check the formation of gas hydrate, which is one of the problems related to the normal transfer of gas through the pipeline. According to Figure 6, it is clear that in the entire length of the pipeline in the dense phase state, the fluid conditions are far from the hydrate formation condition as well as the two-phase fluid formation. Due to the absence of gas hydrates and also the absence of two-phase fluid inside the pipeline, the cost of service and maintenance of the pipeline in the supercritical condition was reduced.

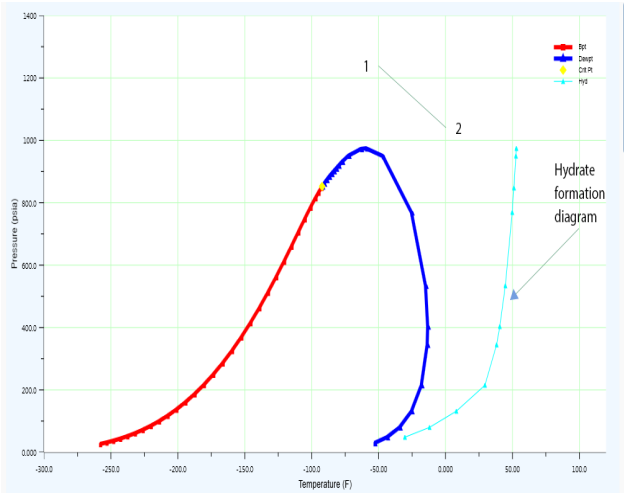

Figure 6. Gas hydrate diagram: 1: Input conditions 2: Output conditions from the pipeline

5.3. Comparison of the outlet pressure in both normal and dense phase modes

Figure 7 shows the comparison between the outlet pressure in both cases of the normal and dense gas transmission. According to Figure 7, the output pressure in the dense phase state is 53% lower than in the normal state. The reason for the lower output pressure in the supercritical state is the lower viscosity of the gas in the supercritical state compared to the normal state.

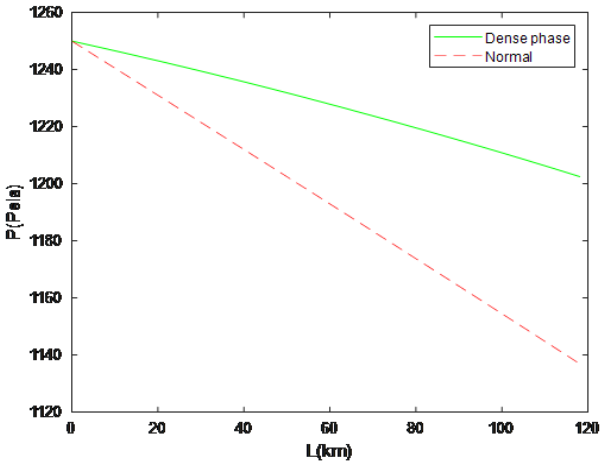

Figure7. Outlet pressure changes in both dense phase and normal cases.

5.4. Checking the pressure drop in both normal and dense phase mode

In order to show the difference between the pressure drops in the pipeline, the amount of pressure drop at a certain distance in the pipeline is compared in both cases. Figure 8 shows the result of this comparison. According to Figure 8, the pressure drop in the supercritical mode is 59% less than the normal mode. Therefore, the number of pressure stations in the supercritical state is reduced compared to the normal state. So, the need to purchase a large number of compressors and the cost of installation and maintenance in the gas transmission path is significantly reduced. Also, due to the high noise created in pressure boosting stations, with the reduction of stations, the amount of noise pollution in the areas will decrease.

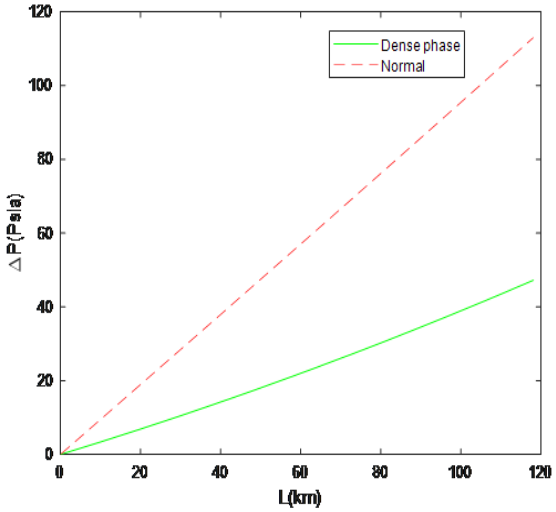

Figure 8. Pressure drop changes in the both dense and normal cases

5.5. Temperature changes in both normal and dense phase states

Figure 9 shows the temperature changes along the pipeline for both normal and dense phase modes. According to the figure, in both cases, the temperature changes were almost the same.

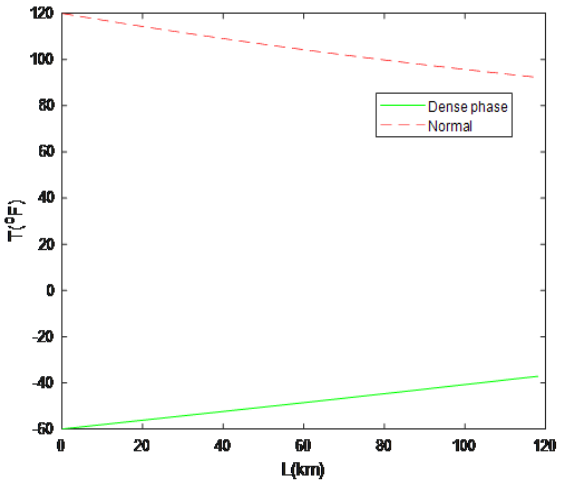

Figure 9. Temperature changes for the two cases

5.6. Comparison of compressor power and heat exchanger energy values in both normal and supercritical modes

Tables 3 and 4 show the power values of compressors and heat exchangers in two modes.

Table 3. Compressor power consumption for the two cases

Compressor power in dense phase mode (hp)	Compressor power in normal mode (hp)
56424	**141060**

According to Table 3, the power values of the compressors in the supercritical mode is 60% less than the normal mode, which indicates the reduction of the problem related to the high power required for the compressors in the normal gas transfer process.

Table 4. Energy required in the heat exchangers

Energy of heat exchangers in supercritical mode (MW)	Energy of heat exchangers in supercritical mode (MW)
563	58.7

According to the results of Table 4, it is clear that the amount of energy required for the heat exchanger in the dense phase mode is more than the normal mode, which is due to the cooling of the gas in the supercritical process.

6. Conclusion

In this research, gas transmission simulations in the pipeline in normal and dense phase conditions have been performed, and the performance of these two cases have been compared. The results of this study showed that by using the fluid in the dense phase mode, the gas transmission performance in the pipeline had been greatly improved so that:

- The outlet pressure in the supercritical mode was 53% less than the normal mode. Also, the pressure drop in the supercritical state was 59% less than usual. Therefore, the number of pressures boosting stations in the supercritical mode has been decreased from 10 stations to 4 stations.
- The cost of installation and maintenance of compressors was reduced due to a significant reduction of the pressure boosting stations. Also, due to the high noise of the station, with the decrease in the station numbers, noise pollution in the areas was reduced.
- The energy requirement of the compressors in the supercritical state was 60% less than the normal state, which shows a solution for the problem related to the high power required for the compressors in the normal gas transfer process.
- No hydrates and two-phase fluid were formed along the pipeline in the supercritical state. So, the cost of servicing and maintaining the pipeline in the supercritical state has been reduced.

Nomenclature

C_v	Heat capacity at constant volume (J/(kg.K))
D	Diameter (m)
F	Friction factor
L	Length (km)
P	Pressure (Pa)
T	Temperature (°C)
U	Heat transfer coefficient (W/ (m^2.K))
u	Velocity (m/s)
T	Temperature (°C)
T_a	Ambient temperature (°C)
Greek letters	
ρ	Density (kg/m^3)

References

Dai, L., Wang, D., Wang, T., Feng, Q., Yang, X., 2017. Analysis and Comparison of Long-Distance Pipeline Failures. Petroleum Engineering, 2017, Article ID 3174636. https://doi.org/10.1155/2017/3174636.

Helgaker, H., Ytrehus, T., 2012. Coupling between Continuity/Momentum and Energy Equation in 1D Gas Flow. Energy Procedia. 26, 82-89. https:// doi. 10.1016/j.egypro.2012.06.013.

Kamal, K.B., 2002. Performance of five equations of state for the prediction of VLE and densities of natural gas mixtures in the dense phase region. Chem. Eng. Comm., 189, 151-172. https://doi.org/10.1080/00986440211837.

Liu, E., Li, CH., Yang, Y., 2014. Optimal Energy Consumption Analysis of Natural Gas Pipeline. The Scientific World Journal. 2014, PMC4053082. https://doi.10.1155/2014/506138.

Moshfeghian, M., 2012., Gas Processing, Process Facilities, http://www.jmcampbell.com/tip-of-the-month/2012/08/transportation-of-natural-gas-in-dense-phase/.

Shiekh, T.M., 2013. The Optimal Design of Natural Gas Transmission Pipelines. Energy Sources, Part B: Economics Planning and Policy. 8, 7-13. https://doi.org/10.1080/15567240802534193.

Thomas, S., Dawe, R., 2003. Review of Ways to Transport Natural Gas Energy from Countries Which Do Not Need the Gas for Domestic Use. Energy. 28, 1461-1477. https://doi.org/10.1016/S0360-5442(03)00124-5.

Wang, T., Xuan, W., Wang, X., Ren, K., 2013. Overview of oil and gas pipeline failure database. International Conference on Pipelines and Trenchless Technology. ICPTT, 2013, 1161-1167. https://doi.org/10.1061/9780784413142.121.

Wenyue, Z., 2013. corrosion cracking of oil and gas pipelines in near neutral pH environment: Review of recent research. Energy Materials: Materials Science and Engineering for Energy Systems. 3, 220-226. https://doi.org/10.1179/174892309X12555944292234.

Wu, X., Li, Y., He., Y., Jia, W., 2018. Operation Optimization of Natural Gas Transmission Pipelines Based on Stochastic Optimization Algorithms: A Review. Mathematical Problems in Engineering, 2018, Article ID 1267045. https://doi.org/10.1155/2018/1267045.

Zivdar, M., Abrofarakh, M., Investigating the Natural Gas Transmission in Supercritical Condition. Iranian Chemical Engineering Journal. 20 (16), 50-63. Doi: 10.22034/ijche.2021.257914.1070.

JOURNAL OF GAS TECHNOLOGY

Volume 6 / Issue 2 / Winter 2021 / Pages 53-64

Journal Homepage: http://jgt.irangi.org

Feasibility Study of Using Waste Heat from Gas Pressure Reducing Stations for Water Desalination

Maryam Karami[1*], Farima Alikhani[2]

1. Faculty of Engineering, Kharazmi University, Tehran, Iran
2. Department of Mechanical Engineering, Alzahra University, Tehran, Iran

ARTICLE INFO

ORIGINAL RESEARCH ARTICLE

Article History:
Received: 26 June 2021
Revised: 01 August 2021
Accepted: 21 September 2021

Keywords:
Gas Pressure Reducing Station (PRS)
Water Desalination
Humidification-Dehumidification Unit
Numerical Simulation
Aspen HYSYS

ABSTRACT

In recent years, recovering waste heat to reduce energy consumption and provide the energy needs has become a promising method to solve the energy crisis. In this study, the waste heat from gas pressure reducing stations is used to produce fresh water using a humidification-dehumidification desalination unit. Using Aspen HYSYS to model the proposed system, the effect of different parameters on the fresh water production rate is evaluated. The results show that optimum saline water and air flow rates are 0.165 kg/s and 0.2 kg/s, respectively, for a gas pressure reducing station by a capacity of 50,000 standard cubic meters per hour. It is also found that by decreasing the gas inlet pressure from 1000 psi to 400 psi, the fresh water production rate is decreases by about 52.2%. The increase of the fresh water production rate by increasing the capacity of the pressure reducing station from 10,000 to 50,000 standard cubic meters per hour is about 62%. Furthermore, the fresh production rate at gas pressure reducing station with 10,000 SCMH increases 4.4% by increasing the saline water temperature entering the humidifier from 40°C to 80°C.

DOR: 20.1001.1.25885596.2021.7.2.5.7

How to cite this article
M. Karami, F. Alikhani. Feasibility Study of Using Waste Heat from Gas Pressure Reducing Stations for Water Desalination. Journal of Gas Technology. 2021; 6(2): 53 -64. (http://jgt.irangi.org/article_251678.html)

* Corresponding author.
E-mail address: karami@khu.ac.ir (M. Karami)

Available online 26 December 2021

1. Introduction

Today, the need for drinking water is increasing rapidly. This is while freshwater resources are limited or running low. Only about 3% of the earth's water resources are drinkable. However, 2% of it is frozen in polar glaciers and only 1% of fresh water (FW) is available to humans. On the other hand, the production of FW in the world faced with problems such as significant consumption of fossil fuels or high costs of installation and maintenance of solar collectors. In addition to the excessive costs, it can be also mentioned the production of greenhouse gases and environmental pollution due to fossil fuels. Therefore, it is necessary to use available free energy, which also has low-cost equipment.

There are numerous studies on using waste heat to produce FW (Elsaida et al., 2020; Olabi et al., 2020). Schwantes et al. (2013) performed an experimental investigation on the FW production using a membrane distillation (MD) unit and the waste heat from the cooling circuit of a diesel power station. Their results indicated that the waste heat-based desalination plant operates more steadily than a solar-based desalination unit and the FW of 3688 l is produced in 24 h. Sharshir et al. (2016) designed a combined solar desalination system that includes a humidifier, a dehumidifier and four systems of evaporation and condensation of water vapor. The new desalination system reuses the outlet hot water form humidifier-dehumidifier to supply the secondary system to prevent the loss of hot water during desalination. Reusing the hot drain water increases the system output ratio by 50% and increases the solar still by about 90%. Using the waste heat from gas fired power station for a direct contact membrane distillation (DCMD) system with 0.67 m^2 of membrane area, Dow et al. (2016) concluded that the FW production is 3 l/(m^2h), which depends mostly on the waste heat temperature. Lokare et al. (2017) used the waste heat from natural gas compressor stations for treatment of water generated during extraction of natural gas from unconventional (shale) reservoirs in Pennsylvania. An ASPEN Plus simulation of DCMD revealed that all the produced water can be treated to 30 wt% regardless of its initial salinity by using the waste heat available from natural gas compressor stations in Pennsylvania.

Lai et al. (2019) recovered the waste heat from the proton exchange membrane fuel cell to produce distilled water using DCMD. They found that the energy utilization degree increases by 201%-266% under maximal energy gain condition. He et al. (2018) proposed a humidification-dehumidification (HDH) system in which seawater is desalinated by heat recovery. The simulation results show that the maximum amount of water production is 99.05 kg/h and the output ratio is 1.51 when the dehumidifier equilibrium conditions appear in the design conditions, while the low cost of water production unit is equal to 37.68 $/kg.h and the air flow is 0.14 kg/h. Santosh et al. (2018) investigated the performance of a combined HDH system using the waste heat of vapor compression refrigeration (VCR) based on the air conditioning unit. It was found that with increasing air conditioning temperature, the average condensate production decreased. In addition, the economic analysis shows that the cost of FW produced by the proposed system is about $ 0.1658 per kilogram. Using waste heat from both the exhaust fumes and the cooling water of submarine engines, Shafieian and Khiadani (2020) reported that a DCMD unit can produce 8.3 kg/m^2h at cooling water flow rate of 0.25 kg/s and diesel exhaust mass ratio of 0.25.

Sorgulu and Dincer (2021) investigated the performance a hybrid multi-effect desalination (MED) and reverse osmosis (RO) units using biomass-based waste heat. The results show that 92.29 kg/s freshwater is produced using 2.498 kg/s of municipal solid and 0.1314 kg/s of olive oil waste. Shakib et al. (2021) studied using the waste hear from gas turbine cycle for water desalination by hybrid multi-effect thermal vapor compression desalination (MED-TVC)

and reverse osmosis (RO). The FW produced by the proposed system varied between 70,000 m^3/day and 140,000 m^3/day. The Summary of previous researches on waste heat-based water desalination is shown in Table 1.

Table 1. Summary of previous researches on waste heat-based water desalination

Author	Desalination unit	Waste heat source	Investigation type	Highlights
Schwantes et al. (2013)	MD	Cooling circuit of a diesel power station	Experimental	• Waste heat-based desalination plant operates more steadily than a solar-based desalination unit. • FW of 3688 l is produced in 24 h.
Sharshir et al. (2016)	HDH and four systems of evaporation and condensation of water vapor	Hot water form HDH	Numerical	• Daily water production rate is 13 L/h. • Reusing the hot drain water increases the system output ratio by 50%. It also increases the solar still by about 90%.
Dow et al. (2016)	DCMD	Gas fired power station	Experimental	• FW production rate is 3 l/(m^2h), which depends mostly on the waste heat temperature.
Lokare et al. (2017)	DCMD	Natural gas compressor stations	Numerical	• All produced water can be treated to 30 wt% regardless of its initial salinity.
Lai et al. (2019)	DCMD	Proton exchange membrane fuel cell	Numerical	• FW mass flow rate can lead to the maximal energy gain. • Energy utilization degree increases by 201%-266% under maximal energy gain condition
He et al. (2018)	HDH	Exhaust gas	Numerical	• Maximum amount of water production is 99.05 kg/h. • Output ratio is 1.51 at the dehumidifier equilibrium conditions. • Low cost of water production unit is 37.68 $/kg.h.
Santosh et al. (2018)	Hybrid HDH-VCR	Vapor compression refrigeration (VCR)	Numerical and Experimental	• By increasing air conditioning temperature, the average condensate production decreased. • Cost of FW produced is about $ 0.1658 per kilogram. • Maximum average freshwater yield is 4.63 kg/h and 4.13 kg/h.
Shafieian and Khiadani (2020)	DCMC	Exhaust fumes and cooling water of submarine engines	Numerical	• Freshwater productivity is more sensitive to temperature than mass flow rate. • FW of 8.3 kg/m^2h produces at cooling water flow rate of 0.25 kg/s and diesel exhaust mass ratio of 0.25
Sorgulu and Dincer (2021)	Hybrid MED-RO	Biomass	Numerical	• Overall energy and exergy efficiencies are 37.04% and 19.78%, respectively • 92.29 kg/s freshwater is produced using 2.498 kg/s of municipal solid and 0.1314 kg/s of olive oil waste.
Shakib et al. (2021)	Hybrid MED-TVC/RO	Gas turbine cycle	Numerical	• FW production rate varied between 70,000m^3/day and 140,000 m^3/day. • Lowest production cost is obtained using the cooling water of MED-TVC as the RO system feed water.

Natural gas pressure reducing stations at the inlets of suburban gas networks are responsible for regulating and reducing gas pressure. This pressure drop is from the range of 1000-1200 psi to about 250 psi. The pressure reduction process that occurs by the regulator reduces the temperature due to the positive Joule-Thomson coefficient. This decrease in temperature is so great that it causes the gas to freeze and condense. To prevent this problem, the gas is heated in the water bath heater before reaching the regulator. Most part of the fuel energy used in the heater is always wasted by exhausting the combustion products. Some attempts have been made to use this waste heat for various applications. Ghaebi et al. (2018) investigated using the waste heat of PRS heater for produce power and hydrogen. They combined a Rankine cycle (RC), an absorption power cycle (APC), and a proton exchange membrane (PEM) electrolyzer. The results indicate that the thermal and exergy efficiency of the combined PRS/PEM-RC systems were 32.9% and 47.9%, respectively, while these values for combined PRS/APC system were 33.6% and 48.9%, respectively. Naderi et al. (2018a) studied the performance of a water reheating system installed on the chimney of the heater. They found that the fuel consumption of the heater reduces by about 45% and the payback period is about 1.3 years. In another study, they reported that the heat exchanger with the coolant flow of 1.3 kg/s and fin per inch of 3.3 has the minimum pressure drop (Naderi et al., 2018b). By using the waste heat of the PRS heater for preheating the water inside the heater, Karami and Noroozi (2019) concluded that the energy consumption of heaters is decreased by about 50% and also, the heater efficiency increases by 20%.

One way to reuse this waste heat is desalinating of salt water to meet the needs of people for FW, which is one of the important issues and crises ahead. In an interesting work, Deymi-Dashtebayaz et al. (2021) proposed a multi-effect desalination thermal vapor compression (MED-TVC) system to produce FW using the waste heat of PRS heater. Their analysis showed that the optimal station capacity for a two effect MED-TVC system is a PRS with capacity of 11.5 kg/s.

As the literature review shows, there is no study on recovering the waste heat of a PRS heater for producing the FW with a small-scale HDH unit. Therefore, in this study, the thermal performance of a humidification-dehumidification desalination unit is investigated using the waste heat from the water bath heater of a PRS. The effect of the operating parameters on the FW production rate is evaluated by simulating the proposed system in Aspen HYSYS.

2. System description and simulation

The schematic of the proposed PRS-HDH system is indicated in Figure 1. The natural gas flow is heated passing the bath water heater to the desired temperature (usually 30 °C) and then, is throttled by the regulator to the desired pressure, which is normally 250 psi. The combustion products, which are still the high temperature heat source, flows in the heater chimney and goes to a heat exchanger, in which transfers its heat to the saline water flow from the dehumidifier. Then, the warm saline water is sprayed into the humidifier and is vaporized and absorbed by the air. This humid air goes to the dehumidifier and can be distilled and recycled by passing from cold surfaces to produce distilled water. The governing mass and energy conservation equations on the performance of the PRS heater and the HDH unit are defined in the following sections.

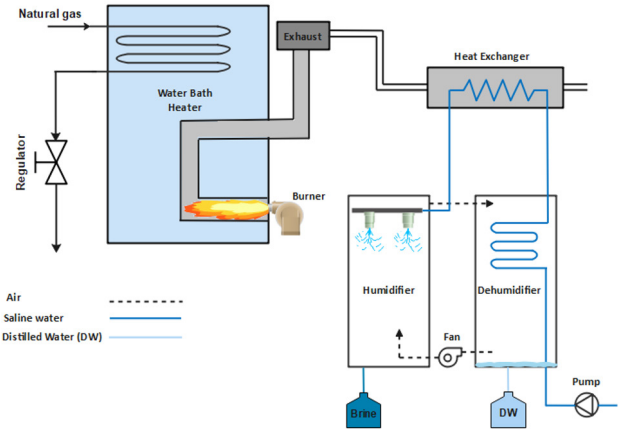

Figure 1. Schematic of the proposed PRS-HDH system

2.1. PRS heater

In water bath heaters, the combustion products outlet from the burner cause the water temperature inside the heater to rise and the water heats indirectly the natural gas inside the tubes. The schematic of the heater is shown in Figure 1. Therefore, considering the water bath heater as a control volume, the law of energy conservation is as follows (Bayat et al., 2016):

$$\dot{Q}_{load} = \dot{Q}_{swf} + \dot{Q}_{NG} + \dot{Q}_{water} \quad (1)$$

where $\dot{Q}_{load}$ is the heating value of the fuel, $\dot{Q}_{NG}$ is the heat transfer rate received by the natural gas, $\dot{Q}_{water}$ is the required heat transfer rate for increasing the water temperature inside the heater, and $\dot{Q}_{shl}$ is the heat loss due to radiation and convection form the heater surface.

The thermodynamics first law is used to calculate $\dot{Q}_{NG}$ as following:

$$\dot{Q}_{NG} = \dot{m}_{NG}\,(h_{out} - h_{in}) = \dot{m}_{NG} \int_{T_i}^{Tou_t} c_{p,NG}\, dT \quad (2)$$

where $\dot{m}_{NG}$ is the mass flow rate of natural gas and $C_{p,NG}$ is its specific heat, which is obtained as a function of temperature from the following relation:

$$c_{p,mix} = \sum Xi \times c_{p,i} \quad (3)$$

where X_i is the mass fraction of the natural gas component and C_{pi} is their specific heats. The combustion process has the constant pressure and all components are considered as ideal gas.

To determine $\dot{Q}_{shl}$, the temperature of the heater inside surface is considered equal to the temperature of the hot water inside heater:

$$\dot{Q}_{shl} = \frac{T_w - T_{am}}{\sum R_t} \quad (4)$$

where T_w is the temperature of heater inside water and R_t is the total thermal resistance of heater wall.

The required heat transfer rate for increasing the water temperature inside the heater ($\dot{Q}_{water}$) is calculated as follows:

$$\dot{Q}_{water} = \int_{i}^{i+1} \dot{m}_w \cdot c_{p,w}\, dT \quad (5)$$

The period of the calculation is one hour:

The heat transfer rate of the heater is calculated using $\dot{Q}_{load}$ and $\dot{Q}_{losses}$:

$$\dot{Q}_{heater} = \frac{\dot{Q}_{load}}{\eta_c} + \dot{Q}_{losses} \quad (6)$$

where η_c is the heater efficiency:

The volumetric flow rate of the fuel is obtained using the following relation:

$$\dot{V} = \frac{\dot{Q}_{heater}}{LHV} \quad (7)$$

2.2. HDH desalination unit

In Figure 2, the schematic of a closed air open water (CAOW) HDH desalination unit and its component is shown. The mass and energy conservation equations and the heat exchanger relations are used to model the performance of the HDH unit. It is assumed that the air flow is steady state and fully developed with constant thermo-physical properties. Considering the dehumidifier as a control volume, the mass, and energy conservation equations are written as follows (Narayan et al., 2010):

$$\dot{m}_{pw} = \dot{m}_a\,(\omega_{a,2} - \omega_{a,1}) \quad (8)$$

$$\dot{m}_w\,(h_{w,1} - h_{w,0}) + \dot{m}_{pw}\,h_{pw} = \dot{m}_a\,(h_{a,2} - h_{a,1}) \quad (9)$$

The mass and energy conservation equations for the humidifier are written as follows (Narayan et al., 2010):

$$\dot{m}_w - \dot{m}_a\,(\omega_{a,2} - \omega_{1,a}) = \dot{m}_b \quad (10)$$

$$\dot{m}_a\,(h_{a,1} - h_{a,2}) = \dot{m}_b\,h_{w,3} - \dot{m}_w h_{w,2} \quad (11)$$

The heat transfer from the collector to the fluid is obtained by using the following equation:

$$\dot{Q}_{heater} = \dot{m}_w\,c_{p,w}\,(T_{w,2} - T_{w,1}) \quad (12)$$

The gained output ratio (GOR) of the HDH is defined as:

$$GOR = \frac{\dot{m}_{fw}.h_{fg}}{\dot{Q}_{in}} \quad (13)$$

where $\dot{m}_{fw}$, h_{fg} and Q_{in} are fresh water mass flow rate, evaporation enthalpy and inlet thermal energy to the HDH

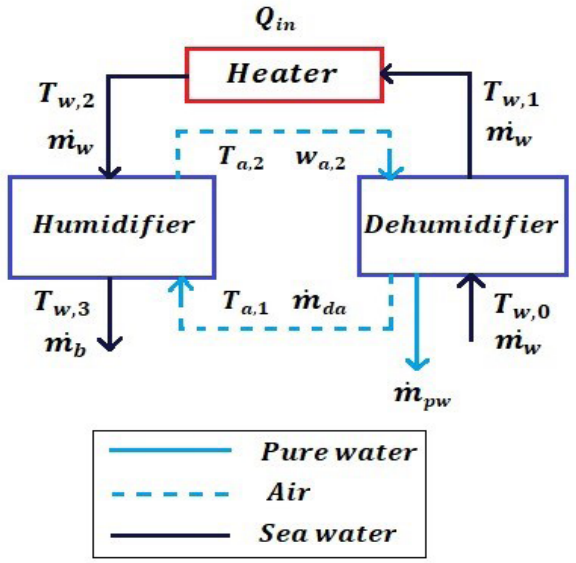

Figure 2. Schematic of a CAOW-HDH desalination system

2.3. Validation

Since there is no experimental data to validate the integrated PRS-HDH system, the PRS and HDH models are separately validated using the experimental results.

For validating the PRS model, the calculated gas outlet temperature from the model is compared with the gas outlet temperature from the PRS of Semnan

(Rastgar and Saedodin, 2013), which have measured in 10 days. The PRS characteristics are entered to the HYSYS model. Figure 3 indicates that the model has the proper accuracy and the mean absolute percentage error (MAPE) is 5.5%.

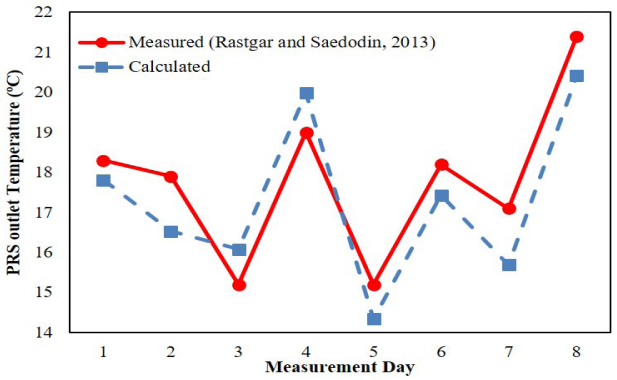

Figure 3. Comparison of measured (Rastgar and Saedodin, 2013) and calculated PRS outlet temperature

The results of the HDH model are compared with the results of the experimental study (Narayan et al., 2010). Table 2 indicates the measured and calculated GOR of the HDH in different saline water inlet temperature. As can be seen in Table 2, the experimental and numerical results were in good agreement by the MAPE of 6.2%.

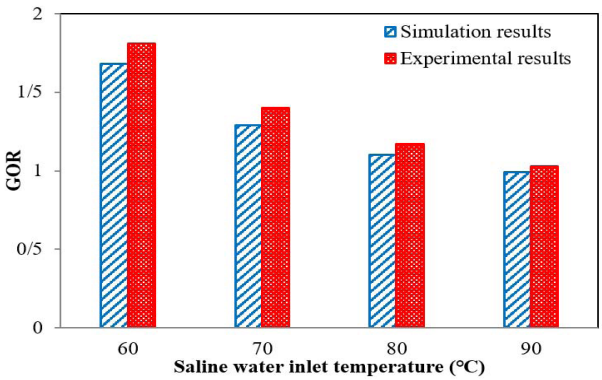

Figure 4. Comparison of the experimental (Narayan et al., 2010) and numerical GOR

2.4. Simulation

Figure 5 indicates the HYSYS model of the proposed PRS-HDH system. The features and HYSYS types of the components used to simulate the system are listed in Table 2. The specifications of the natural gas in the simulated PRS are shown in Table 3. To illuminate the simulation process, a flowchart is shown in Figure 6.

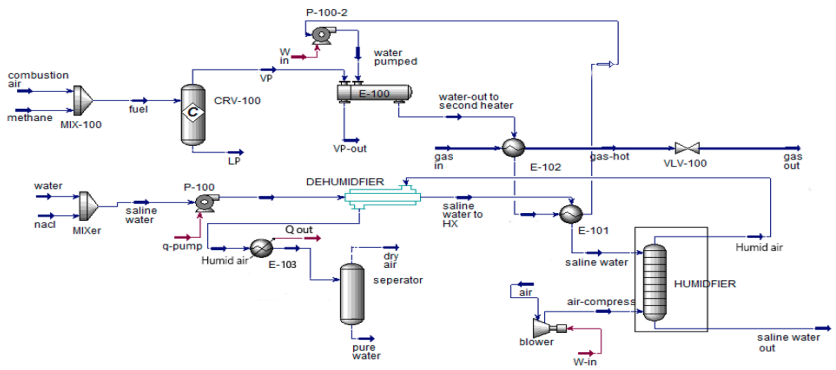

Figure 5. Simulation of the PRS-HDH system in Aspen HYSYS

Table 2. Features and HYSY type of the main components used in the simulation

Component	Features
Regulator	Type: VLV-100 Temperature [ºC]: 30 Pressure [psia]: 994 Volume flow rate [m^3/h]: 50,000
Pump	Type: P-100 Power [kW]: 0.02 Mass flow rate [kg/s]: 1.44 Pressure difference [psia]: 15.23
Reactor	Type: CRV-100 Reaction set: $CH_4 + 2O_2 \rightarrow CO_2 + 2H_2O$ Volume flow rate [m^3/h]: 771.4 Product temperature [ºC]: 1835
Shell and tube heat exchanger	Type: E-100 VP temperature [ºC]: 1835 VP outlet temperature [ºC]: 69 Pumped water temperature [ºC]: 66.95 Water-outlet to second heater temperature [ºC]:158
	Type: E-101 Water inlet temperature [ºC]: 69.85 Water outlet temperature [ºC]: 66.94 Saline water to HX temperature [ºC]: 50 Saline water to humidifier temperature [ºC]: 66
	Type: E-102 Inlet gas temperature [ºC]:10 Outlet gas temperature [ºC]: 30 Water inlet to second heater temperature [ºC]: 158 Water outlet temperature [ºC]: 69.85
Mixer	Mixing water with salt to produce a seawater fluid with mole fraction below: H_2O: 0.9873 NACL: 0.0127 Mass flow rate [kg/s]: 0.28
Separator	Separating H_2O from humid air with phase fractions below: Moisture air [H_2O-air]: 0.0774- 0.9225 Pure water Mass Flow [kg/s]: 0.03 Dry air Mass Flow[kg/s]: 0.66
Dehumidifier	Type: Shell and tube Saline water-pumped temperature [ºC]: 25.01 Saline water to HX temperature [ºC]: 50 Humid air temperature [ºC]: 54.92 Humid air to cooler temperature [ºC]: 45.07
Humidifier	Type: Absorber Add H_2O to dry air with phase fractions below: Humid air[H_2O-Air]: 0.0625- 0.9375

Table 3 Analysis of natural gas

Components	Mole fraction (%)
CH_4	95.4
N_2	0.9
CO_2	0.1
C_2H_6	2.3
C_3H_8	0.75
ISO - C_4H_{10}	0.13
N - C_4H_{10}	0.2
ISO - C_5H_{12}	0.08
N - C_5H_{12}	0.08
C_6H_{14}	0.04
C_7H_{16}	0.02

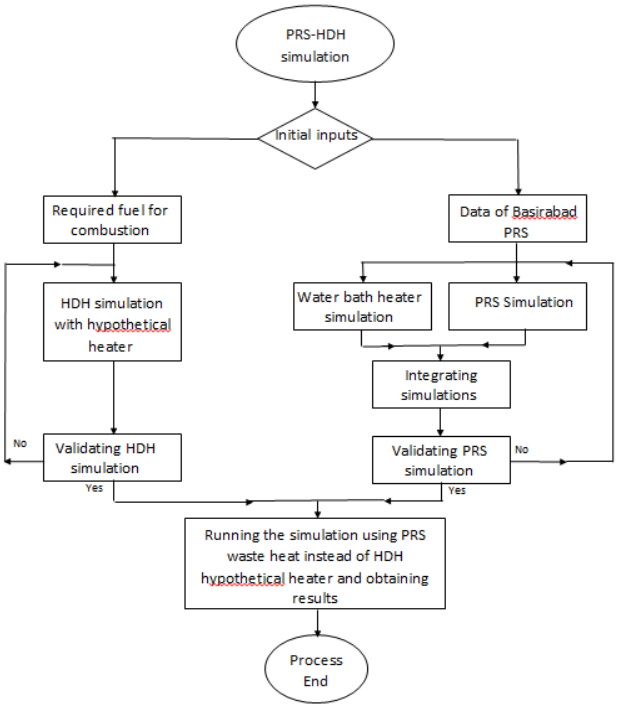

Figure 6. Flowchart of simulation process

3. Results and discussion

Figure 7 indicates the effect of combustion air temperature and excess air percentage on the adiabatic flame temperature and fuel consumption of the PRS burner. By increasing the temperature of air entering the burner, the combustion efficiency increases and the adiabatic flame temperature and thus, the fuel consumption reduces, as can be seen in Figure 7 (a). According to Figure 7 (b), increasing the percentage of excess air reduces the adiabatic flame temperature and thus, reduces the heat transfer from the combustion gases to the fire tube and more fuel is used to compensate for this shortcoming.

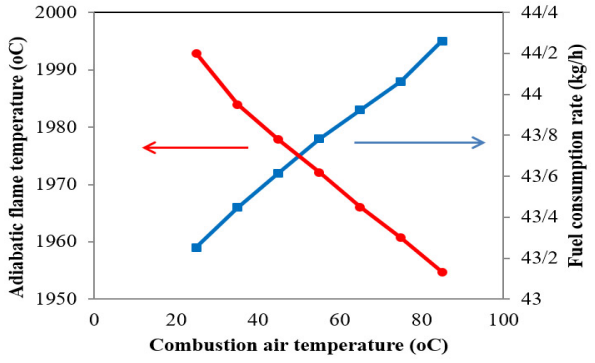

(a)

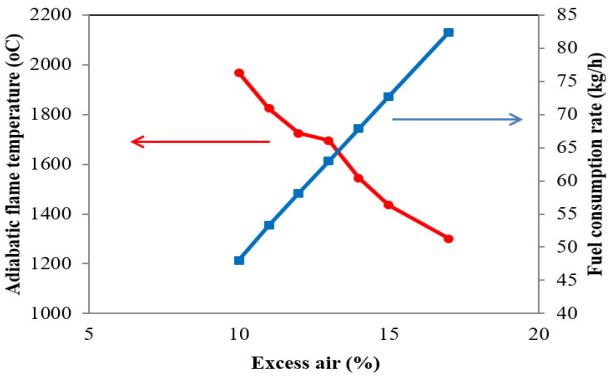

(b)

Figure 7. Variation of adiabatic flame temperature and fuel consumption by (a) combustion air temperature and (b) excess air

The variation of FW production rate by the mass flow rate of saline water and air are depicted in Figure 8. By increasing the mass flow rate of saline water to a desirable point, it is obvious that the production of the FW increases. However, after saturating the air by the water vapor, increasing the saline water flow rate has negative effect on the FW production rate, because the air temperature increases and then, the dehumidification process deteriorated. By increasing the air flow rate, the capacity of the air for absorbing more water vapor increases and therefor, the more FW is produced. However, similar to the saline water flow rate, the FW production rate decreases by increasing the air flow rate beyond the optimum value of the air

flow rate. This is because the water flow rate is constant and therefore, the released heat from the dehumidification process heats up less the air entering the humidifier. The results show that optimum saline water and air flow rate are 0.165 kg/s and 0.2 kg/s, respectively. In other words, the ratio of saline water to air flow rates should be 0.825 to produce the highest FW by the proposed system.

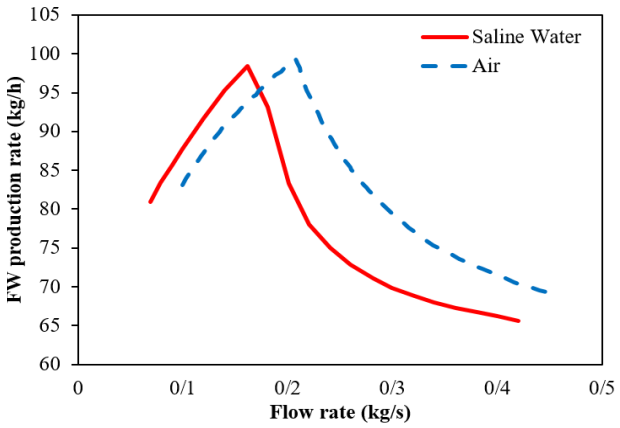

Figure 8. Variation of FW production rate by saline water and air mass flow rate

The variation of the FW production by the gas inlet pressure is indicated in Figure 9. By decreasing the gas inlet pressure, the fuel is required to heat the gas to the desired temperature in the heater reduces and therefore, the lower thermal energy delivers to the saline water and the FW production rate decreases. By decreasing the gas inlet pressure from 1000 psi to 400 psi, the FW production rate is decreases by about 52.2%.

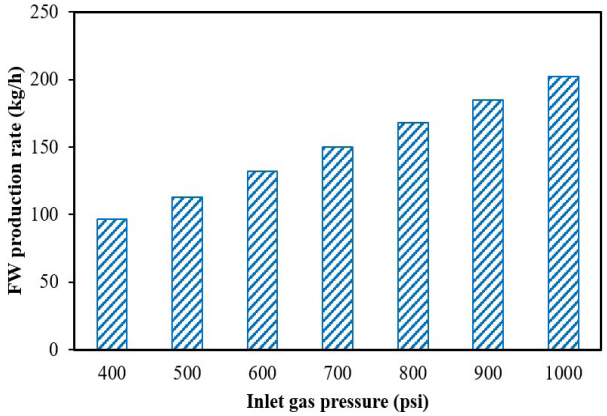

Figure 9. Effect of gas inlet pressure on FW production rate

In Figure 10, the effect of gas flow rate of the PRSs in four different cities of Iran on the FW production rate is indicated. The PRS capacities are listed in Table 4. As observed, the FW production rate increases by increasing the gas flow rate because of the higher thermal energy of the combustion products which are used for heating the saline water entering the humidifier. The increase of the FW production rate by increasing the PRS capacity from 10,000 to 50,000 standard cubic meters per hour (SCMH) is about 62%.

Table 4 Capacity of different PRSs

Station name	Basirabad	Arjan	Bistoon	Shahrood
Station capacity (SCMH)	50,000	30,000	20,000	10,000

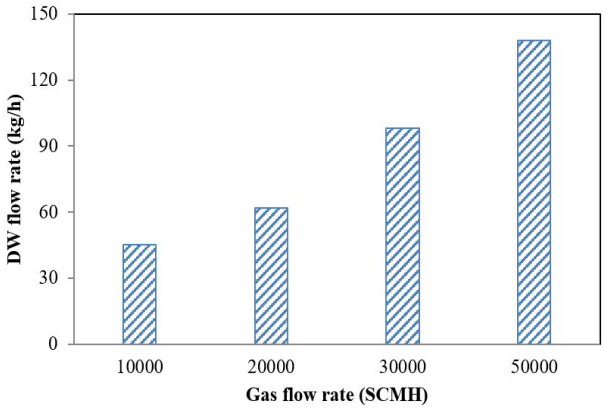

Figure 10. Effect of gas flow rate on FW production rate

The effect of the temperature of spray water into the humidifier and the temperature of saline water into the dehumidifier on the DW production rate is depicted in Figure 11. As can be seen, by increasing the capacity of the PRS, the FW production increases because of more heat transfer rate from the combustion products to the saline water. In Figure 7 (a), it is shown that the higher the temperature of the inlet water to the dehumidifier, the lower the heat exchange and the lower the capacity of the water to absorb heat from the air, and as a result, the air cools less and the water vapor in it becomes less condensed. By increasing the saline water temperature from 10°C to 40°C, the fresh production rate at PRS

with 10,000 SCMH decreases about 73.4%. This value for PRS with 50,000 SCMH is about 73.7%.

According to Figure 11 (b), the higher the temperature of the spray water in the humidifier, the more moisture the air absorbs and the FW production increases. Furthermore, it is found that by increasing the spray water temperature from 40°C to 80°C, the fresh production rate at PRS with 10,000 SCMH increases 4.4%. It should be noted that if the saline water temperature is too low, the spray water temperature reduces, which has an adverse effect on FW production; therefore, there is a limit for saline water temperature.

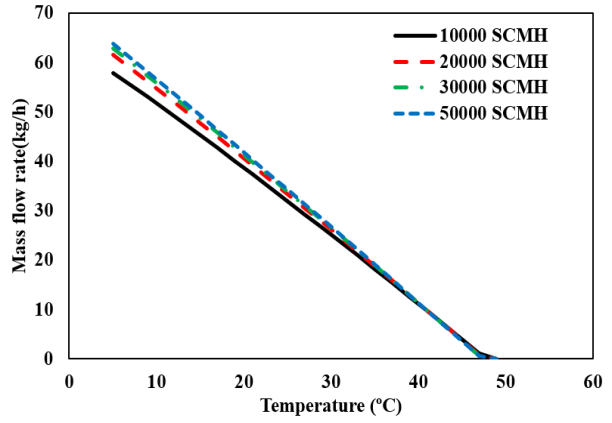

(a)

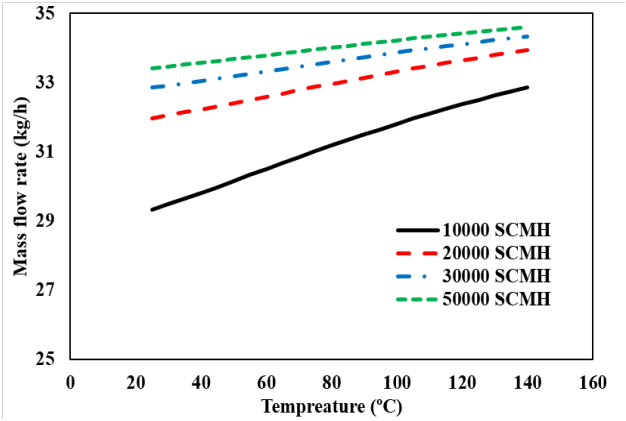

(b)

Figure 11 Effect of temperature of inlet saline water to (a) dehumidifier and (b) humidifier on FW production rate

4. Conclusions

In this study, the thermal performance of the PRS-HDH system integrating PRS heater with HDH desalination unit has been studied. It should be noted that a fixed HDH size is assumed for all PRSs because the fresh water production of the PRSs can be compared. Also, the heat exchangers, humidifier, and dehumidifier are considered insulated. Furthermore, it is assumed that the complete combustion process is occurred in a constant pressure chamber. The findings showed that by increasing the temperature of the combustion air, the combustion efficiency increases and the adiabatic flame temperature and thus, the fuel consumption reduces. Whereas, increasing the excess air percentage reduces the adiabatic flame temperature and thus, fuel consumption increases. It is also found that the production rate of the FW increases by increasing the mass flow rate of saline water, until the air is saturated with water vapor. Then, the production of FW decreases. The higher temperature of the inlet saline water to the dehumidifier results in the lower FW production rate. This is because the less heat exchange between the air and saline water and the lower the capacity of the water to absorb heat from the air. The higher spray water temperature in the humidifier results in the larger FW production rate because of more moisture absorbs by the air. Based on the obtained results, by increasing the air flow rate, the capacity of the air for absorbing more water vapor increases and therefor, the more FW is produced. However, the FW production rate decreases by increasing the air flow rate beyond the optimum value, because the released heat from the dehumidification process heats up less the inlet air to the humidifier. The results show that the ratio of saline water to air flow rates should be 0.825 to produce the highest FW by the proposed system. Considering the operating parameters of the PRS indicated that by decreasing the gas inlet pressure from 1000 psi to 400 psi, the FW production rate is decreases by about 52.2%. Furthermore, the increase of the FW production rate by increasing the PRS capacity from 10,000 SCMH to 50,000 SCMH is about 62%.

Nomenclature

c_p	Specific heat, kJ/kg K
h	Specific enthalpy, J/kg
$\dot{m}$	Mass flow rate (kg/s)
$\dot{Q}$	Heat transfer rate(KJ/h)
R	Thermal resistance, K/W
T	Temperature, K
X	Mass fraction

Greek Symbols

η	Efficiency
ω	Absolute humidity, kg_w/kg_{da}

Subscripts

a	air
am	Ambient
i	Component
in	Inlet
out	Outlet
pw	Product water
max	Maximum
mix	Mixture
t	Thermal
w	Water

Abbreviation

LHV	Low heating value
NG	Natural gas
SWF	Surface heat loss
LP	Liquid product
VLV	Valve
VP	Vapor product

Acknowledgemen

The authors would like to express their thank to Kharazmi University for the financial supports (under a grant presented by Vice Chancellor in Research).

References

Bayat, A., Abbasporsani, K., Heidari, F., Vosough, M., 2016. Thermodynamic analysis of gas preheater at Zanjan city gate station, Applied mechanics research 8(1), 27-32.

Deymi-Dashtebayaz, M., Dadpour, D., Khadem, J., 2021. Using the potential of energy losses in gas pressure reduction stations for producing power and FW. Desalination 497, 114763.

Dow, N., Gray, S., Li, J., Zhang, J., Ostarcevic, E., 2016. A. Liubinas, P. Atherton, G. Roeszler, A. Gibbs, M. Duke, Pilot trial of membrane distillation driven by low grade waste heat: Membrane fouling and energy assessment. Desalination 391, 30–42.

Elsaida, K., Taha Sayed, E., Yousef, B.A.A., Rabaia, M.K.H., Abdelkareem, M.A., Olabi, A.G., 2020. Recent progress on the utilization of waste heat for desalination: A review. Energy Conversion and Management 221, 113105.

Ghaebi, H., Farhang, B., Rostamzadeh, H., Parikhani, T., 2018. Energy, exergy, economic and environmental (4E) analysis of using city gate station (PRS) heater waste for power and hydrogen production: A comparative study. International Journal of Hydrogen Energy 43, 1855-1874.

He, W., Han, D., Zhu, W.P., Ji, C., 2018. Thermo-economic analysis of a water-heated humidification-dehumidification desalination system with waste heat recovery. Energy Conversion and Management 160, 182-190.

Karami, M., Noroozi, A., 2019. Application of Waste Heat Recovery Unit for PRS Heater, Journal of Gas Technology 4 (1), 16-23.

Lai, X., Long, R., Liu, Z., Liu, W., 2018. A hybrid system using direct contact membrane distillation for water production to harvest waste heat from the proton exchange membrane fuel cell. Energy 147, 578-586.

Lokare, O.R., Tavakkoli, S., Rodriguez, G., Khanna,

V. Vidic, R.D., 2017. Integrating membrane distillation with waste heat from natural gas compressor stations for produced water treatment in Pennsylvania. Desalination 413, 144-53.

Naderi, M., Ahmadi, G., Zarringhalam, M., Akbari, O., Khalili, E., 2018a. Application of water reheating system for waste heat recovery in NG pressure reduction stations, with experimental verification. Energy 162, 1183-1192.

Naderi, M., Zargar, G., Khalili, E., 2018b. A Numerical Study on Using Air Cooler Heat Exchanger for Low Grade Energy Recovery from Exhaust Flue Gas in Natural Gas Pressure Reduction Stations, Iranian Journal of Oil & Gas Science and Technology 7 (1), 93-109.

Narayan, G.P., Sharqawy, M.H., Lienhard, V., Zubair, S.M., 2010. Thermodynamic analysis of humidification dehumidification desalination cycles. Desalin. Water Treat. 16 (1-3), 339-353.

Olabi, A.G., Elsaid, K., Rabaia, M.K.H., Askalany, A.A., Abdelkareem, M.A., 2020. Waste heat-driven desalination systems: Perspectiv. Energy 209, 118373.

Rastgar, S., Saedodin, S., 2013. Presenting a thermodynamic model to prevent the formation of gaseous hydrates in Natural gas pressure reducing station, 2nd National Iranian Conference on Gas Hydrate, Semnan, Iran.

Santosh, R., Kumaresan, G., Selvaraj, S., Arunkumar, T., Velraj, R., 2019. Investigation of humidification-dehumidification desalination system through waste heat recovery from household air conditioning unit. Desalination 467, 1-11.

Schwantes, R., Cipollina, A., Gross, F., Koschikowski, J., Pfeifle, D., Rolletschek, M., Subiel, V., 2013. Membrane distillation: Solar and waste heat driven demonstration plants for desalination. Desalination 323, 93-106.

Shafieian, A., Khiadan, M., 2020. A multipurpose desalination, cooling, and air-conditioning system powered by waste heat recovery from diesel exhaust fumes and cooling water. Case Studies in Thermal Engineering 21, 100702.

Shakib, S.E., Amidpour, M., Boghrati, M., Ghafurian, M.M., Esmaieli, A., 2021. New approaches to low production cost and low emissions through hybrid MED-TVC+RO desalination system coupled to a gas turbine cycle. Journal of Cleaner Production 295, 126402.

Sharshir, S., Peng, G., Yang, N., El-Samadony, M.O.A., Kabeel, A.E., 2016. A continuous desalination system using humidification-dehumidification and a solar still with an evacuated solar water heater. Applied Thermal Engineering 104, 734-742.

Sorgulu, F., Dincer, I., 2021. Development and assessment of a biomass-based cogeneration system with desalination. Applied Thermal Engineering 185, 116432.

JOURNAL OF GAS TECHNOLOGY

Volume 6 / Issue 2 / Winter 2021 / Pages 65-82

Journal Homepage: http://jgt.irangi.org

Proposing a New Dynamic Maintenance Model for Reliability Improvement By Antifragility Approach: A Case Study in Iranian Gas Transmission Company-Zone10

Hamid Khedry[1], Gholamreza Jamali[2*],Ahmad Ghorbanpour[3]

1. Ph.D Candidate in Production and Operation Management, Industrial Management Department, Faculty of Business and Economics, Persian Gulf University, Bushehr, Iran
2. Associate Professor in Production and Operation Management, Industrial Management Department, Faculty of Business and Economics, Persian Gulf University, Bushehr, Iran
3. Assistant Professor in Operation Research, Industrial Management Department, Faculty of Business and Economics, Persian Gulf University, Bushehr, Iran

ARTICLE INFO

ORIGINAL RESEARCH ARTICLE

Article History:
Received: 20 September 2021
Revised: 06 November 2021
Accepted: 08 Desember 2021

Keywords:
Maintenance
Reliability
Antifragility
Dynamic System
Gas Transmission
Thematic Analysis

DOR: 20.1001.1.25885596.2021.7.2.6.8

ABSTRACT

Reliability is one of the most important performance evaluation indicators in maintenance and repair filed. The present study is a mixed design attempting to identify the antifragility components and their effect on the system reliability using the system dynamics. In the qualitative section, using by the thematic analysis method, with the participation of 10 organizational and academic experts, antifragility factors were identified in the form of 254 open codes, 18 organizing codes and two global codes with the review of literature and using Maxqda 2020 software. In the quantitative part of the research, the relationship between the antifragility factors with the system reliability was investigated using multiple regression method. The three criteria of learning, redundancy and exploratory discussions were identified and selected as the factors that have the highest impact on system reliability. The effect of these indicators on system reliability in a dynamic environment was simulated using the Vensim software, DDS version. The results show the positive effect of all three criteria of learning, redundancy and exploratory discussions on improving the reliability of the system in the area in gas transmission Company-zone 10. Also, the redundancy index had the highest effect and learning components and explorative discussions were in the next classes of impact on improving the system reliability.

How to cite this article
H. Khedry, G. Jamali, A. Ghorbanpour. Proposing a New Dynamic Maintenance Model for Reliability Improvement By Antifragility Approach: A Case Study in Iranian Gas Transmission Company-Zone10. Journal of Gas Technology. 2021; 6(2): 65 -82. (http://jgt.irangi.org/article_251679.html)

* Corresponding author.
E-mail address: gjamali@pgu.ac.ir (G. Jamali)

Available online 26 December 2021

1. Literature review

Today's community heavily depends on reliable performance and high reliability of complex systems to enhance performance and deal with the increasing uncertainties due to the growing complexities of environment [Kobbacy and Murthy, 2008; Derbyshire and Wright, 2014]. Reliability is defined as the probability of a system operating at a given time under certain environmental conditions [Ben-Daya et al., 2016; Elsayed, 2012]. If t is a random time variable of disruption and f (t) is a function of the disruption probability density, the reliability function will be as follows:

$$R(t) = \int_{t}^{-\infty} f(t)\ d(t) \quad (1)$$

F(t) represents the failure probability until moment t. Given the area under the curve in Figure 1, the probability density function is equal to one, thus we have:

$$R(t) = P(T \geq t) = 1 - P(T < t) = 1 - \int_{o}^{t} f(t)\, dt = 1 - F(t) \quad (2)$$

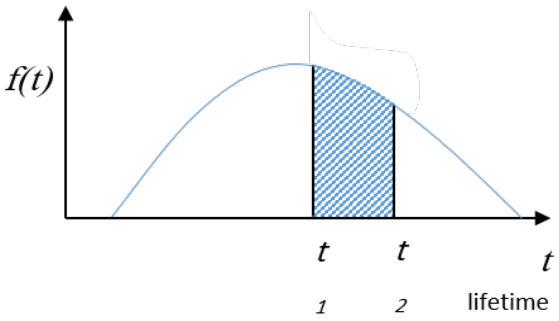

Figure 1. Component lifetime curve [109]

$$h(t).\Delta t = \frac{F(t+\Delta t) - F(t)}{1 - F(t)} \rightarrow h(t) = \frac{\frac{F(t+\Delta t) - F(t)}{\Delta t}}{1 - F(t)}$$

Accordingly, the probability that the lifetime of a system is in the time interval t_1 to t_2 is obtained from the following equation.

$$P(t_1 \leq t \leq t_2) = \int_{t_1}^{t_2} f(t)\, dt = F(t_2) - F(t_1) \quad (3)$$

Failure rate and degradation function are two very important issues in evaluating system reliability. This function indicates the probability of failure at the time interval t and $t + \Delta t$, provided that no failure has occurred until time t. In the calculation of this probability, we are encountered with the conditional probability $(x \mid y)$, where x is the failure event of the system during $t, t + \Delta t$ and y is the system surviving until time t.

$$P(x|y) = \frac{P(x \cap y)}{P(y)} = \frac{P(t \leq T \leq t + \Delta t)}{P(T \geq t)} = \frac{\int_{t}^{t+\Delta t} f(t)\, dt}{\int_{t}^{\infty} f(t)\, dt} = \frac{F(t+\Delta t) - F(t)}{1 - F(t)} \quad (4)$$

Now if we denote the failure rate with the instantaneous failure rate by $r\ (t)$ or $h\ (t)$, the product of $h(t).\Delta t$ is equal to the failure probability during Δt after time t on the condition the system functions until time t, so we have:

$$h(t).\Delta t = \frac{F(t+\Delta t) - F(t)}{1 - F(t)} \rightarrow h(t) = \frac{\frac{F(t+\Delta t) - F(t)}{\Delta t}}{1 - F(t)} \quad (5)$$

In the above limit, Δt approaches to zero, the nominator is the same derivative of $F\ (t)$, ie $f\ (t)$ and we have:

$$h(t) = \frac{F'(t)}{1 - F(t)} = \frac{f(t)}{R(t)} \quad (6)$$

The failure rate function is different for various systems and equipment. When the failure of a device is due to the failure of a large number of system components, its distribution of failure is usually normal [205]. Since one of the methods to find the failure rate in gas transmission is using historical data statistics and system failures in the present study, the normal distribution in the system failure rate has been used. Despite the development of knowledge in reliability field, degradation is a critical factor in this regard. In a division, four general models - remaining useful life, random processes, physics-based and multi-

state processes - have been proposed for it [Zio, 2016].

Remaining useful life statistical models are based on degradation data [Lu and Meeker, 1993]. Zhang and Shi used this model using data geometry in cases where there is no or very little information on system interruptions [Zhang and Shi, 2020]. Wujun Si et al. have used microstructure imagery to model material degradation and predict interruption. The results of their study showed considerable progress in predicting the interruptions caused by material degradation compared to optimal mining models [Si et al., 2018]. Interruptions are rarely found in high reliability systems. There are various methods to overcome this problem. Life cycle acceleration using internal or external covariates is one of these cases. Vilijandas Bagdonaviius and Mikhail Nikulin used time-lapse regression models, most commonly, to examine the data on degradation and remaining useful life. They defined interruptions as traumatic and non-traumatic. If degradation reaches the specified limit Z_0, it is called non-traumatic, otherwise it is traumatic [Bagdonavičius and Nikulin, 2009]. In many industrial applications, it is possible to build a database of time-consuming and non-economical interruptions. Accordingly, Nagi et al. used the interruption data - preparing which is easier compared to sensor installation approaches, considering maintenance history - in Bernstein distribution, and used its parameters to estimate the initial distribution of the degradation model [Gebraeel et al., 2009]. Given the problems mentioned, stochastic process modeling methods were developed and various investigations [Kjell et al., 1992; Chen et al., 2015; Lawless and Crowder, 2004] were conducted in this regard. In most of the studies conducted in this area, the error rate in degradation process is considered a function of Wiener-process or Gamma-process [Tseng and Peng, 2007].

Physical models are used in cases where statistical model information is not enough due to the high reliability of the system such as nuclear power plants and are based on knowledge of degradation physics and factors such as mechanical loads frequency and environmental critical conditions in modeling fatigue, corrosion, destruction mechanism or cavity corrosion [Chookah et al., 2011; Ma et al., 2016; Keedy and Feng, 2012; Zhu et al., 2016; Hao et al., 2010; Wang and Pham, 2012]. Multi-stage models describe and examine the underlying processes of degradation in the finite states such as Semi-Markov simulations. In this model, the state of the system is divided into several stages from full performance to full stop. It is crucial to obtain time-dependent probabilities in this method to evaluate the system reliability dynamically [Yu et al.,].

Besides the mentioned divisions, other approaches are also seen in the literature to predict the role of degradation in system reliability, which are generally categorized into four groups: experience-based, knowledge-based, model-based, and data-based. The latter two approaches are more common in reliability evaluation. The knowledge-based approach is mostly used in combination with other approaches such as data mining. Experience-based approaches need less data and are the simplest approach since they do not consider the degradation index in predicting the lifetime of the equipment. Such approaches are widely used when historical information on maintenance and interruptions is based on the distribution of logs from a population of identical and similar items. Many conventional reliability approaches, such as exponential distributions, log-normal and Weibull have been used to model equipment reliability. Weibull distribution approach is more popular than other materials because of the capability to cover various types of behaviors in bathtub curve [Gorjian et al., 2010]. Model-based approaches are commonly used with the mathematical dynamics models and are sometimes incorporated into physics-based or statistics-based models. Knowledge-based approaches are suitable for solving problems solved by expert individuals and do not require

a specific model. Expert and rational fuzzy systems are among these approaches [Shin et al., 2018; Zhou and Thai, 2016; Zhang et al., 2015].

Data-based approaches have been shaped based on statistical and learning techniques derived from pattern recognition theory. Various methods from multivariate statistical methods, partial least squares, and so on to the black box, Bayesian network, Hidden Markov Model (HMM), and neural networks are among them, of which neural networks and HMM are the most widely used ones in recent studies [Song et al., 2017; Li et al., 2007; Saidi et al., 2017; Eleuteri et al., 2003].

Nassim Nicholas Taleb introduces unknown events around the world in his book "Black Swans" to further explore risk. Black swan has three characteristics: it is unpredictable, it has a huge consequence, and seems predictable after incidence if it cannot be predicted before occurrence. According to the antifragility theory, systems are divided into three categories: fragile, stable, and antifragile. Figure 2 shows the response of these three types of systems to stress exposure [Taleb, 2012, 2010]. Table 1 depicts some recent researches on antifragility applications in various businesses.

The knowledge development, methods, techniques, multiple models and finally the increase of information sharing about reliability assessment have provided the opportunity for analysts to present new methods [Zio, 2016]. Some of the mentioned methods have been used in assessing the reliability of gas transmission companies [Ren et al., 2020; Chen and Wu, 2020; Gaur et al., 2019; Yu et al., 2018].

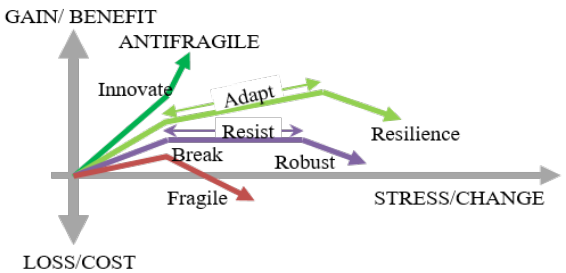

Figure 2. The evolution of systems from failure to antifragility [31]

The present study was conducted to present a new antifragility approach in evaluating system reliability. On the other hand, identifying the antifragility components are the additional results but important and practical results of the present study that have not been addressed in any research so far and can be used as a suitable basis in other researches. Their impact on the reliability index by systems dynamics are among the major stages of this research.

The identification of antifragility components, their relationship with reliability and examining Innovations of this research include simultaneous attention to structural and behavioral factors in assessing reliability, considering the small risks with serious consequences called black swan, reducing the complexity of the problem and the possibility of adding or reducing other variables using a dynamic approach and finally defining different strategies and observation of the long-term and short-term effects of decisions on the reliability index

Table 1. Some recent researches on antifragility

Year	Title	Author/ authors.
2020	Relativistic antifragility [36]	Succi and Sauro
2020	Approach to resilience and antifragility in business ecosystems	Ramezani et al.,
2020	Dynamic model of optimization in development of water supply with uncertain flow	Moudi et al.,
2019	Multilayer structures in production of antifragile systems in Boolean Network	Kim et al.,
2019	Anatomy of an incident: A hydrogen gas leak showcases the need for antifragile safety systems	Smith
2018	Resilience and anti-fragility engineering: accident occurring on a mobile elevating work platform	Martiny et al.,
2018	Antifragile communications	Lichman et al.,

2. Methodology and model structure

As shown in Figure 3, the present study is a mixed design and designed in four stages. In the qualitative section, antifragility components have been identified using the content analysis method and Maxqda 2020 software. The qualitative method of thematic analysis is used to analyze the textual data and diverse data in five stages: data familiarization, creation of raw codes, search of themes through selective codes, review of themes and creation of organizing themes and definition and naming of main themes to detailed data [Braun and Clarke, 2019]. In researches such as the present study where the number of texts and their data is high, the themes format is used Guest et al., 2012]. Then, the most important antifragility factors affecting reliability have been identified using stepwise multiple regression method. Multiple stepwise regression identifies significant input variables and eliminates multicollinearity between variables; multicollinearity would incur when the selected input variables are correlated. Several recent studies have applied stepwise regression as the variable selection technique [Mohsenijam et al., 2017].

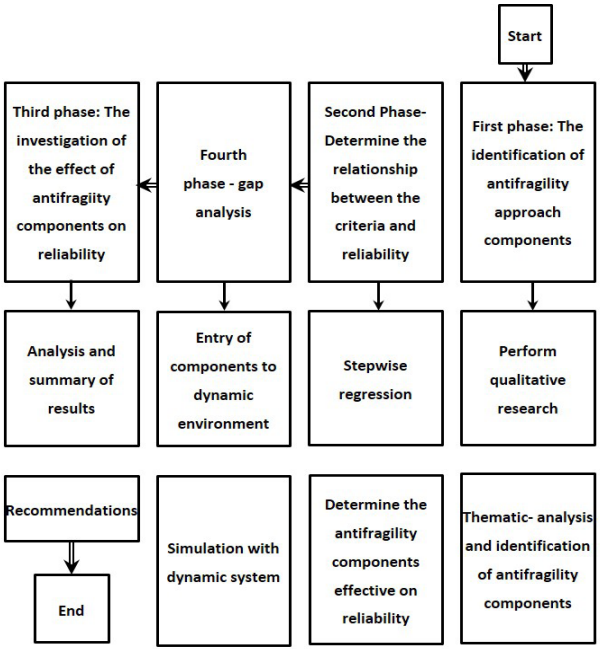

Figure 3. Flowchart of research implementation method

Then, the effective indicators on reliability were entered into the dynamic model of maintenance and repair using the systems dynamics approach and their separate and simultaneous impact on the reliability of the system has been simulated and evaluated.

System dynamics is a methodology for framing, understanding and discussing complex issues and problems [Sterman, 2018]. It allows a system to be represented as a feedback system. Compared to other simulation approaches, a system dynamics model is more beneficial to explain the developing trends of dynamics behaviors in the long-term (simulation duration) due to its feedback structure and capability to function under different parameter setting and initial inputs [Sterman, 2000]

Unlike other approaches that have a linear view to the problem and its effect, the system dynamics focuses on the information returned from the problem variables and cause-and-effect loops [Sterman, 2018]. According to system dynamics' standpoint, system dynamics model judges object system's changing trend by simulating object system dynamically in order to study and plan future action and corresponding decision-making of the object system. This approach, which focuses on cause-and-effect processes based on information retrieval processes, is designed to overcome complex problems. In this method, a combination of quantitative and qualitative methods using mathematical equations is used to simulate system behavior [Sterman, 2000].

As antifragility has many components, the inclusion of each variable in the model is well investigated and analyzed in system dynamic approach. Figure 4 shows the Causal loop diagram representing the main loops of the antifragile model structure [De Bruijn et al., 2020].

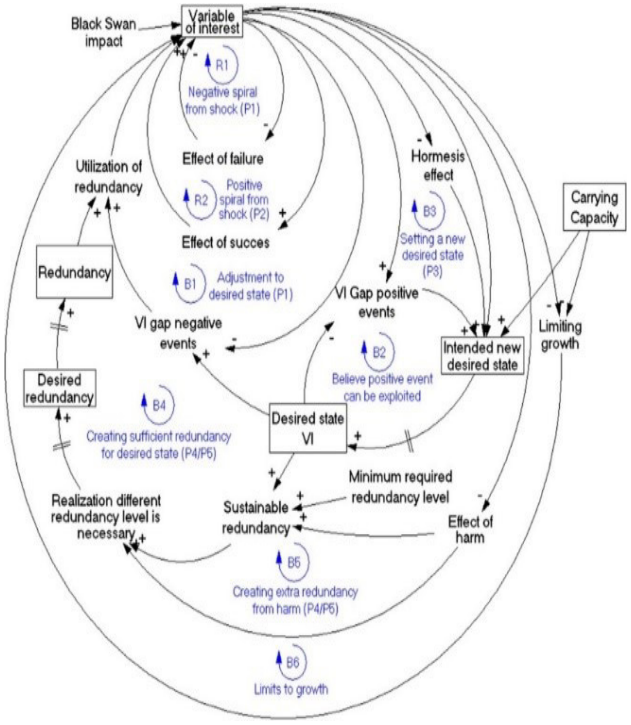

Figure 4. Main loops of the antifragile model Causal loop diagram [De Bruijn et al., 2020]

Recognizing rate and state variables and shaping cause and effect diagrams are so important in dynamic systems. In maintenance systems, the reliability has a key role and is influenced by most of other performance indices of the organization. As shown in Figure 5, total shutdown is one of the factors contributing to the decrease in system reliability. Reliability is calculated by dividing the number of hours of operation by the number of interruptions. Non-stop hours will be the system reliability, which decreases with interruption increasing rates.

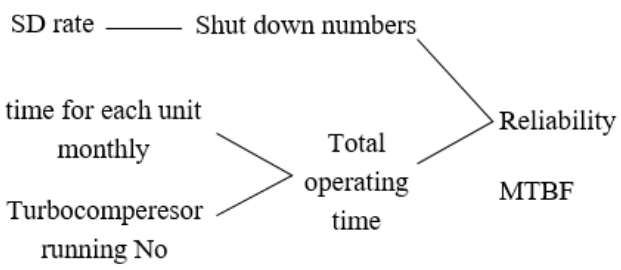

Figure 5. Reliability tree diagram

Figure 6 shows that many interruptions are resolved with emergency repairs and preventive repairs. The role of preventive maintenance is well seen in enhancing reliability in this dynamic model. Increasing preventive maintenance processes reduces the rate of system failures. The role of emergency repairs in reducing existing failures, as shown in the models, is minimized over time and in reducing the amount of existing failures, preventive repairs affect the rate of occurrence of failures and decrease them. Figure 7 shows depots and flows related to the volume of gas transmitted, the volume of gas discharged to the environment, and the internal uses of the facilities. Overall interruptions that reduce system reliability will directly affect production rates as well. Moreover, this increase in facility interruptions will result in increased gas loss due to rebooting and reducing overall system efficiency and greater environmental pollution. Although the purpose of the study is not to discuss the environmental issues and the volume of the transmitted gas, one can deduce the direct relationship of reliability of the system with the volume of gas transmitted and its inverse relationship with the discharge of gas to the environment and its environmental effe

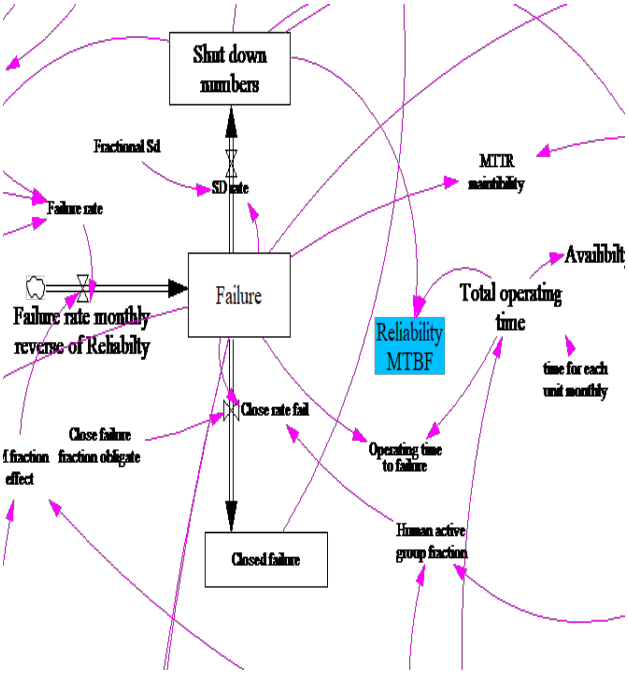

Figure 6. Reliability and failure rate

Preventive maintenance activities to reduce system failures and increase system reliability have a positive effect on environmental performance evaluation indices. This can be very significant in expressing the mission of industrial organizations in responding to the social mission.

Figure 8 depicts the cost savings, flows, and the effective factors on various costs of maintenance. The level of reliability is defined depending on the type of industry and equipping. This strategy means that maximizing reliability depends on factors like budget and cost savings.

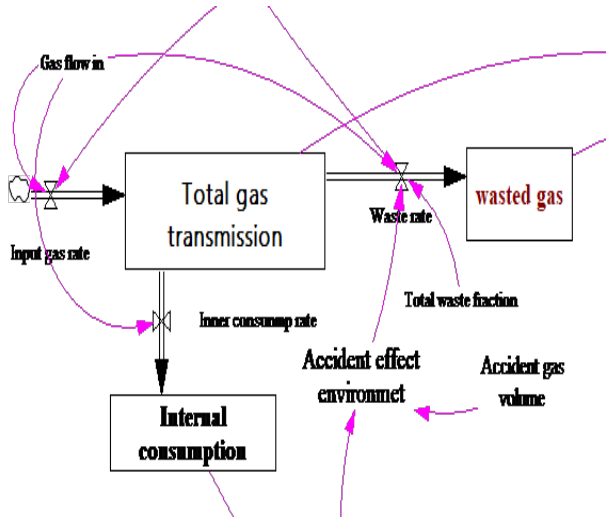

Figure 7. Reliability and environmental effects

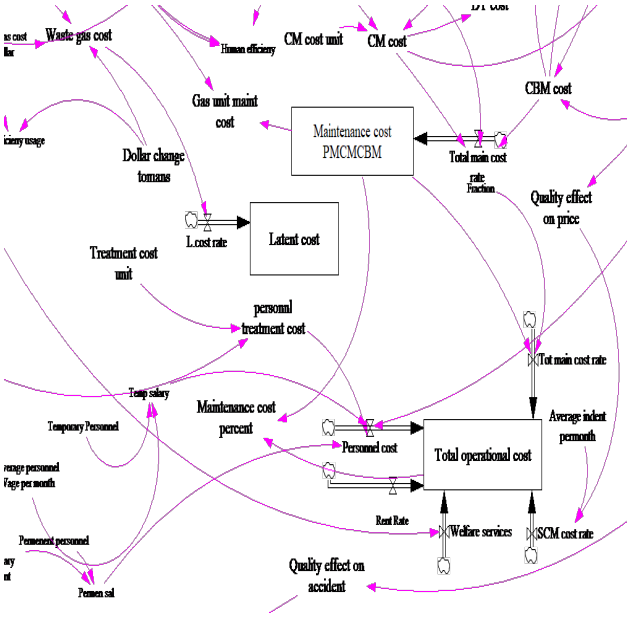

Figure 8: Reliability and total costs

At first glance, it seems that we need to invest in emergency, preventive measurements, salaries and equipment to maximize reliability. Although in some industries it may be true to some degree, the situation in the gas industry is different. Some maintenance processes done to increase system reliability lead to hidden costs such as non-production and export or discharge of gas to the environment, which also results in the cost of wasted gas and environmental pollution. Reaching an acceptable level of risk in maintenance processes and using new and technological approaches coupled with designing a supply chain in the industry can greatly help improve the status of costly and agile processes. Finally, maintenance processes cannot maximize the reliability of a gas transmission network or any industrial organization without neglecting other effective limiting or facilitating components. The dynamic system shows all cases to the researcher in a defined timeframe with a comprehensive view.

Figure 9 shows the event flow diagram. Some events stop operations and, in turn, reduce the reliability of the complex. Accidents that occur in maintenance systems have a variety of factors.

Human errors and deficiencies in the equipment and tools used are among the major causes in this regard. Accidents in addition to having negative effects on the reliability of the gas transmission network or any industry in need of high reliability result in a variety of overt and covert human resources costs. These include the cost of training new personnel, the various risks of new employees, and the cost of lost equipment and non-production. In addition, accidents have negative effects on the organization's reputation and the cost of losing market share is predictable in some industries.

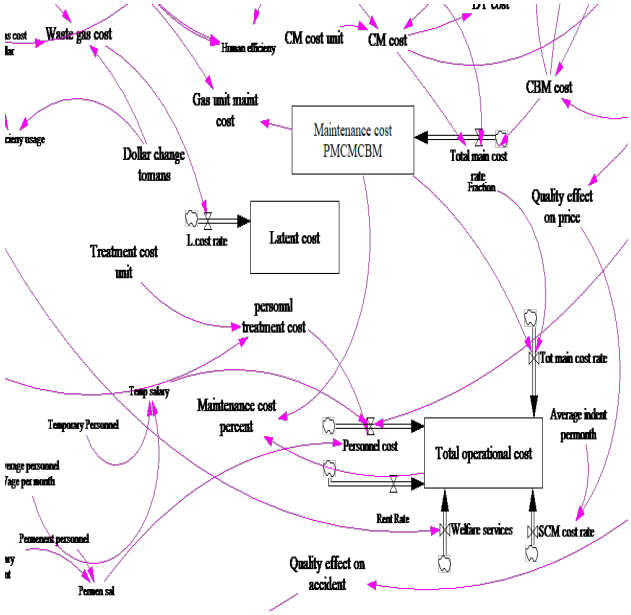

Figure 9. Reliability and human accidents

Establishing a training system in the safety field in repair and improving the supply chain in supplying quality items are some of the solutions that can be used to improve the performance of repair teams. With a dynamic approach and controlling the overall factors affecting the accident rate can ensure the reliability of the system to an optimal level. Doing this necessitates a knowledge-based and comprehensive approach to all issues of the organization to manage the ultimate reliability of other performance indices such as cost and accidents besides the ultimate desirability.

Figures 6 to 9 show the structure of the dynamic maintenance model. Now as is shown in Figures 10 and 11, the learning criterion and exploration discuss are added to the maintenance system model. In the resulting model, the total operation interruptions and failures are resolved in a specific process by analyzing the root cause of the failures in the expert operating sessions and are grouped into different categories. Improper use of equipment, improper installation, improper design and construction, incomplete and ineffective maintenance and installation are the areas that can be examined in each case. After examining each case and recognizing the basic roots, the items related to the manufacturing companies are sent to them and those that need organizational learning are dealt with in problem-based training processes. The manufacturing companies will take steps to improve equipment quality by obtaining reports on defects in design and manufacture. In this case, learning happens outside the organization but its effect can be seen with appropriate delays in the maintenance system.

Figure 10 shows the effect of human resource learning and the results of rooting failures and improving the quality of equipment in design and manufacturing on the monthly failure process. Although failures impose problems and costs on the organization, they can help staff experience equipment and repairs effectively if they are system-based and problem-based. Moreover, in the highly competitive market, suppliers find the best way to compete to create an effective supply chain by obtaining information from the end consumer to survive. These will reduce failure.

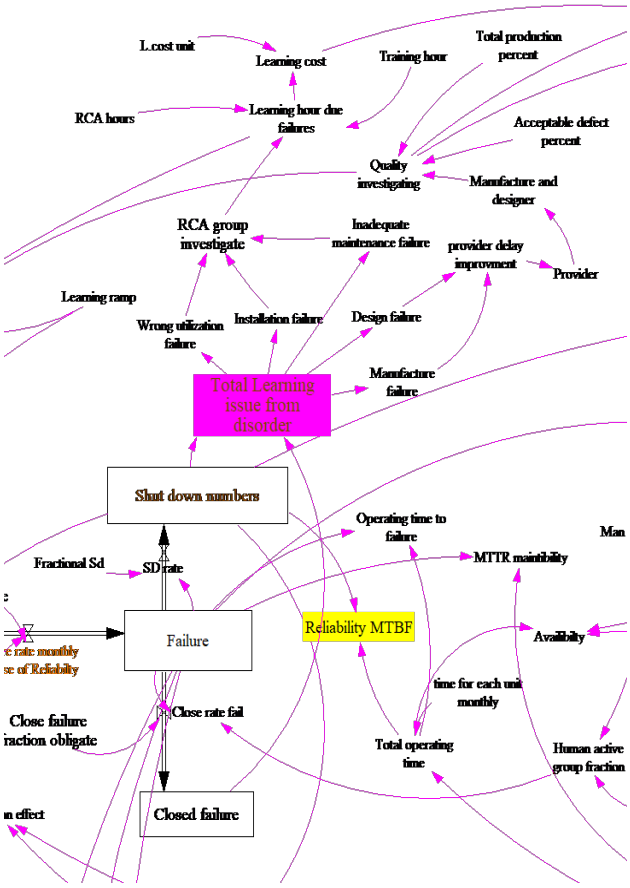

Figure 10. Learning and failure rates

As the reduction in failures has a positive effect on system reliability, the role of the learning mechanism in improving reliability will be undeniable. Figure 11 shows the effect of increased exploration discuss on the maintenance system. The partnership system is the main symbol of heuristic discourses in the organization. Indeed, personnel identifies problems or points of improvement in the organization and reports on the systematic processes according to their experiences and knowledge. Most of the suggestions made in this area are the same black swans that Nassim Taleb has mentioned in his study: significant risks that can pose numerous problems for industry and other stakeholders if they occur, though unlikely. The elimination of black swans, the risks of unforeseen events in the organization will reduce, adversely affecting the possible events and making the maintenance system more reliable.

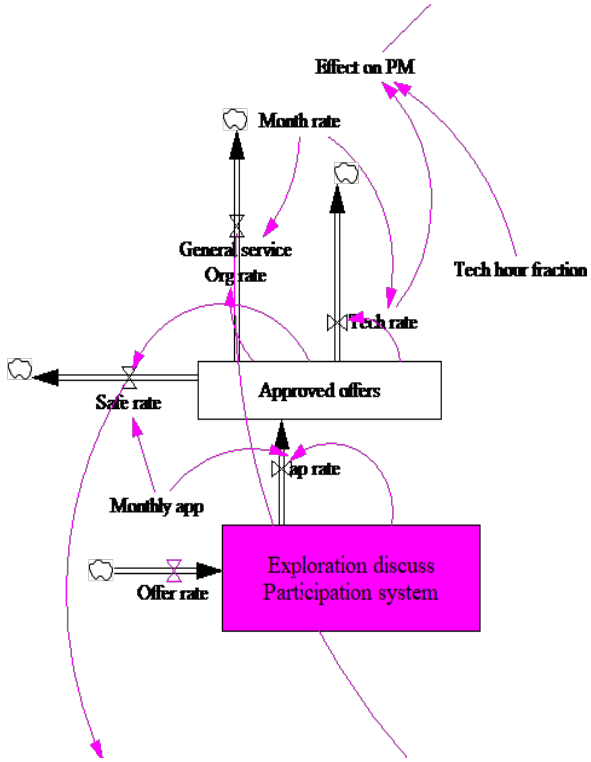

Figure 11. Exploration discussion and the effects on reliability

Figure 12 shows the effect of redundancy, an important criterion of antifragility on the maintenance system. There have been many studies on the effect of redundancy on reliability, but so far, there have been no studies using a dynamic approach examining some simultaneous criteria. It is critical to develop replacement unit designs and layouts according to systems that require high reliability.

As the cost of designing, purchasing, installation and operating spare parts is a decisive factor in any industry, one cannot independently and certainly hope for an increase in spare units or backup systems. Purchasing expensive turbochargers or designing and implementing high-pressure gas transmission lines needs more budgets; this must be addressed in a dynamic process with other organizational criteria in mind.

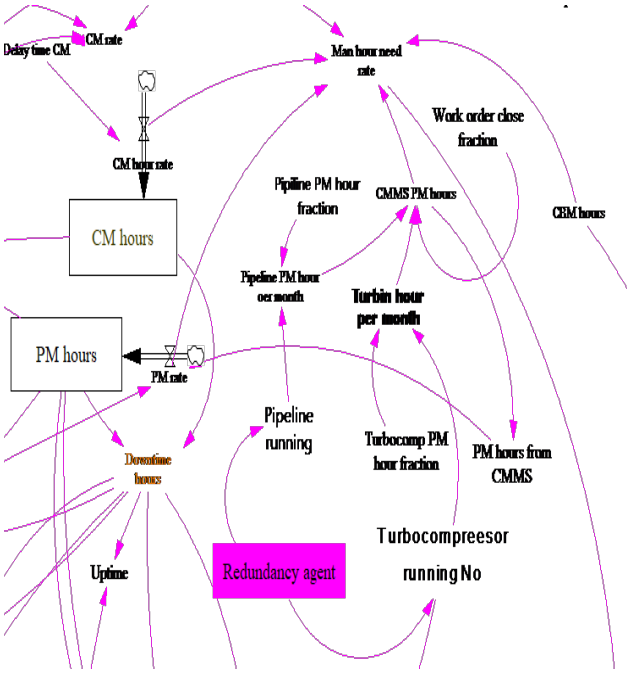

Figure 12. Redundancy and the relationships affecting reliability

3. Results of running model

In the qualitative part of the present study, the data were reviewed and their meanings were searched while taking notes. These notes were obtained from the study of more than 50 papers and books that were recorded in Maxqda 2020 software in addition to the manual method.

At this stage, parts of the texts that were conceptualized for the research questions were selected and labeled. At first, 491 open codes were identified at this stage[1]. By interpreting the open initial codes, the themes were identified again and the extracted codes were placed in the form of selective codes. The open and selective codes identified were categorized into 254 themes. By re-examining and further refining the themes, it was attempted to make have comprehensive and on-repetitive themes. As shown in Table 2, at this stage, 18 organizing themes and two structural and behavioral global themes were extracted.

An appropriate combination of non-fragile components can be a good predictor of reliability. To determine which variables can be a good predictor of reliability; Stepwise multiple regression method was used for six important criteria. The results of statistical analysis of this test are summarized in figures 13-15 and Table 3. Three learning, redundancy and exploratory discussion variables explain 69.4% of the variance of reliability and therefore, have been selected as the most influential antifragility factors and entered into the dynamic model of reliability assessment.

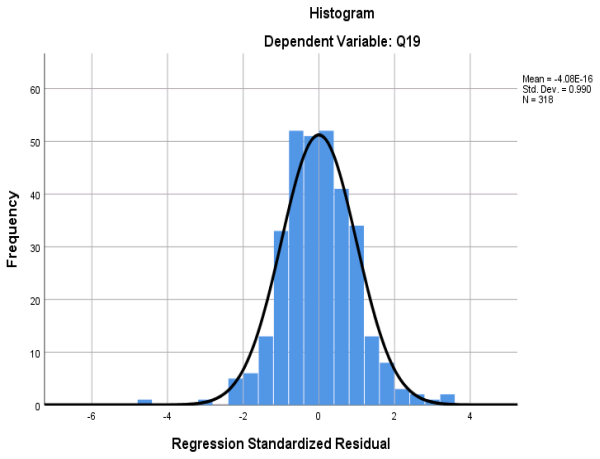

Figure13. Depenent variable histogram

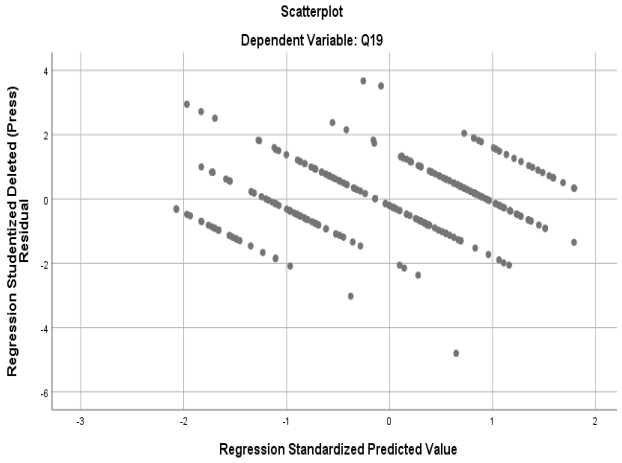

Figure 14. dependent variables scattplot

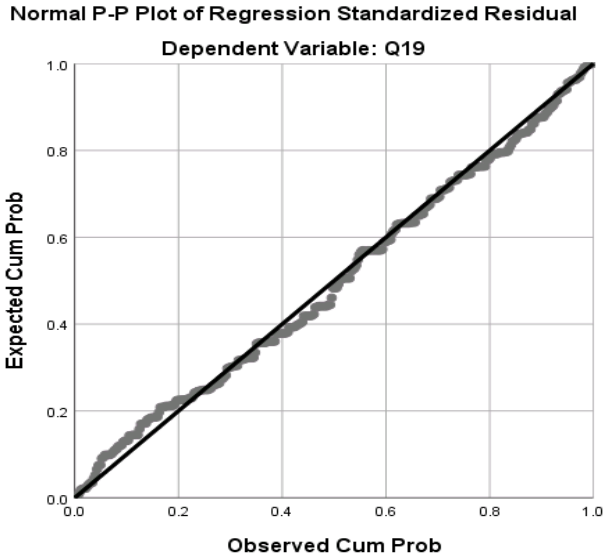

Figure 15. Normal P plot of regression standard residual

1. Selective Codes

Table 2. Final modified themes of antifragility

Basic	Organizing	global
The system facing the environmental stress with learning processes uses the existing mistakes and become stronger. 85 cases.	Learning and growth	Behavioral components
In facing the environmental uncertainties, the system has more ascending movement more than descending movement. 12 cases.	Asymmetry	
For antifragility, the smaller components should be designed as they will be destroyed for the survival of the main system. 19 cases.	Creative-based panarchy of antifragility	
The unplanned results can create new structures in some cases in the system. 12 cases	Emergence approaches	
The simple rules that the system learns over the time to face with the problems. 4 cases.	Heuristic	
Non-interference of low-experienced experts in the affairs can increase the system performance. 5 cases.	Experience and specialization	
It causes that the organizations have better performance in the face of threats. 8 cases.	Resilience	
Anti-fragility is defined as a part of agility activities of the system. 4 cases.	Agility	
Full elimination of negative factors is harmful for the system. 12 cases.	Hormesis	
The system ability in recognition of black swans helps its anti-fragility. 16 cases	Unknown risks	
The risk management considers the important issues in short and long-term periods. 6 cases.	Barbell strategy	
Unfragile organizations have high entropy but this feature cannot degrade them because they are based on some layers. 3 cases.	Entropy	Structural components
Unfragile organizations have flexible and multi-sectional structure. The balance between the limitations and degree of freedom has required optimization conditions for a system. 26 cases.	Flexibility and operational adjustment with the connection and freedom degree of system	
Redundancy makes the system sustainable and in unfragility, it is considered investment. In the long-term, redundancy has many benefits to optimization for an organization. 11 cases.	Redundancy	
High reliability is necessary for system but they don't become unfragile. Fragility is controlled by high reliability. 2 cases.	High reliability	
The increase of system entry has not the same output increase.	Non-linearity	
There are many different environments that their work rules can not be defined clearly and maximum participation is required (participation system). 9 cases.	Transparent procedures	
The higher the number of system elements, their higher its complexity. 10 cases.	Complexity	

The results show that all three components of exploratory discussions, redundancy and learning affect the reliability of the system and the effect of redundancy is higher than the other components. The initial model in which no antifragile criterion is entered is called original and the final model, with the simultaneous effect of entering antifragility criteria into the model is called antifragile reliability.

Table 3. Summary of stepwise multiple regression analysis results

Durbin-Watson	Estimation standard error	Adjusted R^2	R^2	R	Model
1.973	0.72572	0.582	0.583	0.764[a]	First step
	0.63277	0.673	0.675	0.822[b]	Second step
	0.61184	0.694	0.697	0.835[c]	Third step
	0.60472	0.701	0.705	0.840[d]	Fourth step
	0.59967	0.706	0.711	0.843[e]	Fifth step
	0.59683	0.709	0.715	0.845[f]	Sixth step
Learning and growth			0.675	0.822b	Predictors in the first step
Learning and growth, redundancy			0.675	0.822b	Predictors in the second step
Learning and growth, redundancy, transparent procedures and exploratory discussions			0.675	0.822b	Predictors in the third step
Learning and growth, redundancy, transparent procedures and exploratory discussions, high reliability			0.675	0.822b	Predictors in the fourth step
Learning and growth, redundancy, transparent procedures and exploratory discussions, high reliability, Barbell strategy			0.675	0.822b	Predictors in the fifth step
Learning and growth, redundancy, transparent procedures and exploratory discussions, high reliability, Barbell strategy, Panarchy creativity-based fragility.			0.675	0.822b	Predictors in the sixth step
Dependent variable: Reliability					

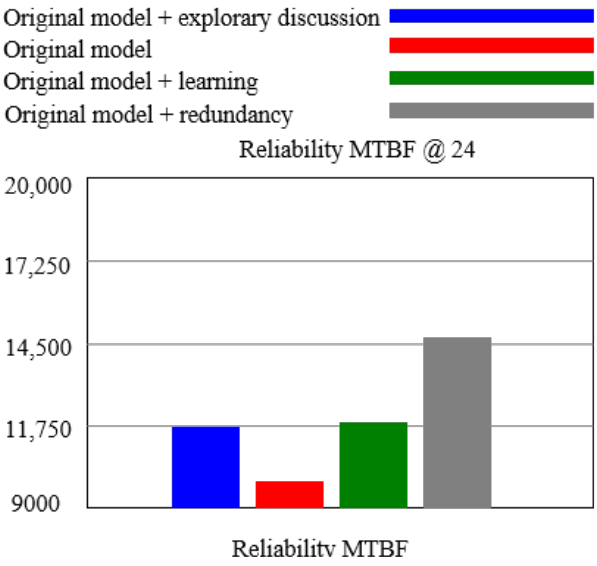

Figure16 . Column diagram of reliability and impact of antifragility components

The results show that after redundancy, which has a significant effect on reliability, the learning component has a higher impact on reliability compared to exploratory discussions. The results are shown based on Figure 16.

4. Model validation

Validation of dynamic models is more based on confirming the structure and ensuring its design and does not have the zero and one aspect [226].

Various methods are used to validate dynamic models [Sterman, 2018, 2000]. Some tests are so important in confirming the method that they can be considered mandatory [Barlas and Carpenter, 1990]. The first test that can be stated is the confirmation of the model structure, which is derived from qualitative judgments.

To confirm the structure, the present model has been investigated by maintenance experts in Gas Transmission Company-zone 10, and managers and experts have emphasized the comprehensiveness of the model structure.

In the next method, the dimensional validation test of the model was evaluated

and confirmed. State and rate variables must have dimensional compatibility and the variables with no significance in the model are eliminated. This can be done well using the software. By performing this test, no error has occurred in the model and the simulated model was run and confirmed.

Another test was done in this study that was examining the model boundary conditions. In this test, very small or very high extreme values, the variables are entered into the model and their effect on the model and the model response is evaluated. In case of failure rates entering the system become zero, not only the reliability of the maintenance system increases up to maximum operating hours, but also it makes emergency repair hours zero.

To perform this test, the time period of the model is extended to 24 months and the result is confirmed based on the output of the model shown in Figure 17.

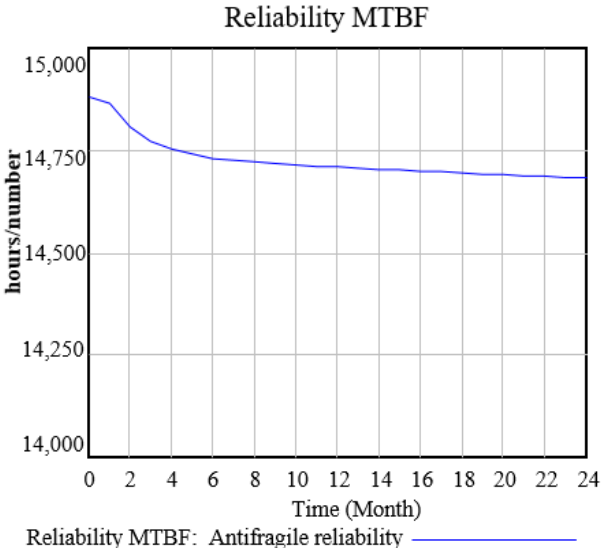

Figure 17. Test of the limit condition of increasing the time interval

On the other hand, since the reliability of the system is determined based on working hours and the number of stops, the model response can be investigating by setting the stops to zero. At this stage, the system response is as expected and confirmed, which is shown in Figure 18 of the test result.

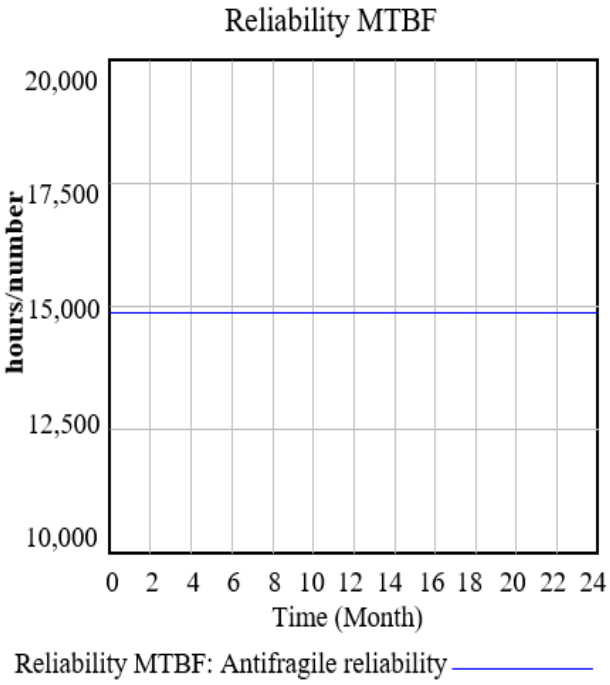

Figure 18 . Zero stops and failures in the limit test and reliability

Sensitivity analysis is used for the overall evaluation of the model functioning. The method is to identify the variables on which the model relies heavily. It is then examined whether this sensitivity and significance exist in the real environment. With a few changes, the system response is examined and various work policies are extracted.

Validity of policy content, determine the validity of policy content is the last step in model validation. Increasing system redundancy has been the policy under investigation at this stage. In increasing redundancy, the experts expect to improve the system reliability, and as shown in Figure 19, the present model explains this well and the sensitivity test of the redundancy policy is approved.

On the other hand, with the increase of redundancy and increasing reserved machineries, it is expected that the working hours of preventive maintenance and repairs will increase, which was also confirmed in the model simulation. Figure 19 depicts this goal.

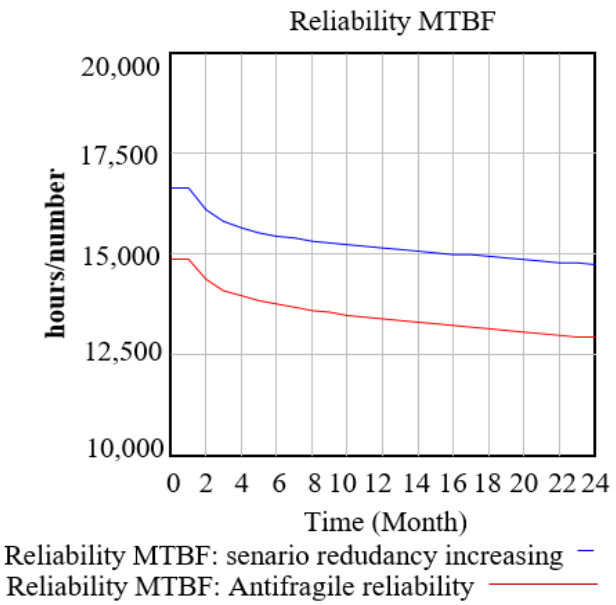

Figure 19. Increasing PM hours in sensitivity test by increasing redundancy

Finally, increasing the number of machineries can lead to higher repair costs than before. Figure 20 shows that the model predicts this goal well.

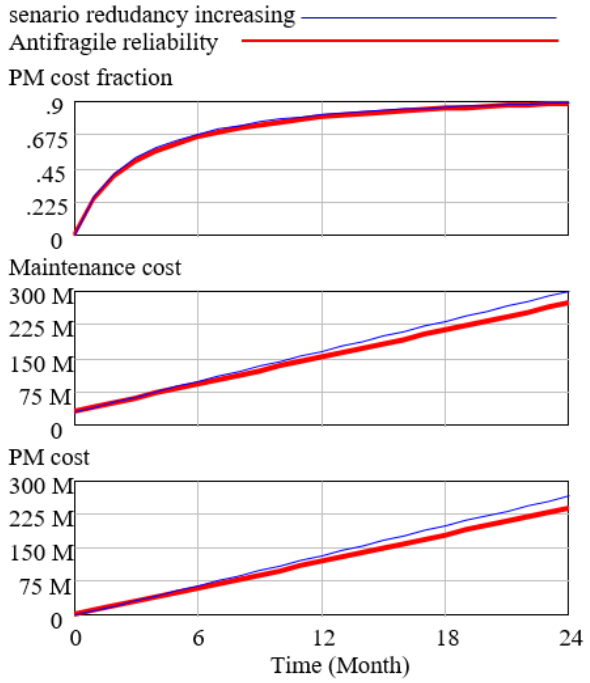

Figure 20. Increasing costs in sensitivity test of increasing redundancy

The utility and fitness test with the audience is also included in the proposed model. Model size, simplicity or complexities of the model are some of the items that are considered important to the audience. The present study has been approved in the zone 10 of operation and applied by the system's audience of the net. Since the researcher himself is experienced in the field of refinery and power plant industry management, he has helped to improve the fit of the model with the audience.

Finally, Monte Carlo sensitivity test is done by changing redundancy factor, failure rate, CBM hours and according to figure 21 the results showed that our model works properly and is valid.

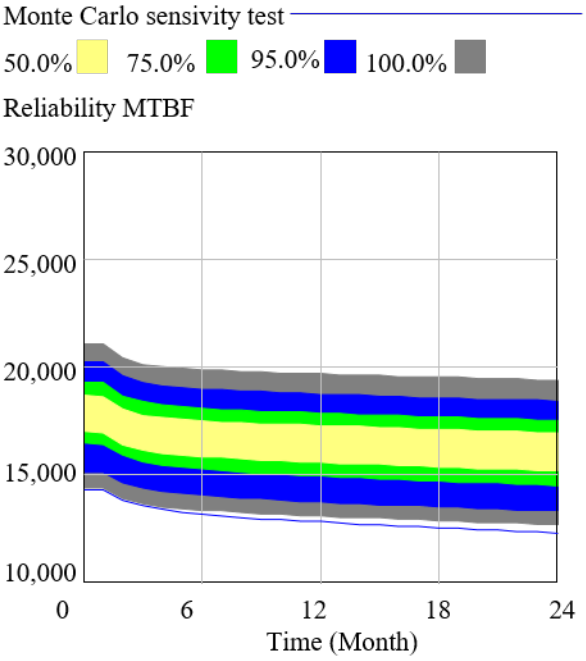

Figure 21- Monte Carlo sensitivity test

5. Discussion

The results show that the antifragility components are effective on the reliability index in gas transmission Company of zone 10. The components of organizing themes in the antifragility approach, learning and growth, have a significant impact on improving reliability. Learning criteria in competitive business scorecard models [Gopal, 1998] and BSC Balanced Scorecard [Kaplan and Norton, 1992] have been identified as one of the

important performance evaluation indicators and are consistent with the present study.

The participation of beneficiaries with the exploratory discussions is one of the well-known indicators in the antifragile reliability approach, which is also mentioned in the evaluation charter model [Adams and Neely, 2000].Learning index is a common element of the present research and the mentioned models.

The results of the present study on the importance of redundancy are similar to other studies in system reliability [Yadav et al., 2008]. The important point is that in other approaches, redundancy optimization is emphasized, but in antifragility, redundancy optimization is not approved and is not justified by the long-term view of redundancy optimization. Although more studies are needed, preliminary studies on the interruption of the country's gas transmission and the damage caused by gas supply problems to power plants and other social problems confirm the reliability approach of antifragility and emphasis on the lack of necessity of optimization in gas transmission processes.

5. Conclusions

The present study investigates the effect of antifragility approach on the reliability of the maintenance system. Research findings show that the concept of antifragility includes two global, 18 organizing and 254 basic themes. Studies show that among the organizing themes of antifragility, three components of learning and growth, redundancy and exploratory discussions are related to system reliability. After entering these criteria into the dynamic model of maintenance performance evaluation, it was found that all three components have a positive effect on reliability, but the role of redundancy in improving system reliability is more significant than the other two components and learning and exploratory discussion are in the next ranks.

The conclusion that can be made is that reliability heavily depends on invisible factors such as learning from errors and collaborative system. The traditional view of maintenance systems to improve the situation will not be fully effective and the present study provides an opportunity to examine the effect of other antifragility criteria, besides reliability, on other performance evaluation criteria for maintenance systems. Among the limitations of the study is the time-centered and deterministic method of system dynamics, which is an inseparable property of the aforementioned method.

It is suggested that in future researches, the effects of other antifragility variables in a dynamic environment at different time intervals and compare the results. Be integrated to monitor the effects of black swans on the organization's risk management more effectively. Finally, it is recommended that in the design of utilities and lines of pressure optimization, the issue of redundancy beyond the short-term optimization is considered in order that the long-term benefits are not affected by a few short-term benefits.

Acknowledgements

Hereby, we appreciate all the respected colleagues of IGTC zone 10 who did their best in the study and sincerely assisted us.

References

Adams, C., & Neely, A., 2000. The performance prism to boost M&A success. Measuring business excellence.

https://doi.org/10.1108/13683040010377818

Bagdonavičius, V., & Nikulin, M., 2009. Statistical models to analyze failure, wear, fatigue, and degradation data with explanatory variables. Communications in Statistics - Theory and Methods, 38(16-17), 3031-3047.

https://doi.org/10.1080/03610920902947519

Barlas, Y., & Carpenter, S., 1990. Philosophical roots of model validation: two paradigms.

System Dynamics Review, 6(2), 148-166.

https://doi.org/10.1002/sdr.4260060203

Ben-Daya, M., Kumar, U., & Murthy, D. P., 2016. Introduction to maintenance engineering: modelling, optimization and management. John Wiley & Sons.

https://doi.org/10.1002/9781118926581

Braun, V., & Clarke, V., 2019. Reflecting on reflexive thematic analysis. Qualitative Research in Sport, Exercise and Health, 11(4), 589-597.

https://doi.org/10.1080/2159676X.2019.1628806

Chen, F., & Wu, C., 2020. A novel methodology for forecasting gas supply reliability of natural gas pipeline systems. Frontiers in Energy, 14(2), 213-223. https://doi.org/10.1007/s11708-020067 2-5

Chen, N., Ye, Z. S., Xiang, Y., & Zhang, L., 2015. Condition-based maintenance using the inverse Gaussian degradation model. European Journal of Operational Research, 243(1), 190-199. https://doi.org/10.1016/j.ejor.2014.11.029

Chookah, M., Nuhi, M., & Modarres, M., 2011. A probabilistic physics-of-failure model for prognostic health management of structures subject to pitting and corrosion-fatigue. Reliability Engineering & System Safety, 96(12), 1601-1610. https://doi.org/10.1016/j.ress.2011.07.007

De Bruijn, H., Größler, A., & Videira, N., 2020. Antifragility as a design criterion for modelling dynamic systems. Systems Research and Behavioral Science, 37(1), 23-37.

https://doi.org/10.1002/sres.2574

Derbyshire, J., & Wright, G., 2014. Preparing for the future: development of an 'antifragile'methodology that complements scenario planning by omitting causation. Technological Forecasting and Social Change, 82, 215-225.

https://doi.org/10.1016/j.techfore.2013.07.001

Eleuteri, A., Tagliaferri, R., Milano, L., De Placido, S., & De Laurentiis, M., 2003. A novel neural network-based survival analysis model. Neural Networks, 16(5-6), 855-864.

https://doi.org/10.1016/S0893-6080(03)00098-4

Elsayed A., 2012. Reliability engineering. https://doi.org/10.1109/TR.2012.219410

Gaur, V., Yadav, O. P., Soni, G., & Rathore, A. P. S., 2019. A review of metrics, algorithms and methodologies for network reliability. In 2019 IEEE International Conference on Industrial Engineering and Engineering Management (IEEM) (pp. 1129-1133). IEEE.

https://doi.org/10.1109/IEEM44572.2019.8978688

Gebraeel, N., Elwany, A., & Pan, J., 2009. Residual life predictions in the absence of prior degradation knowledge. IEEE Transactions on Reliability, 58(1), 106-117.

https://doi.org/10.1109/TR.2008.2011659

Gopal K.Kanji, 1998. Measurement of business excellence, Total Quality Management, 9:7, 633-643, https://doi.org/10.1080/0954412988325

Gorjian N., Ma L., Mittinty M., Yarlagadda P., Sun Y., 2010. A review on degradation models in reliability analysis. In: Kiritsis D., Emmanouilidis C., Koronios A., Mathew J. (eds) Engineering Asset Lifecycle Management. Springer, London.

http://dx.doi.org/10.1007/978-0-85729-320-6_42

Guest, G., MacQueen, K. M., & Namey, E. E., 2012. Introduction to applied thematic analysis. Applied thematic analysis, 3(20), 1-21.

https://dx.doi.org/10.4135/9781483384436

Hao Peng, Qianmei Feng & David W. Coit, 2010. Reliability and maintenance modeling for systems subject to multiple dependent competing failure processes, IIE Transactions, 43:1, 12-22. https://doi.org/10.1080/0740817X.2010.491502

Kaplan, R. S., & Norton, D. P., 1992. The balanced scorecard--measures that drive performance. Harvard Business Review, 70(1), 71-79.

Keedy, E., & Feng, Q., 2012. A physics-of-failure based reliability and maintenance modeling framework for stent deployment and operation. Reliability Engineering & System Safety, 103, 94-101.

https://doi.org/10.1016/j.ress.2012.03.005

Kjell A. Doksum & Arnljot Hbyland, 1992. Models for Variable-Stress Accelerated Life Testing Experiments Based on Wener Processes and the Inverse Gaussian Distribution, Technometrics, 34:1, 74 82.

https://doi.org/10.1080/00401706.1992.10485235

Kobbacy, K. A., & Murthy, D. P., 2008. Complex system maintenance handbook. London: Springer. https://doi.org/10.1007/978-1-84800-011-7

Lawless, J., & Crowder, M., 2004. Covariates and random effects in a gamma process model with application to degradation and failure. Lifetime data analysis, 10(3), 213-227.

https://doi.org/10.1023/B:LIDA.0000036389.14073.dd

Li, C., Tao, L., & Yongsheng, B. , 2007. Condition residual life evaluation by support vector machine. In 2007 8th International Conference on Electronic Measurement and Instruments (pp. 4-441). IEEE.

https://doi.org/10.1109/ICEMI.2007.4351178

Lu, C. J., & Meeker, W. O., 1993. Using degradation measures to estimate a time-to-failure distribution. Technometrics, 35(2), 161-174.

https://doi.org/10.1080/00401706.1993.10485038

Ma, K., Wang, H., & Blaabjerg, F., 2016. New approaches to reliability assessment: Using physics-of-failure for prediction and design in power electronics systems. IEEE Power Electronics Magazine, 3(4), 28-41. https://doi.org/10.1109/MPEL.2016.2615277

Mohsenijam, A., Siu, M. F. F., & Lu, M., 2017. Modified stepwise regression approach to streamlining predictive analytics for construction engineering applications. Journal of Computing in Civil Engineering, 31(3), 04016066. https://doi.org/10.1061/(ASCE)CP.1943-5487.0000636

Ren, Y., Cui, B., Feng, Q., Yang, D., Fan, D., Sun, B., & Li, M., 2020. A reliability evaluation method for radial multi-microgrid systems considering distribution network transmission capacity. Computers & Industrial Engineering, 139, 106145.

https://doi.org/10.1016/j.cie.2019.106145

Saidi, L., Ali, J. B., Bechhoefer, E., & Benbouzid, M., 2017. Wind turbine high-speed shaft bearings health prognosis through a spectral Kurtosis-derived indices and SVR. Applied Acoustics, 120,1-8.

https://doi.org/10.1016/j.apacoust.2017.01.005

Shin, I., Lee, J., Lee, J. Y., Jung, K., Kwon, D., Youn, B. D., ... & Choi, J. H., 2018. A framework for prognostics and health management applications toward smart manufacturing systems. International Journal of Precision Engineering and Manufacturing-Green Technology, 5(4), 535-554.

https://doi.org/10.1007/s40684-018-0055-0

Si, W., Yang, Q., & Wu, X., 2018. Material degradation modeling and failure prediction using microstructure images. Technometrics. https://doi.org/10.1080/00401706.2018.1514327

Song, Y., Liu, D., Yang, C., & Peng, Y. , 2017. Data-driven hybrid remaining useful life estimation approach for spacecraft lithium-ion battery. Microelectronics Reliability, 75, 142-153. https://doi.org/10.1016/j.microrel.2017.06.045

Sterman, J. D., 2000. Business dynamics: System thinking and modeling for a complex world Irwin McGraw-Hill. Massachusetts Institute of Technology, Engineering Systems Division:

Cambridge, MA, USA.

https://doi.org/10.2307/41166098

Sterman, J. D., 2001. System dynamics modeling: tools for learning in a complex world. California management review, 43(4), 8-25. https://doi.org/10.2307/41166098

Sterman, J., 2018. System dynamics at sixty: the path forward. System Dynamics Review, 34(1-2), 5-47. https://doi.org/10.1002/sdr.1601

Succi, S., 2020. Relativistic anti-fragility. The European Physical Journal Plus, 135(2), 1-7. https://doi.org/10.1140/epjp/s13360-020-00255-5

Taleb, N. N., 2010. The Black Swan. The Impact of the Highly Improbable. Random House Incorporated.

Taleb, N. N., 2012. Antifragile: Things that gain from disorder. Random House Incorporated.

Tseng, S. T., & Peng, C. Y., 2007. Stochastic diffusion modeling of degradation data. Journal of data Science, 5(3), 315-333.

https://doi.org/10.6339/JDS.2007.05(3).351

Wang, Y., & Pham, H., 2012. Modeling the dependent competing risks with multiple degradation processes and random shock using time-varying copulas. IEEE Transactions on Reliability, 61(1), 13-22. [6045314].

https://doi.org/10.1109/TR.2011.2170253

Yadav, O. P., Choudhary, N., & Bilen, C., 2008. Complex system reliability estimation methodology in the absence of failure data. Quality and reliability engineering international, 24(7), 745-764. https://doi.org/10.1002/qre.920

Yu, J., Zheng, S., Pham, H., & Chen, T., 2018. Reliability modeling of multi-state degraded repairable systems and its applications to automotive systems. Quality and Reliability Engineering International, 34(3), 459-474.

https://doi.org/10.1002/qre.225

Yu, W., Wen, K., Min, Y., He, L., Huang, W., & Gong, J., 2018. A methodology to quantify the gas supply capacity of natural gas transmission pipeline system using reliability theory. Reliability Engineering & System Safety, 175, 128-141. https://doi.org/10.1016/j.ress.2018.03.007

Zhang, F., & Shi, Y., 2020. Geometry on the statistical manifold induced by the degradation model with soft failure data. Journal of Computational and Applied Mathematics, 363, 211-222. https://doi.org/10.1016/j.cam.2019.06.003

Zhang, X., Wang, B., & Chen, X., 2015. Intelligent fault diagnosis of roller bearings with multivariable ensemble-based incremental support vector machine. Knowledge-Based Systems, 89, 56-85

https://doi.org/10.1016/j.knosys.2015.06.017

Zhou, Q., & Thai, V. V., 2016. Fuzzy and grey theories in failure mode and effect analysis for tanker equipment failure prediction. Safety science, 83, 74-79.

https://doi.org/10.1016/j.ssci.2015.11.013

Zhu, S. P., Huang, H. Z., Peng, W., Wang, H. K., & Mahadevan, S., 2016. Probabilistic physics of failure-based framework for fatigue life prediction of aircraft gas turbine discs under uncertainty. Reliability Engineering & System Safety, 146, 1-12. https://doi.org/10.1016/j.ress.2015.10.002

Zio, E., 2016. Some challenges and opportunities in reliability engineering. IEEE Transactions on Reliability, 65(4),1769-1782. https://doi.org/10.1109/TR.2016.259154

تولید LNG به روش مبرد آمیخته تک‌مرحله‌ای در مقیاس قابل‌حمل: انتخاب پیکربندی و آنالیز حساسیت

- لاله شیرازی [1*]، مهران سرمد[1]، پیمان معین[1]، رضا حیاتی[1]، ساناز آناهید[1]، مرضیه زارع[2]

۱. پژوهشکده گاز، پژوهشگاه صنعت نفت، تهران، ایران

۲. مدیریت پژوهش و فناوری شرکت ملی گاز ایران، تهران، ایران

(ایمیل نویسنده مسئول: shirazil@ripi.ir)

چکیـــــــده

بررسی صاحبان فناوری مایع سازی گاز طبیعی در مقیاس قابل‌حمل، نشان می‌دهد که فرآیندهای مبرد آمیخته تک‌مرحله‌ای، سیکل انبساطی نیتروژن و فرآیندهای خود سرمایش، برای تولید گاز طبیعی مایع‌شده، استفاده‌شده است. در بین فرایندهای نامبرده شده، فرآیندهای مبرد آمیخته تک‌مرحله‌ای از بازده انرژی بالاتری برخوردار بوده و از تجهیزات دوار کمتری استفاده می‌کند. با توجه به مطالعات پژوهشگاه صنعت نفت در مورد فرآیندهای تجاری سیکل مبرد آمیخته تک‌مرحله‌ای و مطالعه بیش از ۱۰۰ اختراع در این رابطه، فرایند مبرد آمیخته تک‌مرحله‌ای با یک جداکننده فازی (با ۳۴٪ اشتراک در فرآیندهای مبرد آمیخته تک‌مرحله‌ای)، برای تولید گاز طبیعی مایع‌شده در مقیاس قابل‌حمل، انتخاب‌شده است. با توجه به پیچیدگی فرآیندهای مبرد آمیخته تک‌مرحله‌ای با چند جداکننده فازی، این نوع چرخه‌ها انتخاب‌نشده‌اند. از طرفی فرآیند مبرد آمیخته تک‌مرحله‌ای بدون جداکننده فازی به دلیل احتمال یخزدگی هیدروکربن‌های سنگین موجود در مبرد، انتخاب‌نشده است.

چندین فرآیند مبرد آمیخته تک‌مرحله‌ای با یک جداکننده فازی بر اساس چیدمان تجهیزات در بخش‌های مایع سازی و سردسازی قابل‌استفاده است. بامطالعه گسترده و با توجه به محدودیت‌های طراحی در مقیاس قابل‌حمل (به‌عنوان‌مثال حداقل تعداد تجهیزات ثابت و دوار، حداقل پیچیدگی فرآیند و ابعاد و غیره)، دو آرایش فرآیندی در این مقاله انتخاب، شبیه‌سازی و بهینه‌سازی شده است. آنالیز حساسیت بر روی فشار و دمای خوراک و همچنین اجزاء مبرد آمیخته و ترکیب درصد خوراک انجام‌شده است. انرژی مصرفی این دو آرایش محاسبه‌شده و پیچیدگی آن‌ها با یکدیگر مقایسه شده است. با توجه به پایین بودن میزان تولید LNG و لزوم سادگی فرآیند در مقیاس قابل‌حمل و با توجه به نتایج اقتصادی بهترین گزینه توصیه‌شده است.

واژگان کلیدی: LNG، مبرد آمیخته تک‌مرحله‌ای، بهینه‌سازی، آنالیز حساسیت و اقتصادی، طراحی قابل‌حمل

ارتقاء سرعت انتقال حرارت توسط قطعه تعبیه شده در گرم‌کن ایستگاه گاز شهری

- بهنام رنجبر[۱]، فائزه محمدی[۱]، مسعود رحیمی[۲*]، بهزاد خسروی[۳]، نادر عباسی[۳]

۱. گروه مهندسی شیمی، دانشکده مهندسی شیمی، واحد کرمانشاه، دانشگاه آزاد اسلامی، کرمانشاه، ایران

۲. گروه مهندسی شیمی، دانشگاه رازی، کرمانشاه، ایران

۳. شرکت ملی گاز ایران، کردستان، سنندج، ایران

(ایمیل نویسنده مسئول: masoudrahimi@yahoo.com)

چکیـــــــده

در این تحقیق به‌منظور افزایش سرعت انتقال حرارت در یک گرم‌کن ایستگاه گاز شهری (CGS) نوع کلاسیک قطعه تعبیه‌شده در داخل کویل‌های حرارتی قرارگرفته است. استفاده از این قطعات باعث افزایش افت فشار می‌شود که استفاده از آن در اکثر مبدل‌های حرارتی یک عیب به‌حساب می‌آید. آما در این مورد پدیده کاملاً مطلوب است فشار در خط انتقال شهری بایستی کاهش یابد. نوع بکار گرفته قطعه موردنظر از نوع مارپیچی است از استیل بدون درز بر طبق استاندارد شرکت گاز ساخته‌شده است. قطعات در هر هشت مسیر مارپیچ ایستگاه تقلیل فشار ماویان شهر کامیاران استان کردستان با ظرفیت ۲۵۰۰ مترمکعب بر ساعت نصب‌شده است. ارتقاء سرعت انتقال حرارت تا ۷۴٪ به دست آمد که ازنظر صرفه‌جویی در انرژی و کنترل آلودگی کاملاً مهم است.

واژگان کلیدی: قطعه تعبیه‌شده در لوله، ایستگاه تقلیل فشار، گرم‌کن، رگلاتور، ایستگاه گاز شهری

تجزیه و تحلیل فنی و اقتصادی فرآیند تبدیل گاز فلر به بنزین (FGTG) از طریق تولید دی‌متیل‌اتر

- مصطفی جعفری[1]، علی وطنی[1*]، محمد شهاب دلجو[1]، امیرحسین خلیلی گرکانی[2]

۱. انیستیو گاز طبیعی مایع (I-LNG)، دانشکده مهندسی شیمی، پردیس دانشکده های فنی، دانشگاه تهران، تهران، ایران

۲. گروه پژوهشی شیمی و فرآیند، پژوهشگاه نیرو، تهران، ایران

(ایمیل نویسنده مسئول: avatani@ut.ac.ir)

چکیـــــــده

مسئله سوزاندن گازهای فلر و رهاسازی آن‌ها به اتمسفر، به یکی از مشکلات صنایع نفت ، گاز و پتروشیمی تبدیل‌شده است. اگر این صنایع بتوانند انرژی یا مواد ارزشمندی را از گازهای فلر تولید کنند، بسیار سودآور خواهد بود و همچنین محیط‌زیست هم آسیب کمتری خواهد دید. هدف از این تحقیق، طراحی، شبیه‌سازی و ارزیابی اقتصادی فرآیند تبدیل گاز فلر به دی‌متیل‌اتر به‌منظور تولید هم‌زمان بنزین، گاز مایع و هیدروژن در نرم‌افزار Aspen HYSYS v.11 است. فرآیند تبدیل گاز فلر به بنزین (FGTG) می‌تواند از دو مسیر تولید مستقیم یا غیرمستقیم دی‌متیل‌اتر صورت بگیرد (دو سناریو). در مقایسه اقتصادی این دو سناریو، هزینه فروش محصول، سود عملیاتی ، کل هزینه سرمایه‌گذاری، نرخ بازده سرمایه‌گذاری و بازگشت سرمایه محاسبه خواهد شد. نتایج ارزیابی اقتصادی نشان می‌دهد که استفاده از فرآیند FGTG با تولید مستقیم دی‌متیل‌اتر (سناریوی دوم) به‌جای فرآیند FGTG با تولید غیرمستقیم دی‌متیل‌اتر (سناریوی اول) فروش محصول و سود عملیاتی را حدود ۵۵ درصد و ۶۵ درصد افزایش می‌دهد و همچنین کل هزینه سرمایه‌گذاری و هزینه یوتیلیتی به ترتیب حدود ۳۰ درصد و ۵۰ درصد کاهش پیدا می‌کند. سرانجام ، نرخ بازده سرمایه‌گذاری در فرآیند FGTG با تولید مستقیم دی‌متیل‌اتر و تولید غیرمستقیم دی‌متیل اتر به ترتیب ۵۲ درصد در سال و ۳۳ درصد در سال است و همچنین بازگشت سرمایه در سناریوی دوم ۱/۱ سال زودتر از سناریوی اول است.

واژگان کلیدی: گاز فلر، دی‌متیل‌اتر، بنزین، هیدروژن، سود عملیاتی، عسلویه

انتقال گاز طبیعی در حالت فوق بحرانی

- مرتضی زیودار[1*]، مسلم ابروفراخ[2]

۱. استاد مهندسی شیمی، دانشکده مهندسی شیمی، دانشگاه سیستان و بلوچستان، زاهدان، ایران

۲. دانشجوی کارشناسی ارشد مهندسی شیمی، دانشگاه سیستان و بلوچستان، زاهدان، ایران

(ایمیل نویسنده مسئول: mzivdar@eng.usb.ac.ir)

چکیـــــــده

در فرایند انتقال گاز طبیعی در خط لوله مشکلاتی نظیر هزینه‌ی بالای خرید و نگهداری کمپرسورها در ایستگاه‌های تقویت فشار، تشکیل هیدرات گازی، تشکیل جریان دوفازی، آلودگی صوتی و هزینه بر بودن سرویس و نگه داری خطوط لوله وجود دارد . برای کاهش این مشکلات انتقال گاز طبیعی در حالت فوق بحرانی پیشنهاد می‌شود. متأسفانه اطلاعات بسیار محدودی در زمینه انتقال گاز طبیعی در حالت فوق بحرانی وجود دارد. در این تحقیق انتقال گاز طبیعی خط لوله سراسری چهارم ایران در حالت فوق بحرانی بررسی شده و نتایج آن با انتقال گاز در حالت معمولی مقایسه شده است. با انجام فرایند در حالت فوق بحرانی، تعداد ایستگاه‌های تقویت فشار از ۱۰ ایستگاه در حالت معمولی به ۴ ایستگاه کاهش یافت. همچنین نتایج این تحقیق نشان داد که افت فشار و انرژی کمپرسورها در حالت فوق بحرانی به ترتیب به اندازه ۵۹٪ و ۶۰٪ نسبت به حالت معمولی کاهش یافته است.

واژگان کلیدی: حالت فوق بحرانی، انتقال گاز طبیعی، خطوط لوله، شبیه‌سازی

امکان‌سنجی استفاده از گرمای اتلافی ایستگاه کاهش فشار گاز برای شیرین سازی آب

- مریم کرمی[1*] ، فریما علیخانی[2]

۱. گروه مهندسی مکانیک، دانشکده فنی مهندسی، دانشگاه خوارزمی، تهران، ایران

۲. گروه مهندسی مکانیک، دانشگاه الزهرا، تهران، ایران

(ایمیل نویسنده مسئول: karami@khu.ac.ir)

چکیـــــــده

در سال‌های اخیر، بازیابی گرمای اتلافی برای کاهش مصرف انرژی و تأمین انرژی موردنیاز به یک روش امیدبخش برای حل بحران انرژی تبدیل‌شده است. در این مطالعه، از گرمای اتلافی ایستگاه‌های کاهش فشار گاز برای تولید آب شیرین با استفاده از یک واحد آب‌شیرین‌کن رطوبت زنی- رطوبت‌زدایی استفاده‌شده است. با مدل‌سازی سیستم پیشنهادی در نرم‌افزار اسپن هایسیس، تأثیر پارامترهای مختلف بر میزان تولید آب شیرین ارزیابی‌شده است. نتایج نشان می‌دهد که میزان بهینه دبی آب‌شور و جریان هوا برای یک ایستگاه کاهش فشار گاز با ظرفیت ۵۰،۰۰۰ مترمکعب استاندارد بر ساعت (SCMH)، به ترتیب ۰/۱۶۵ کیلوگرم بر ثانیه و ۰/۲ کیلوگرم بر ثانیه است. همچنین مشخص‌شده است که با کاهش فشار ورودی گاز از ۱۰۰۰ psi به ۴۰۰ psi، میزان تولید آب شیرین حدود ۵۲/۲٪ کاهش می‌یابد. افزایش نرخ تولید آب شیرین با افزایش ظرفیت ایستگاه کاهش فشار از ۱۰،۰۰۰ SCMH به ۵۰،۰۰۰ FGTG حدود ۶۲٪ است. علاوه بر این، میزان تولید آب شیرین در ایستگاه کاهش فشار گاز با ۱۰،۰۰۰ SCMH با افزایش دمای آب‌شور ورودی به رطوبت زن از ۴۰°C به ۸۰°C حدود ۴/۴٪ افزایش می‌یابد.

واژگان کلیدی: ایستگاه کاهش فشار گاز، شیرین سازی آب، واحد رطوبت زنی-رطوبت زدایی، شبیه سازی عددی، اسپن هایسیس

ارایه مدل نوینی از نگهداری و تعمیرات پویا با رویکرد شکست ناپذیری در بهبود قابلیت اطمینان (مطالعه موردی: منطقه ده عملیات انتقال گاز ایران)

- حمید خدری[1]، غلامرضا جمالی[2*]، احمد قربانپور[3]

۱. دانشجوی دکتری مدیریت تولید و عملیات،دانشکده اقتصاد و کسب‌وکار، دانشگاه خلیج‌فارس، بوشهر، ایران

۲. دانشیار دانشکده اقتصاد و کسب‌وکار، دانشگاه خلیج‌فارس، بوشهر، ایران

۳. استادیار دانشکده اقتصاد و کسب‌وکار، دانشگاه خلیج‌فارس، بوشهر، ایران

(ایمیل نویسنده مسئول: gjamali@pgu.ac.ir)

چکیـــــــده

قابلیت اطمینان یکی از مهم‌ترین شاخص‌های ارزیابی عملکرد در حوزه نگهداری و تعمیرات محسوب می‌شود. تحقیق حاضر که به‌صورت آمیخته انجام‌شده است به دنبال شناسایی مؤلفه‌های شکست‌ناپذیری و بررسی تأثیر آن‌ها بر قابلیت اطمینان سیستم با استفاده از پویایی سیستم‌ها انجام‌شده است. در بخش کیفی تحقیق با استفاده از روش تحلیل مضمون، با مشارکت ۱۰ متخصص خبره سازمانی و دانشگاهی، عوامل شکست‌ناپذیری در قالب ۲۵۴ کد باز، ۱۸ کد سازمان دهنده و دو کد فراگیر با مرور ادبیات تحقیق و استفاده از نرم‌افزار ماکس کیودا[1] نسخه ۲۰۲۰ شناسایی و دسته‌بندی گردید.در ادامه و در بخش کمی تحقیق ارتباط مؤلفه‌های سازمان دهنده شکست‌ناپذیری به روش رگرسیون چندگانه باقابلیت اطمینان سیستم موردبررسی قرار گرفت. سه معیار یادگیری، افزونگی و بحث‌های اکتشافی به‌عنوان عواملی که بیشترین تأثیر بر قابلیت اطمینان سیستم را دارند شناسایی و انتخاب شدند. تأثیر این شاخص‌ها بر قابلیت اطمینان سیستم در محیطی پویا و با استفاده از نرم‌افزار ونسیم نسخه DDS شبیه‌سازی گردید. نتایج بیانگر تأثیر مثبت هر سه معیار یادگیری، افزونگی و بحث‌های اکتشافی در بهبود قابلیت اطمینان سیستم در منطقه ده عملیات انتقال گاز است و شاخص افزونگی بیشترین تأثیر و مؤلفه‌های یادگیری و بحث‌های اکتشافی در رده‌های بعدی تأثیرگذاری در بهبود قابلیت اطمینان سیستم قرار دارند.

واژگان کلیدی: نگهداری و تعمیرات، قابلیت اطمینان، شکست‌ناپذیری، پویایی سیستم، انتقال گاز، تحلیل موضوعی

1. Maxqda 2020

Iran Gas Institute

JOURNAL OF GAS TECHNOLOGY

VOLUME 6 • ISSUE 2 • WINTER 2021

EISSN: 2588-5596

Contents